ABSTRACT

Title of Document: METHODS TO INCREASE VELOCITY OF MAKEUP AIR FOR ATRIUM SMOKE CONTROL - A CFD STUDY

Christine Pongratz, Masters of Science, 2014

Directed By: Associate Professor, Dr. Arnaud Trouvé, and Professor and Chair, Dr. James Milke
Fire Protection Engineering Department

NFPA 92 currently restricts the velocity of makeup not exceed 1.0 m/s in atria smoke control systems. This requirement imposes a restriction on atria design due to the need for large area makeup vents. The objective of the research project is to evaluate the effects of velocity and location of makeup airflow on potential design fires within atria using Fire Dynamics Simulator 6.0 (FDS). A series of simulations are developed with fire size, makeup air vent flow velocity, and makeup air vent location as primary variables. The numerical results are analyzed in terms of possible adverse changes on smoke layer depth and fire spread propensity. The analysis is formulated in terms of a simplified engineering design tool, which allows for makeup air to exceed the 1.0 m/s limitation. The design tool proposed determines a modified volumetric exhaust rate for the system configuration, by a factor related to the smoke production increase.

METHODS TO INCREASE VELOCITY OF MAKEUP AIR FOR ATRIUM SMOKE CONTROL - A CFD STUDY

By

Christine Anderer Pongratz

Thesis submitted to the Faculty of the Graduate School of the
University of Maryland, College Park, in partial fulfillment
of the requirements for the degree of
Masters of Science
2014

Advisory Committee:
Dr. James Milke, Professor and Chair
Dr. Arnaud Trouvé, Associate Professor
Dr. Andre Marshall, Associate Professor

Dedication

I dedicate this report to my parents, Nancy and Simon Pongratz.

For living a life full of determination, integrity, and dedication- my every achievement only mirrors the empowerment that you have instilled in me. Thank you for your unyielding support, and continuous commitment in facilitating my success.

Acknowledgements

This research was supported by ASHRAE (project 1600-TRP) under the technical direction of Paul Turnbull.

I would like to sincerely thank my thesis advisors for their guidance and support during my pursuit of this research project. I would like to thank my advisor, Professor Arnaud Trouvé, for his guidance during this past year- for his support and patience as I became familiar with FDS, and for his perceptive strategies during the analysis process. I would like to acknowledge my Professor Andre Marshall, for his involvement as an advisory committee member. I am especially thankful for his insightful approaches to numerical scaling, and assisting with my specific scaling analysis process.

Finally I would like to express my sincere gratitude to my advisor, Professor Jim Milke, for introducing me to what has become my passion for fire protection engineering. For guiding me through my graduate research with limitless patience, continuous motivation, and for instilling confidence in me during times I did not have it myself. I am truly thankful for his genuine dedication to my education during my five years at the University of Maryland. I am privileged to call him my mentor and truly appreciate his positive impact on my life. Most importantly I am thankful for his effortless ability to make me laugh.

Table of Contents

List of Tables

List of Figures

Chapter 1

Introduction

1.1 Atria and Smoke Management Systems

The use of atria has become an increasingly popular design feature within large commercial space, lavish hotels, and multi-level shopping centers. Modern atria serve as prominent aesthetic features, often several stories high with undivided space. Many atria have glazed roofs and large windows to give the grandeur feel of space and light.

The opening in the floors created to form an atrium pose fire and smoke challenges. The large space allows for easier smoke spread between floors and adjacent openings. A principal design objective for fire protection systems in an atrium is to protect occupants from the adverse effects of smoke and contain the fire and smoke to its room of origin. As atria fashion larger openings, the ability to compartmentalize smoke and fire decrease. Consequently, design approaches must be altered to maintain the life safety objectives.

The primary objective of all fire protection systems is to protect occupants from the adverse effects of smoke and fire. In atria especially, managing the spread of smoke due to fire is compulsory. Building codes address the potential event of a fire by requiring automatic sprinkler installation throughout the building, limiting the

combustible materials on the floor of the atria, and providing tenable conditions for occupants.

Untenable conditions can be created from the presence of smoke. The hazard of smoke spread in atria must be addressed to satisfy identified objectives. These objectives are detailed in NFPA 92: Standard for Smoke Control Systems [3]. The objectives include:

- Maintain a tenable environment in the means of egress from large-volume building space during the time required for evacuation;
- Control and reduce mitigation of smoke between the fire area and adjacent spaces;
- Provide conditions within and outside the fire zone to assist emergency response personnel in conducting search and rescue operations and in locating and controlling the fire;
- Contribute to the protection of life and reduction of property loss;
- Aid in post-fire smoke removal.

In order to accomplish the design objective(s), an engineered smoke management system is considered for all atria. NFPA 92 includes requirements for the design of smoke management systems. By evaluating the design characteristics of the atrium, numerous types of smoke management approaches may be considered.

There are various design approaches for atria that are intended to maintain tenable conditions for occupants. The steady mechanical smoke exhaust system is the most commonly used approach in North America [2]. The system is designed to use mechanical exhaust to stabilize the bottom of the smoke layer at the predetermined height for the design fire. The exhaust removes smoke from the upper levels of the atrium to prevent accumulation of heat and smoke and prevent the descent of the smoke layer interface below the predetermined height [2]. An idealized version of a smoke management system in an atrium with multiple levels is illustrated in Figure 1.1.

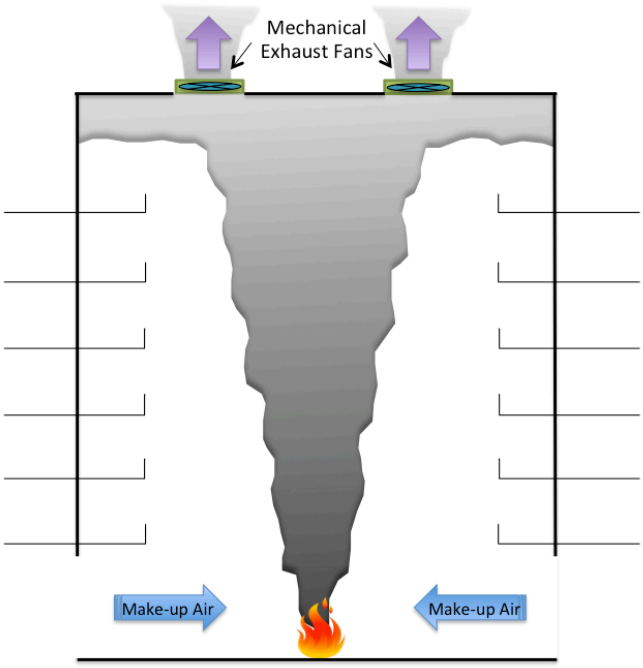

Figure 1.1: Mechanical Atrium Smoke Management System

The mechanical ventilation system assumes the formation of a smoke layer at the ceiling. Factors that may affect the smoke layer include sprinkler activation, HVAC systems, air currents striking the plume, upward thrusting airflows, and air forced into

the upper layer by means other than the plume.

In order to provide effective mechanical ventilation, a makeup air supply must be provided. The supply of makeup air may enter into the compartment from passive openings such as doors or windows, or additional mechanical ventilation. The amount of air that must be supplied is not dictated in the model building codes, but several restrictions are addressed in the design of this component of the system.

High makeup air velocity may cause high velocity air entrainment into a flame to significantly affect the fire development and smoke movement within a compartment. Increased air entrainment will increase mixing between ambient air and smoke to upsurge the volume of smoke produced. Also the additional air velocity may tilt the flame and disturb the upward trajectory of fire plume, which may expose occupants to additional radiant heat flux and smoke. A schematic of increased makeup air velocity on the fire plume is shown in Figure 1.2. The image illustrates a disturbed fire plume, with smoke entering the balcony levels of the atrium. The adverse effect of the makeup air compromises the ability of the mechanical exhaust system to achieve the design goals of maintaining the smoke layer above a particular elevation.

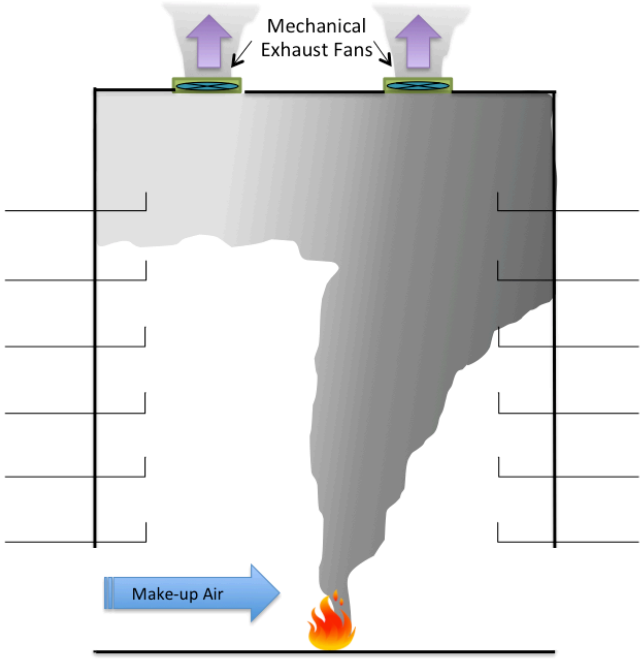

Figure 1.2: Makeup Air Velocity adverse effects on Fire Plume in Atrium

Currently NFPA 92 restricts the makeup air velocity not to exceed 1.02 m/s, (200 ft/min) to prevent significant plume deflection and disruption of the smoke layer interface. This limitation is further discussed in ASHRAE/SFPE publication, Handbook for Smoke Control Engineering [22]. This restriction, however, is based on limited research into the effect of wind on flames. The work is cited in the SFPE Handbook of Fire Protection Engineering [13]. NFPA 92 permits greater velocities of makeup air if the design is supported by engineering analysis.

Although there is no restriction on the overall volumetric flow of makeup air, NFPA 92 suggests makeup air be designed at 85 percent to 95 percent of the exhaust, not including the leakage through small paths [3]. Coupled with the limitation on the maximum makeup air velocity, this suggestion can lead to large areas for makeup air

vents. Engineering designers and architects are therefore limited by the need for large area makeup air vents, especially if makeup air is injected at low elevation of the atrium. Overall, the requirement often presents design challenges and increased costs.

1.2 Separation Distance of Fuel Packages

In addition to the increasing smoke production due to increased makeup air velocity, the thermal radiation from the design fire to exposed items close to the fire may also increase due to the flame tilt. When determining a design fire, NFPA 92 requires that the design must consider the type of fuel, fuel spacing, and configuration [3]. The base fuel package is considered as the maximum probable size of fuel that is likely to be involved in a fire situation. A fuel package can include any fuel item that may be located in a large space such as chairs, tables, furniture, or additional decorative items that may be found in an atrium [3].

The base fuel package in an array of potential fuels is selected as the one with the greatest heat release rate (often being the largest fuel package in the array). In addition, the configuration of the design fire must consider the impact of the fire's radiant heat flux value to its surroundings. If the radiant heat flux is sufficient to ignite other fuel packages in the array then the design fire must be increased to include this additional fuel [3]. The following study will use FDS coupled with a point source model, to report on the appropriate separation distance under additional airflow conditions.

1.3 Research Objectives and Project Scope

The following study will investigate the adverse effects of makeup air velocity specifically on the smoke layer interface position and the separation of fuel packages.

The study is completed using a state-of-the-art computational fluid dynamics (CFD) model, specifically Fire Dynamic Simulator (FDS) Version 6. FDS is an open-source freeware fire model developed by the Fire Research Division of the National Institute of Standard and Technologies (NIST) and has emerged in recent years as the leading fire simulation software used by fire safety engineers and fire researchers around the world.

Past Research by Heskestad [19], Beyler [13], Hadjisophocleous [15], and Kerber & Milke [16] using FDS, suggests that velocities above 1 m/s can alter an axisymmetric smoke plume, resulting in an increase in the amount of air entrained into the plume. While the study by Kerber [16] showed that high makeup air flow velocities may result in substandard operation of the smoke control system, it did not provide a detailed understanding of the exact conditions that lead to substandard behavior and whether there may be a range of makeup air flow velocities beyond the current 1 m/s limit that still provide acceptable design solutions. The objective of the present study is to evaluate the impact of makeup airflow velocity on the smoke layer interface and fuel package separation distance. Further, an engineering tool is proposed in order to provide guidance on possible adjustments in the

mechanical exhaust when exceeding the current 1.02 m/s limitation as a function of fire size, supply vent area, and vent elevation.

The following study uses FDS 6.0. An FDS model grid analysis is completed in order to evaluate the proper grid resolution for the study. As further explained in Chapter 2, two previous studies have been completed to evaluate the effects of makeup air, using FDS Version 4.0. The present study will first revisit the simulations created in the previous study to confirm similar results in FDS Version 6.0.

This study will specifically isolate the affects of makeup air by introducing the air through a vent located on one side, at a close distance to the base of the fire. The fire will be a propane burner, centrally located within a10-meter tall atrium. The intent is to study the effects of makeup air at the base of the fire plume to investigate the increased mass flow rate of the smoke plume in order to develop and quantify the results. The vent is a dedicated, duct-mounted makeup air vent, and supplies makeup air velocities of 1 m/s, 1.25 m/s, 1.5 m/s and 1.75 m/s directed at the fire.

The fire sizes included in the study are 1 MW, 2.5 MW, and 5 MW. The duct mounted makeup air vent will vary in size and elevation for each simulation.

An analysis of the FDS simulations is conducted to isolate the effects of the duct-mounted makeup air vent airflow on the fire. The analysis concentrates on the effects of the increased makeup air on the mass flow rate of the plume and in turn on the

smoke layer interface height within the atria. Also, additional simulations are run to investigate the outcome of increased makeup air on radiant heat flux and in turn the separation distance of fuel packages.

A parameter to measure the strength of the forced horizontal air flow with respect to the buoyant vertical flow generated by the combustion process is created, and compared to the FDS results of smoke production and heat flux. An engineering design tool correlation for both increases in smoke production and heat flux is formulated as corrections to the expressions for smoke flow rates and separation distances used in the NFPA 92 Standard for Smoke Control Systems.

Chapter 2

Literature Review

This chapter reviews the key algebraic equations used for the design of atrium smoke exhaust systems, along with the assumptions utilized for the specific FDS model fire conditions and chosen configuration details used in this study.

2.1 Axisymmetric Pool Flame Geometry

In fire safety engineering applications, the accidental fire is most commonly described as having buoyant, turbulent diffusion flame. A diffusion flame refers to the condition that the oxygen and fuel are originally separated and mixed through the process of diffusion. Molecular diffusion is the mechanism of molecules being transported from high to low concentration. This mixing process will sustain burning when the process is favorable to combustion [14]. The flame geometry for a pool fire is modeled as a cylindrical solid. The dimension of the flame is defined by the diameter of the pool fire, the flame height, and flame tilt.

2.2 Fire Plume

The most commonly used plume in fire safety engineering for basic atrium smoke control is the buoyant axisymmetric plume. The plume is generated from a diffusion flame above the burning region. The axis of symmetry is along the vertical centerline of the plume. The plume is typically idealized as a cone shape [13].

The additional plume types include wall and corner plumes. Fires located at a wall and in a corner entrain less air along the edge of the plume in contact with the corner or wall. Therefore, the amount of smoke produced is less for these locations. Conservative hazard assessments, such as atria smoke control calculations consequently apply axisymmetric plume conditions [2].

The fundamental equations for continuity, momentum, and buoyancy derive the simplified analytical solutions for the mass flow, velocity, and temperature equations of the plume [14]. The driving force of the plume is assumed to be caused by the density differential of the hot air above the fire and the cold surrounding air. Along the edges of the smoke plume, air is entrained horizontally from all directions [2]. The entrainment rate of the ambient air is proportional to the velocity of the plume at the specific elevation (z).

An idealized axisymmetric smoke plume is shown in Figure 2.1. The overall height of the compartment is defined as H, while the mean flame height is defined as z_l, and the

diameter of the plume is defined as d. Generally, the height, z, of interest in atrium smoke control design is the position located at the smoke layer interface. As the mass flow rate from the plume continues to enter the smoke layer, the smoke layer interface height will descend.

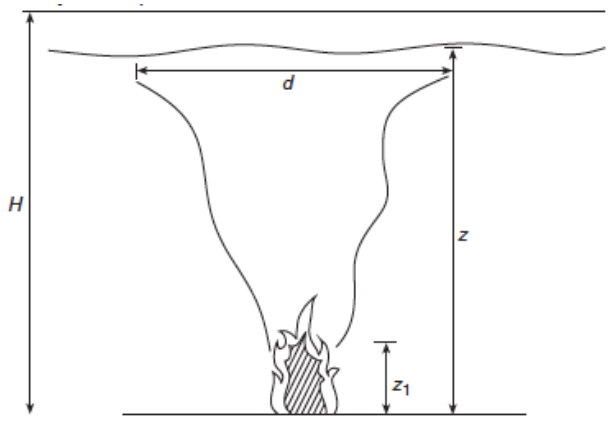

Figure 2.1: Axisymmetric Plume [21]

The diameter of the plume (d) increases with elevation (z) as ambient air continuously is entrained in to the dense smoke. The diameter of an axisymmetric plume is approximated by Equation 2.1.

$$d_p = K_d z \qquad (2.1)$$

d_p = plume diameter (m)

z = distance above the base of the fire (m)

K_d = diameter constant (dimensionless)

The diameter can vary significantly, such that the K_d value is defined between 0.25 to 0.5.

2.3 Compartment Enclosure Effects

As a fuel package burning inside an enclosure the fire can develop in numerous ways depending on the compartment geometry, fuel type, fuel size, and ventilation factors [14].

2.3.1 Fire Plume Dynamics in Compartment

After ignition a fire grows and produces increasing amounts of energy. The products from combustion form hot gases rise upward due to the density difference defined as the buoyant force.

The hot gases rise within the cold air and form a smoke plume. In a compartment, the plume will impinge on the ceiling and spread horizontally to reach the boundaries of the compartment. The hot smoke moving across the ceiling is defined as the ceiling jet. This will cause a layer of hot gases to form defined as a smoke layer. As the smoke plume continues to transport hot products of combustion to the upper layer of the compartment the smoke layer will descend.

Empirical and theoretical methods address the phenomenon of the smoke filling process by using the conservation of mass and energy to determine the characteristics of the upper hot layer. Conservation of mass accounts for the mass supplied from the plume to the smoke layer. Conservation of energy accounts for the energy supplied by the plume along with heat losses from the layer.

Within an enclosure, the compartment is set as a control volume and the conservation equations can therefore be applied to address the mass flow rate and temperature conditions within the system.

2.3.2 Enclosure Geometry and Boundary Conditions

As the ignited fuel burns within a compartment and a smoke layer forms, the upper layer conditions can greatly affect the properties within the lower layer. The radiant heat can increase the burning rate of the fuel, and the increase in the hot upper layer can have a considerable effect on the fire growth. In addition, the area and compartment size greatly affect the temperatures within the enclosure. The amount of cold ambient air entrained into the plume directly depends on the distance between the smoke layer interface and the base of the fire. An enclosure with a low ceiling will create high temperatures within the smoke layer, and also will also provide radiant heat to the fuel, causing fire growth to occur more rapidly. A taller ceiling will allow for more cold ambient air entrainment into the plume and smoke layer.

Although the smoke temperature may be lower in a tall space, the large amount of air entrained into the smoke creates a rapid smoke filling process [14].

The compartment boundary conditions considerably affect the heat transfer process within the system. The boundary material comprised of good insulating materials will limit the amount of heat flow to the surface to retain energy within the system [14]. The role of a boundary material is dependent on thermophysical material properties of conductivity (k), density (ρ_s), and heat capacity (c_p).

2.3.3 Ventilation factors

The air that enters the compartment through the inlet vents or openings is defined as the makeup air. The velocity of the introduction of ambient air into the compartment is an important consideration. Increased airflow at the base of the fuel can create flame tilt. The additional velocity will also increase entrainment rates into the fire. Additional air entrainment will increase the mass flow rate of the plume, to increase the rate of smoke production [19].

2.4 Smoke Management in Atria

The approximation of the smoke filling process and the position of the smoke layer interface (z) is applied to smoke management system design to achieve the safety objectives. The design of a system is specifically influenced by the characteristics of

the atrium itself; these features include the geometric shape and dimensions, the relative location within the building, and separation from communicating space [21].

2.4.1 Smoke Exhaust Design Approaches

Many smoke management systems are designed to restrict the smoke from descending below a designated height during the operation of the system. Numerous investigators have applied the physical phenomena of smoke filling in large spaces to develop potential design approaches of smoke management systems. The most common approaches include natural smoke filling, steady mechanical smoke exhaust, unsteady mechanical smoke exhaust, steady natural smoke venting, and unsteady natural smoke venting [2]. This study considers the design of a steady mechanical smoke exhaust system.

2.4.2 Mechanical Smoke Exhaust System

Steady mechanical smoke exhaust is a commonly used approach in North America. Typically, the system is designed to use mechanical exhaust to stabilize the bottom of the smoke layer at the predetermined height for the design fire. The exhaust removes smoke from the upper levels of the atrium to prevent accumulation of heat and smoke and prevent the descent of the smoke layer interface below the predetermined height [2].

The International Building Code (IBC) section 909.8.1 specifically requires that a smoke layer must remain at least 6 ft (1.8 m) above the highest walking surface [23]. The mechanical exhaust system must be designed to create enough smoke extraction to keep the smoke layer at this designated height. An idealized version of a smoke control system in an atrium with multiple levels is illustrated in Figure 2.2. The figure illustrates an atrium smoke control system with mechanical exhaust fans located at the ceiling. The schematic diagram in Figure 2.2 illustrates the atrium smoke control design objective to maintain a clear height of 1.8 meters with the inclusion of the mechanical exhaust vents.

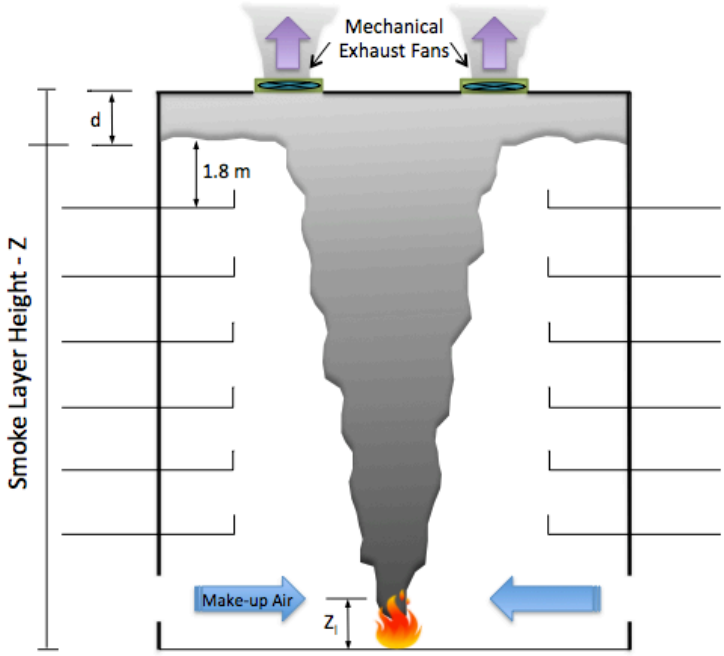

Figure 2.2 Atrium Smoke Control Design

2.4.3 Algebraic Equations for Mechanical Exhaust System

The following equations address the calculations for a mechanical exhaust system for a simplified axisymmetric plume as outlined in NFPA 92. The calculations include the volumetric exhaust, and also the number of inlets, and separation between inlets. These equations represent a sufficiently buoyant plume, where the temperature rise of the plume exceeds at least 4°C above ambient [2]. The intent of the smoke management system is to exhaust smoke at a rate that will arrest the smoke layer descent. In order to arrest the layer at the designed design height, the volumetric exhaust rate of the smoke exhaust must equal the volumetric rate of the smoke supplied to the layer at the designated design height.

Mean Flame Height

The mean flame height, also referred to as the limiting elevation, is defined by averaging the visible flame height, specifically where flames are present 50% of the time [13]. The following simplified equations for an axisymmetric plume, provided in NFPA 92, do not include the distance to the virtual origin z_o. NFPA 92 defines the limiting elevation (Z_l) of an axisymmetric plume in Equation 2.2

$$z_l = 0.166\dot{Q}_c^{2/5} \tag{2.2}$$

$\dot{Q}_c$ = convective portion of the heat release rate (kW)

z_l= limiting elevation (m)

The rate of smoke production is a key consideration in the design of atrium smoke exhaust systems. The convective portion ($\dot{Q}_c$) of the heat release rate affects the rate of smoke production. The convective portion of the heat release rate can be calculated by Equation 2.3.

$$\dot{Q}_c = \chi_c \dot{Q} \qquad (2.3)$$

$\dot{Q}_c$ = Convective Portion of the heat release rate (kW)

$\dot{Q}$ = heat release rate of fire (kW)

χ_c = convective fraction of heat release rate, dimensionless

The convective fraction of heat release rate (χ_c) can vary from 0.4 to 0.9 depending on fire size and fuel type [2].

Mass Flow Rate of Axisymmetric Plume

The volumetric rate of the smoke plume can be approximated from the empirical correlations for the mass entrainment rate of the plume. The mass flow rate of an axisymmetric plume is related as a function of heat release rate ($\dot{Q}_c$) and elevation (z). Numerous investigators such as Zukoski, Heskestad, and McCaffrey carried out experiments to collect data on the entrainment rate of a plume.

NFPA 92 outlines the following approach based on the equation for mass entrainment rate developed by Heskestad. The method utilizes the concept of conservation of mass and energy in order to approximate the volumetric exhaust rate at an intended height.

The conservation equations simplify the method to assume the mass flow rate into the smoke layer is only from the fire plume, and the only mass flow out of the plume is from the exhaust system. It is assumed this transfer of flow is at equilibrium and the heat transfer between the smoke layer and the surroundings has reached steady state. It is intended that the exhaust is removing only smoke from the smoke layer [2]. The system therefore stabilizes the smoke layer height when the vertical mass flow rate in axisymmetric plume at the intended height ($\dot{m}_p$) is equal to the mass flow rate required to exhaust the smoke ($\dot{m}_e$).

The mass flow rate of the plume and temperature and density of the smoke layer are correlated as follows. The simplified axisymmetric mass flow rate is shown in Equation 2.4 or 2.5 with the dependence on the limiting elevation value.

$$\dot{m}_p = 0.071\dot{Q}_c^{\frac{1}{3}}z^{\frac{5}{3}} + 0.0018\dot{Q}_c \qquad z \geq z_l \qquad (2.4)$$

$$\dot{m}_p = 0.032\dot{Q}_c^{\frac{1}{3}}z \qquad z \leq z_l \qquad (2.5)$$

Smoke Layer Temperature

The temperature of the upper layer is then estimated using Equation 2.6.

$$T_s = T_o + \frac{K\dot{Q}_c}{\dot{m}_p c_p} \quad (2.6)$$

c_p= specific heat of plume gases (1.0 kJ/kgK)

$\dot{m}_p$ = vertical mass flow rate in axisymmetric plume at smoke elevation (kg/s)

T_o= ambient temperature (°C)

T_s = average smoke layer temperature (°C)

$\dot{Q}_c$= convective portion of the heat release rate (kW)

K = fraction of convective heat release contained in smoke layer, dimensionless

NFPA 92 suggests a value of K equal to 1. This value produces the greatest temperature and hence the greatest volume of smoke to provide a conservative estimate of hazard [4].

Density of Smoke

The density of smoke is then estimated from the temperature expression, in Equation 2.7.

$$\rho = \rho_o + \frac{T_o}{T_s} \quad (2.7)$$

T_o= ambient temperature (K)

T_s = average smoke layer temperature (K)

ρ = density of smoke (kg/m^3)

ρ_o = density of air at ambient (kg/m^3)

Volumetric Exhaust Rate Required

The volumetric flow rate is then determined by dividing the mass flow rate of the axisymmetric plume at elevation z, by the density of the smoke. The volumetric flow rate at z is equal to the required volumetric exhaust rate of the system to maintain the smoke layer at z.

$$\dot{V} = \frac{\dot{m}_p}{\rho} \tag{2.8}$$

$\dot{V}$ = volumetric flow rate of smoke exhaust (m^3/s)

$\dot{m}_p$= vertical mass flow rate in axisymmetric plume at smoke elevation (kg/s)

ρ = density of smoke (kg/m^3)

Maximum Volumetric Exhaust Rate per Inlet Without Plugholing

In order to properly design the size and location of the volumetric exhaust inlets, the physical phenomenon of plugholing must be considered. Plugholing refers to the circumstance where ambient air from below the smoke layer is pulled through the smoke layer due to the high exhaust rate of the inlet [2]. The number of inlets is chosen based on the maximum volumetric flow rate for one inlet to avoid plugholing.

To calculate the maximum volumetric flow rate to avoid plugholing the absolute temperature of the smoke layer is determined using Equation 2.6. However, NFPA 92 suggests a K value of 0.5 to estimate a low average smoke layer temperature therefore maximizing the possible fan size.

The maximum volumetric flow rate that can be exhausted by a single exhaust inlet without plugholing can be calculated by Equation 2.9. The equation can be applied for round or rectangular inlets. The equation stems from the research conducted by Spratt and Heselden at the Fire Research Station in the UK [24].

$$\dot{V}_{max} = 4.16\gamma d^{\frac{5}{2}} \left(\frac{T_s - T_o}{T_o}\right)^{\frac{1}{2}} \quad (2.9)$$

γ = exhaust location factor, dimensionless

d = depth of smoke layer below lowest point of exhaust inlet (m)

T_o= absolute ambient temperature (K)

T_s= absolute temperature of smoke layer (K)

$\dot{V}_{max}$ = maximum volumetric flow rate without plugholing at T_s (m^3/s)

For ceiling mounted inlets, the exhaust location factor may vary as one or one-half. The following criterion depends on the inlets diameter (D_i) and distance from the wall (L) [2].

$L > 2D_i, \gamma = 1$

$L \leq 2D_i, \gamma = \frac{1}{2}$

To determine the number of fans required for the system to avoid plugholing, the volumetric flow rate required ($\dot{V}$) is divided by the maximum volumetric flow rate per fan ($\dot{V}_{max}$).

Separation of Vents

The separation distance of the vents are strategic, in order to avoid two vent acting as one inlet with respect to plugholing. The minimum separation distance with respect to plugholing is shown in Equation 2.10 [2].

$$S_{min} = .9(V_e)^{\frac{1}{2}} \quad (2.10)$$

S_{min} = minimum edge to edge separation between inlets (m)

$\dot{V}_e$ = volumetric flow rate of one exhaust inlet (m^3/s)

2.4.4 Makeup Air in Smoke Management System

For smoke management systems that utilize mechanical exhaust to remove smoke, makeup air must be provided to ensure the exhaust fans are able to move the design air quantities. As the exhaust removes air from the compartment, additional air must

enter the room to maintain stable pressures and door-opening force requirements. NFPA 92 permits makeup air to enter through large openings such as doors, open windows, or mechanical vents. As previously discussed the amount of makeup air is not mandated by the code, however, it is suggested that makeup air be designed at 85 percent to 95 percent of the exhaust. The introduction of makeup air into the compartment is vital in order to reduce disturbances to the fire plume and smoke layer interface [3].

2.4.4.1 Makeup Air Velocity

The maximum value of makeup air permitted by the NFPA 92 standard is 1.02 m/s. This velocity refers to the velocity subject to strike the design flame or plume. The primary reason for this restriction is to prevent plume disturbance or deflection, which could increase air entrainment and produce higher smoke volume [2]. The smoke management system design is contingent on the smoke plume moving upward and forming a layer at the ceiling. Plume deflection will create smoke control failure because the predictions used during design become invalid. The velocity restriction is also established to prevent potential fire growth and spread due to airflow and wind effects [2].

2.4.4.2 Makeup Air Past Research

Several research studies have been completed through experimental testing and CFD studies in order to provide evidence on the adverse effects of makeup air. Heskestad [19] and Mudan and Croce [18] suggest that velocities that exceed 1 m/s alter the smoke plume and increase in the amount of air entrained into the plume. NFPA 92 requires the supply points for the makeup air shall be located beneath the smoke layer interface. There is little additional guidance in the codes and standards on the location or arrangement of the makeup air supply vents.

In 2004, Souza and Milke present an FDS version 3.0 study to model both symmetric and asymmetric intake vent configurations in a simple 30 m atrium, with a 3 MW design fire centrally located within the atrium [20]. The study includes makeup air vents centrally located on the bottom of each wall. The velocity through the vents included 0.5 m/s, 1.0 m/s, 1.5 m/s, and 3.0 m/s. The study concludes that for symmetric intake vent positioning, velocities less than 2 m/s do not negatively affect the smoke layer thickness. However, for asymmetric intake vent configurations, velocities exceeding 2 m/s result in impingement of hot gases on the opposite lower atrium wall [20].

2.4.5 Relevant Past Studies and Verification in FDS 6.0

2.4.5.1 Carleton University Study

In 2007 Professor George Hadjisophocleous of Carleton University investigated the topic of makeup air in atria and published the final report titled “Maximum Velocity of Makeup Air for Smoke Management Systems in Atria and Other Large Spaces” [15]. This study was initiated by ASHRAE and was undertaken by Carleton University.

The study uses FDS to model the conditions of different atrium sizes (ranging from 10 – 60 m) makeup air velocities (ranging from 0.5 m/s - 1.5 m/s), and fire sizes (ranging from 1 MW – 5 MW) [15].

The results from this study indicated [15]:

- the least disruption to the plume occurs when the makeup air is injected at ground level elevation
- that for all fire sizes and atrium heights the fire plume and the interface height are affected by the minimum incoming makeup air of 1 m/s
- the impact of makeup air velocity is more pronounced when dealing with atria of 20 m tall and less and for larger atria the impact on the interface height decreases
- the imposed 1 m/s velocity limit is not too restrictive

2.4.5.2 University of Maryland Study

Also in 2007, University of Maryland student, Steve Kerber, advised by Dr. James Milke, completed a report titled "Using FDS to Simulate Smoke Layer Interface Height in a Simple Atrium"[16]. The study examines the possible effects of various makeup air supply arrangements and velocities in an atrium smoke management system.

In this study FDS is used to simulate makeup air introduced through side vertical walls of an atrium at different velocities (ranging from 0 to 3.0 m/s) and under different supply configurations (i.e., different horizontal positioning with respect to the fire source and different vertical elevations with respect to flame height). A total of ten simulations are reported with a 30.5 m cubical domain and a fire source simulating a stack of pallets with an approximate peak heat release rate of 5 MW.

The results from this study indicated [16]:

- Makeup air should be supplied to the fire symmetrically for the best chance of not disturbing the fire plume and suggests makeup air supply velocities should be diffused such that little to no velocity effects reach the fire
- Disturbing the fire and smoke plume results in a significant increase in the smoke production rate, as evidenced by a deeper smoke layer.
- High makeup air flow velocities may result in smoke layer elevations that are lower than those intended in the design of the smoke venting system

2.4.5.3 Verification in FDS 6.0

As included in the project scope, before original research is developed, the following Carleton University and University of Maryland studies are re-investigated. Example simulations from both studies are closely re-created to confirm the results of the studies in FDS version 6.0. Chapter 4 of this report presents the re-creations of the simulations and the results obtained.

2.5 Flame Tilt

Atrium smoke control systems may also be designed to limit potential wind effects. Increased wind conditions can disturb a flame. Under wind conditions the flame can exhibit a tilt, creating a disturbance or tilt in the fire plume as well. Multiple investigators have studied the flame tilt angle under wind conditions. The schematic diagram of a potential flame tilt is shown in Figure 2.3 where a crosswind at a velocity (u_∞) moves toward the flame from one side of the fire. The pool fire flame follows a curved trajectory and the angle (θ) approximates the trajectory [18].

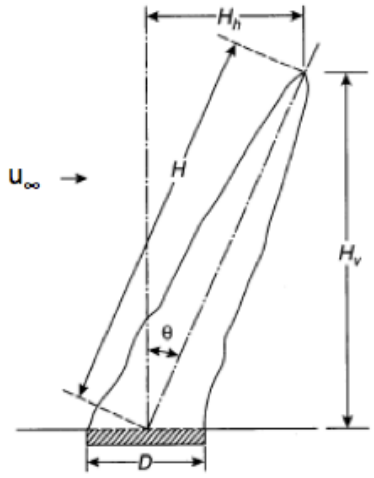

Figure 2.3: Flame inclinations due to wind [18]

In order to calculate the curved trajectory angle, Thomas [17] developed the correlation presented as Equation 2.11. The correlation is based on data from fires involving two-dimensional wood cribs.

$$\cos(\theta) = 0.7\left[\frac{u_w}{\left(g\dot{m}''D/\rho_{air}\right)^{1/3}}\right]^{-0.49} \tag{2.11}$$

u_w = wind velocity

g = acceleration due to gravity (m/s^2)

$\dot{m}''$ = mass flow rate (kg/m^2-s)

D = Diameter of fuel (m)

ρ_{air} = density of air (kg/m^3)

The vertical and horizontal flame length components can also be determined from the flame tilt angle.

2.6 Heat Flux and Separation Distance of Fuel Packages

2.6.1 Heat Flux Defined

Heat flux, refers to the rate of energy transfer between different surface mediums per unit area. Heat flux is an essential variable in fire growth as it influences ignition, flame spread, and burning rate. Heat transfer through gaseous mediums includes both radiative and convective forms of energy transfer. The general net fire heat flux condition is defined by Equation 2.12[10].

$$\dot{q}'' = \dot{q}''_{f,c} + \dot{q}''_{f,r} + \dot{q}''_{e} - \epsilon\sigma T_s{}^4 \qquad (2.12)$$

$\dot{q}''_{f,c}$ = flame convective heat flux $\left(\frac{kW}{m^2}\right)$

$\dot{q}''_{f,r}$ = flame radiative heat flux $\left(\frac{kW}{m^2}\right)$

$\dot{q}''_{e}$ = external environmental radiative heat flux $\left(\frac{kW}{m^2}\right)$

$\epsilon\sigma T_s{}^4$ = surface radiative heat loss $\left(\frac{kW}{m^2}\right)$

The surface radiative heat loss refers to the losses at the target's surface, where ϵ is the emissivity, σ is the Stefan-Boltzmann constant, and T_s is the surface temperature of the target.

2.6.2 Heat Flux Gauge in FDS

Equation 2.12 defines the multiple components of total heat flux including both radiant and convective heat transfer. However, the radiant heat flux components are isolated as the primary consideration when defining the effects in regards to separation distance. The convective proportion of the heat flux is primarily transferred through the plume's hot and dense smoke, which is transferred upward due to natural buoyancy. The convective component of the heat flux does not significantly impact the space lateral to the flame, and is considered negligible. The net radiative heat flux, $\dot{q}''_{r,net}$, is reduced to Equation 2.13.

$$\dot{q}''_{r,net} = \dot{q}''_{f,r} + \dot{q}''_{e} - \epsilon\sigma T_s^{\,4} \tag{2.13}$$

In FDS, heat flux gauges are used to evaluate conditions at a specific location away from the fire. The data from a gauge can be used to evaluate the threat of ignition to other sources due to thermal radiation. The measured heat rate is divided by the surface area of the sensor to determine the heat rate per unit area, defined as the heat flux. To isolate only the radiative effects of the total heat flux, the sensors utilized in FDS are defined as radiative heat flux gauges. The gauges only consider the net

radiative heat flux, defined as the radiative heat flux subtracted by the surface gauges radiative heat loss, as shown in Equation 2.13.

2.6.3 Point Source Model

NFPA 92 requires the evaluation of heat flux in regards to separation distance between fuel packages in a large space. The separation zones of fuel packages must be assessed in order to justify the fuel arrangement. In order to determine the separation of fuel packages, the point source model approximation in Equation 2.15 is utilized [13]. The point source model is used to predict the thermal radiation from flames by defining the fuel source as a point located at the center of the real flame. The approximation is most accurate provided that the distance from the center of the flame is greater than twice the diameter of the fire. The separation distance in reference to the location of the fuel package is defined in Figure 2.4. The radiant heat release of the fire depends on the material burned and the diameter of the fire, however, a radiative fraction between 0.2-0.3 is common. The radiant heat release rate can be determined using Equation 2.14.

$$\dot{Q}_r = \chi_r \dot{Q} \tag{2.14}$$

$$R = \left(\frac{\dot{Q}_r \cos(\theta)}{4\pi \dot{q}_r''}\right)^{1/2} \tag{2.15}$$

R = separation distance from target to center of fuel package (m)

θ = angle between the normal to the target and the line of sight from the target to the point source location

$\dot{Q}_r$= radiative portion of the heat release rate of the fire (kW)

$\dot{q}''_{r,net}$= radiant flux required for piloted ignition (kW/m^2)

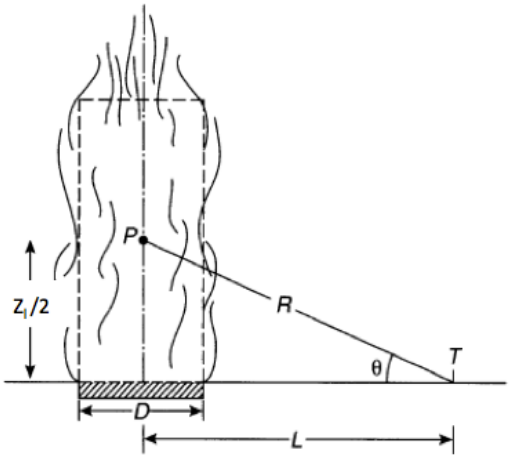

Figure 2.4: Nomenclature for use with point source model
(Modified Image from Belyer [13])

The distance from the point source location to the target is given by the Pythagorean theorem. In reference to Figure 2.4, z_l is defined as the height of the flame, and $z_l/2$ is the height of the equivalent point source, L is the distance from the center of the pool to the target, and D is the diameter of the pool fire.

NFPA 92 suggests an average incident heat flux value of 10 kW/m^2 for piloted ignition. This value was defined by Nelson for fuels that are "easily ignited"[12]. The value is typically defined for thin materials such as curtains or draperies, which would

be considered a worst-case scenario. In Equation 2.15, the separation distance, R, will be calculated by defining the radiant heat flux value, $\dot{q}''_{r,net}$, equal to 10 kW/ m^2.

As suggested by Modak, the point source model provides 90% accuracy if the separation distance, R, is greater than the twice the burner diameter, D. For separation distances between one or two times the burner diameter, the accuracy is estimated closer to 80% [11].

Chapter 3

Description of Model

3.1 CFD Modeling

Computational Fluid Dynamics (CFD) is a form of fluid mechanics that utilizes numerical methods and algorithms to solve fluid flows problems. CFD models are sophisticated tools that rely on computers to perform the calculations required to simulate the interaction of liquids and gases [9]. CFD allows for reliable and efficient simulation of fluid flow and heat transfer.

CFD models are utilized in the Fire Protection Engineering field. The tool applies the fundamental laws of physics to offer a versatile approach to solving the challenges of fire dynamics.

3.1.1 FDS Modeling

Fire Dynamics Simulator (FDS) is a CFD software program developed by the Building and Fire Research Laboratory of NIST (National Institute of Standards and Technology). This fire-modeling tool approximates heat transfer physics, flow physics, and combustion process. NIST explains that the software solves numerically a form of the Navier-Stokes equations appropriate for low-speed, thermally-driven

flow, with an emphasis on smoke and heat transport from fires. FDS is a Fortran program that computes a numerical solution to the governing equation by reading the input parameters, and generating user-specific output data. Smokeview is a code developed by BFRL/NIST as a plotting and visualization tool to display results from FDS [7]. Smokeview is a visualization program that can read the output generated by FDS to display animations.

FDS is used to model the physical phenomena of fire to assist in determining solutions to practical fire problems such as pyrolysis, flame spread, fire growth, radiative and convective heat transfer, mixing of heat and combustion products, and most recently sprinkler sprays and suppression by water [8].

As described by the FDS Validation Guide, the basic governing equations of mass, momentum and energy are approximated with a finite differences method (FDM) and the thermal radiation solver is computed using a finite volume technique (FVT). The solutions of the equations are then updated in time on a three-dimensional rectilinear grid [8]. In fluid flow it is essential to define the method of turbulent flow. FDS uses the Large Eddy Simulation (LES) model. In this model turbulence in the flow is averaged at scales smaller than the mesh size. Therefore, the LES model assumes the numerical mesh is fine enough to allow the formation of eddies responsible for mixing. FDS requires an appropriate mesh to obtain accurate results, and can therefore be demanding computationally.

FDS is constantly validated against various physical experiments and empirical correlations. The FDS Technical Reference Guide describes the experimental models and its validity to the FDS assumptions governed by the conservation equations. The FDS user guide and technical reference guide are constantly referenced throughout the following FDS study.

3.2 Design Diagnostic Tools

In order to evaluate FDS results, diagnostic tools must be developed for analysis. The following diagnostic tools developed are used to establish the smoke layer height within the compartment and the mass flow rate of the plume. Both diagnostics are used as comparative tools to relate the results to the changing velocity variables. The diagnostic tools are also used to establish an optimum grid resolution further detailed in Section 3.3.1, and applied to obtain results for the simulations further described in Section 3.4.

3.2.1 Smoke Layer Height Diagnostic Tool

NFPA 92 outlines an approach to define the smoke layer interface and the first indication of smoke from the use of CFD models [3]. This approach specifically defined by Cooper et al. [5]; Madrzykowski and Vettori [6], uses linear interpolation of the temperature data at the height measurements available in the CFD model. The temperature data is used to define the smoke layer interface and first indication of

smoke by locating the elevation at which the temperature data reaches the defined layer temperatures. NFPA defines the relative temperature value for both layer types in Equation 3.1.

$$T_n = C_n(T_{max} - T_b) + T_b \quad (3.1)$$

T_{max} = temperature in the smoke layer (°C)

T_n = temperature at the interface height (°C)

T_b = temperature in the cold lower layer (°C)

C_n = 0.9 - 0.8 = interpolation constant for the smoke layer interface, dimensionless

C_n = 0.2 - 0.1 = interpolation constant for the first indication of smoke, dimensionless

The maximum temperature in the layer is calculated using Equation 2.6. For the present study a convective fraction of heat release rate (χ_c) is defined as 0.65.

The Smoke Layer Height Diagnostic Tool correlates the relative T_n value for the smoke layer interface height, and first indication of smoke temperature as defined by Equation 3.1 and applies it to the temperature data retrieved by FDS. The tool records the time the temperature of the layer reaches the reference temperature T_n.

Due to the assumptions and approximations made by this diagnostic tool, a margin of error must be considered. The FDS temperature gauges are placed at 0.4 m intervals

in elevation. FDS data is collected at these specific heights, so the diagnostic must consider this constraint. Consequently, the uncertainty of the smoke layer position is $\pm$ 0.8 m.

Temperature gauges are placed 2 m away from the center of each wall as shown in Figure 3.1. The gauges are placed at 0.2 m and 0.4 m intervals in height at each location. The temperature values are averaged over each elevation to provide strong statistical significance.

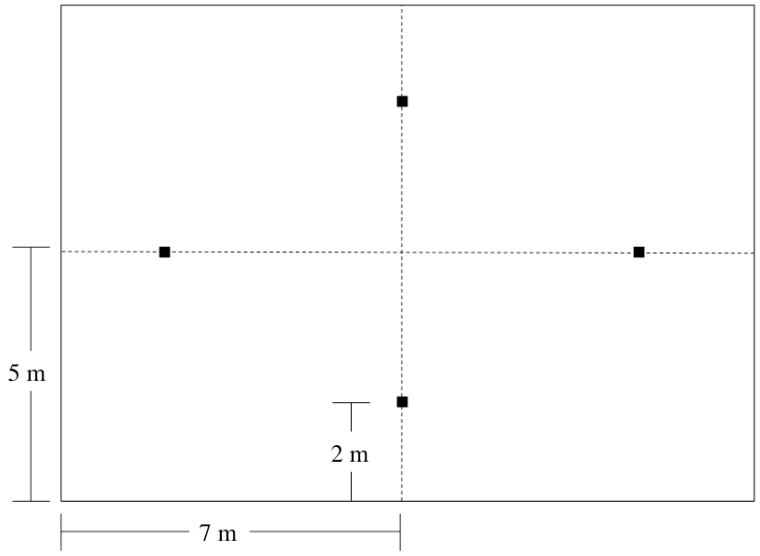

Figure 3.1: Plan view of Temperature Gauge Location in 10 m compartment

In Equation 2.6, the K value is typically defined between 0.5 - 1. A K value of 1 estimates conservative results and is modeled for adiabatic systems. As the boundary conditions for the model are defined as gypsum plaster, the system will not show adiabatic conditions. The appropriate K value is estimated based on the smoke layer temperature conditions reported by FDS for a 1 MW fire in the 10 m compartment.

The average temperature found at each elevation is graphed with respect to time is shown in Figure 3.2. Also, the temperature Smokeview image is shown in Figure 3.3.

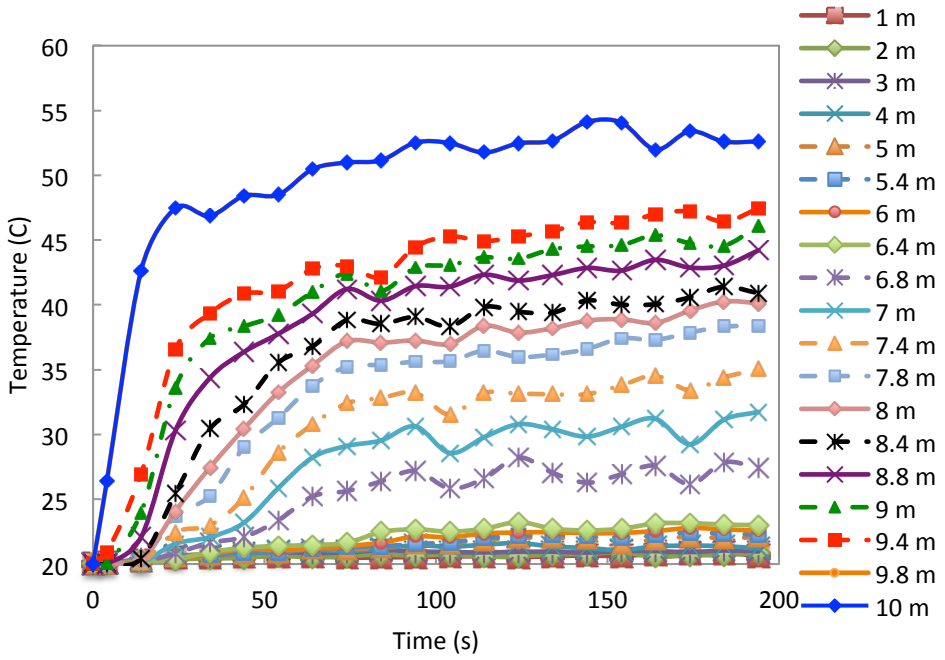

Figure 3.2: Average temperatures recorded by FDS at each elevation for 1 MW fire

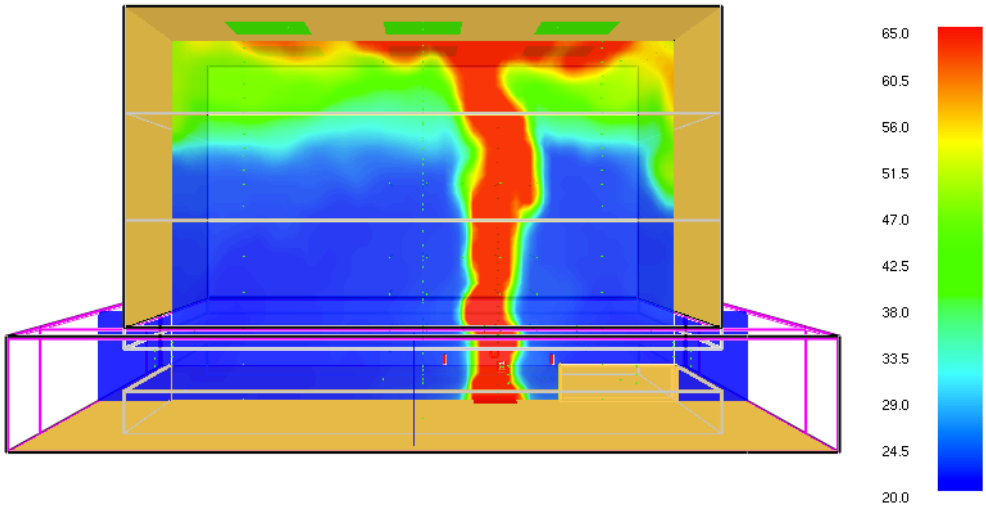

Figure 3.3: Temperature (°C) Smokeview image of 1 MW fire at 150 seconds

The temperature increases significantly in the upper portion of the compartment in the first 50 seconds due to the formation of the smoke layer. The temperature is relatively

constant during the remaining time of the simulation. It is clear from the figure that the distribution of temperature in the smoke layer features a certain level of vertical stratification with the highest temperatures being found at the ceiling. The smoke layer height is designed for an 8 m clear height. The temperature values reported by FDS in the upper layer range from about 35 to 50 °C. In this example, the smoke layer diagnostic appropriately defines the layer at 8 m when a K value of 0.7 is defined. Therefore, a K value of 0.7 estimates the conditions within the layer given the compartment boundary conditions and is set for all 10 m compartment calculations in order to develop consistent comparisons.

As NFPA 92 defines a range of values for C_n, the midrange value is utilized. A C_n of 0.15 is used to define the first indication of smoke and a C_n value of 0.85 is used to define the smoke layer interface. An example of the smoke layer height tool is shown in Figure 3.4, by plotting the smoke layer height vs. the simulation run time. The example includes a 1 MW fire in a 10 m high compartment. The layer is designed to stabilize at 8 meters. The temperature at each elevation is averaged in steady state conditions and graphed vs. elevation in Figure 3.4. Using this approach explained by Equation 3.1 the first indication of smoke value is 23.2 °C and the smoke layer interface is approximately 38.3 °C. The results from Figure 3.4 suggest the first indication of smoke at approximately 6.5 m and the smoke layer interface at approximately 7.9 m, respectively.

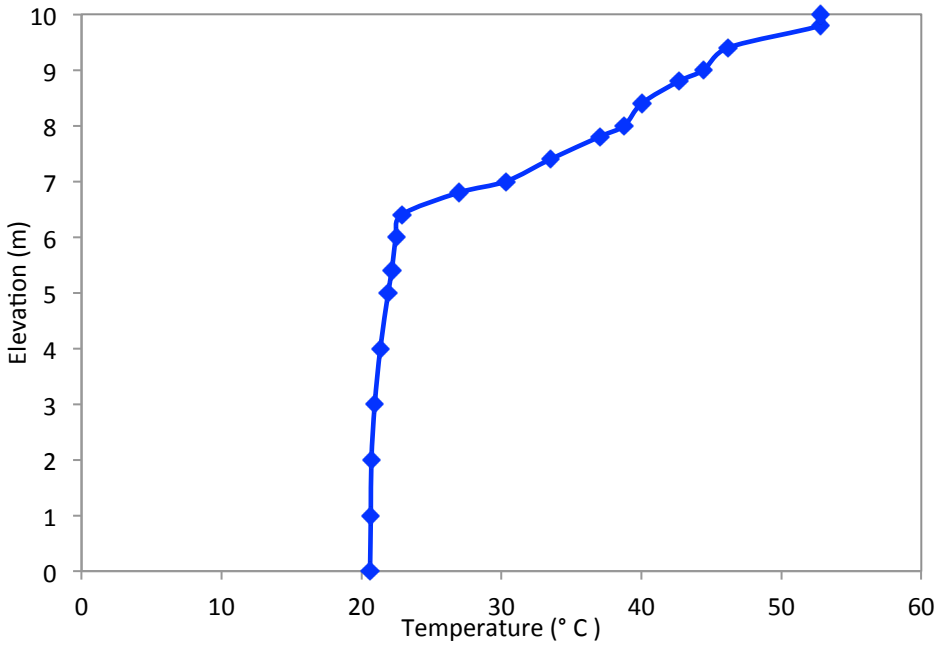

Figure 3.4: Temperature average in steady state conditions for 1 MW fire

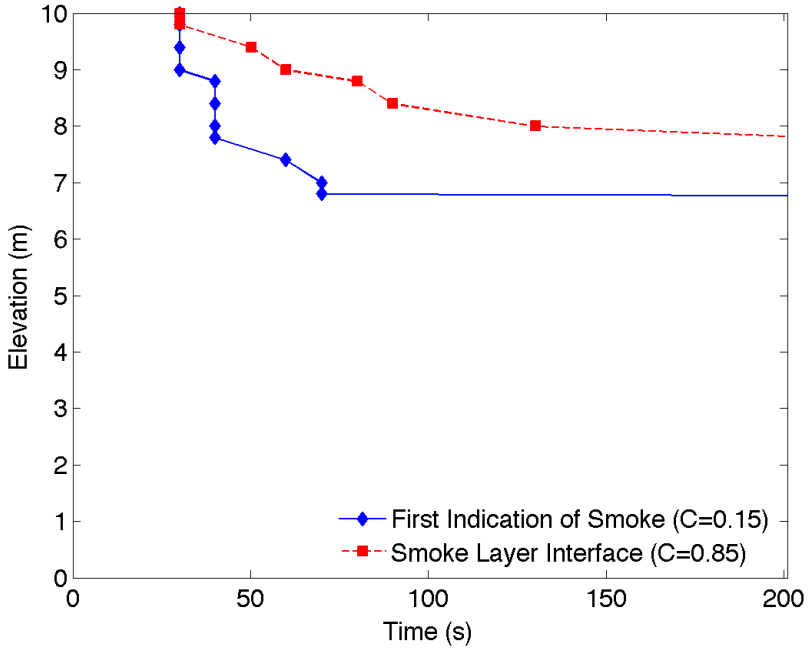

Figure 3.5: Smoke Layer Height Diagnostic Tool for 1 MW fire

The results from Figure 3.5 indicate that the first indication of smoke stabilizes at about 6.8 meters, while the smoke layer interface stabilizes at approximately 7.8

meters. The smoke layer height tool, in Figure 3.5 confirms the approximations by Figure 3.4 over the simulation time.

The intent of the study is to examine the smoke layer height, which is considered the smoke layer interface in the design tool. Therefore, a C_n value of 0.85 is used throughout the study to indicate the smoke layer height.

3.2.2 Mass Flow Diagnostic Tool

In order to examine the effect of makeup air on the fire plume, a mass flow rate diagnostic is created to assess the changes in the plume dynamics. Increased airflow at low elevations is expected to increase the mixing of ambient air and the products of combustion, resulting in an increase in the volume of smoke produced. The purpose of the mass flow diagnostic tool is to track this increased rate of smoke production by observing the mass flow rate of the plume through the FDS mass flow rate tool.

In order to properly confirm the FDS results, a simulation is compared to results from the correlation for the mass flow rate of the plume provided in the NFPA 92, presented here as equation 3.2.

$$\dot{m}_p = 0.071\dot{Q}_c^{\frac{1}{3}}z^{\frac{5}{3}} + 0.0018\dot{Q}_c \qquad (3.2)$$

$\dot{m}_p$ = mass flow in axisymmetric plume at height z (kg/s)

$\dot{Q}_c$ = convective portion of the heat release rate (kW)

z = elevation (m)

3.2.2.1 Mass Flow Rate correlation assessment

The mass flow diagnostic tool in FDS defines the total mass flow rate moving through an area. In order to develop a mass flow rate diagnostic for the study, results from use of the FDS mass flow rate device are compared to those from the NFPA 92 correlation. In order to isolate the mass flow rate of the plume without influence from other variables, the FDS simulation to develop the diagnostic is designed as a completely open system, i.e. the compartment did not include any walls or obstructions.

The simulation created includes a centrally located 1 MW fire, with 1 x 1 m propane burner. The compartment is 10 m x 10 m x 10 m. In order to compare diagnostic approaches the area over which the mass flow rate in FDS is taken in two ways. The first approach defines the mass flow rate device over a consistent area 8 m x 8 m at every 0.3 m elevation. The second approach defines the mass flow rate device over areas that increase with every elevation. This approach defines the square area diameter at each 0.3 m elevation equal to the diameter of the plume estimated by Equation 3.3 [2]. A plume diameter constant K_d is equal to 0.5, which estimates conservative results.

$$d_p = K_d z \tag{3.3}$$

d_p= plume diameter (m)

z = distance above base of fire (m)

K_d = diameter constant

The results are averaged in time once steady state conditions are reached. The FDS results for the two mass flow rate diagnostic approaches are compared with the NFPA 92 correlation in Figure 3.6.

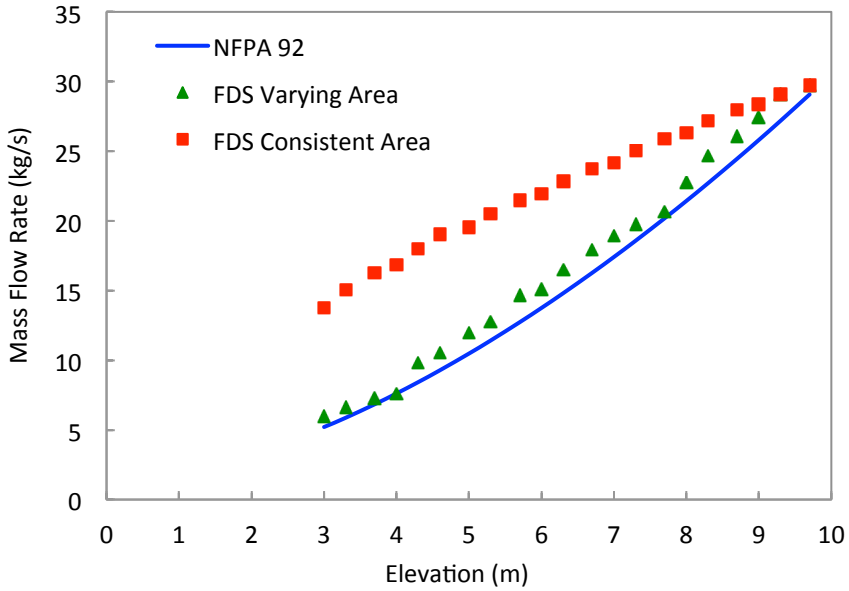

Figure 3.6: Mass Flow Rate method comparisons, 1 MW fire

The two approaches compare to the NFPA 92 correlation differently. The FDS results varying over each elevation according to plume diameter show a close correlation to

the NFPA 92 expression. However, the FDS approach using a consistent area over which the mass flow rate is recorded shows almost two times the mass flow rates at elevations directly above the flame height. The NFPA 92 expression relates elevation with a 5/3 power, while the FDS result shows a linear trend

In order to confirm that the FDS approach using consistent area produces mass flow rate results exceedingly high at low elevations, the same approach is taken with a 5 MW fire. The compartment size is 20 m x 20 m x 20 m. The fire is located centrally within the compartment and has a square propane burner with a diameter of 2 m. The simulation is run to compute the mass flow rate through the entire compartment, beginning at the limiting elevation of the flame. The FDS mass flow rate device is used to capture the mass flow rate at every 0.3 meters in elevation. The mass flow rate is analyzed over an 18 m x 18 m area, which is a consistent 324 m^2 over every elevation. The results are averaged over time once steady state conditions are reached. The mass flow rate vs. elevation is plotted against the NFPA 92 correlation shown in Figure 3.7.

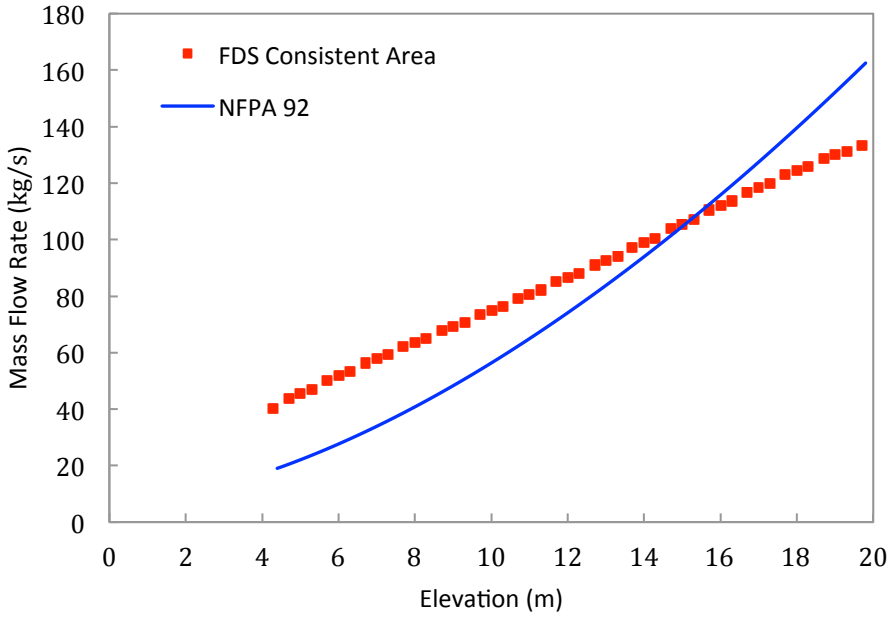

Figure 3.7: Mass Flow Rate method comparisons, 5 MW fire

The FDS results from this study also show a large discrepancy compared with the NFPA 92 correlation. At lower elevations the mass flow rate of the 5 MW FDS simulation is about double the mass flow rate calculated by the correlation. In upper elevations the FDS results show a mass flow rate lower than the NFPA 92 correlation. The FDS results show a linear trend as opposed to an exponential trend reflected in the NFPA 92 correlation.

The discrepancy between the FDS consistent area method compared to the NFPA 92 expression is most likely related to the movement of the makeup air within the compartment. The natural movement of air entrainment towards the fire begins at distances away from the fire source. As the fire source constantly requires ambient air mixing, air is constantly moving towards the fire. In addition, ambient air is

constantly entrained into the smoke plume. A Smokeview image of W-velocity is shown in Figure 3.8 and 3.9, for both a 1 MW fire in a 10 m tall compartment, and a 5 MW fire in a 20 m tall compartment respectively. The w-velocity isolates the w-component of the overall velocity, which is the motion in the upward z-direction.

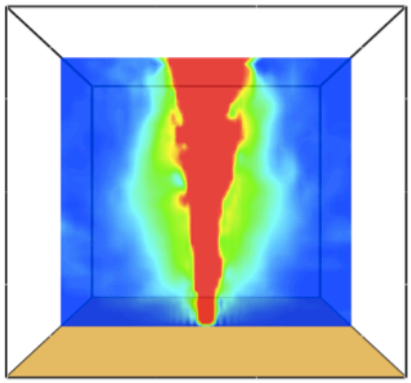

Figure 3.8: 1 MW Fire,
10 m compartment

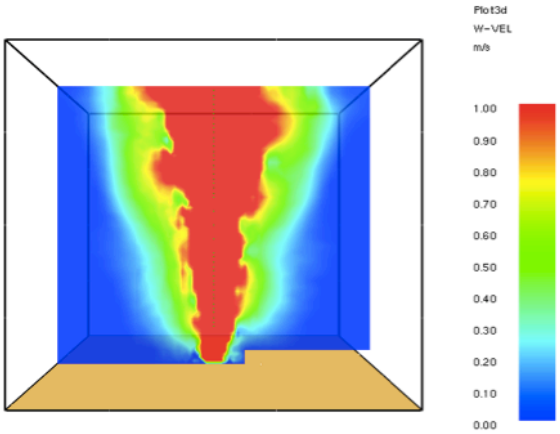

Figure 3.9: 5 MW Fire,
20 m compartment

In Figure 3.8, air is moving with an upward trajectory at distances further from the fire. The magnitude of the upward velocity is small as shown by the 0 – 1 m/s scale, however, velocity is still present. The FDS consistent area method to track mass flow rate includes these small velocities. This method, therefore, over predicts mass flow rates at low elevations, when the plume diameter is expected to be small.

While the FDS results of mass flow rate taken over varying area closely compares to the NFPA 92 correlation, this method cannot be used. The purpose of this study is to increase the makeup airflow to velocities exceeding 1 m/s to analyze the increased smoke production. Therefore, it is expected the flame will tilt and the fire plume will become disturbed. The area over which the mass flow rate is taken cannot be

predefined over a central location as it will not properly account for the anticipated tilt and disturbance. The most effective approach in order to account for tilt and disturbance is to define a consistent area over the entire compartment. However, the FDS results do not confirm a consistent agreement with the NFPA 92 correlation. Therefore, a modification to the FDS source code is created.

3.2.2.2 FDS Source Code Modification

As discussed, the mass flow rate at lower elevations exceeds the NFPA 92 correlation due to makeup air entrainment from the compartment. In order to isolate the movement of smoke for this diagnostic, a modification to the FDS source code is written. The modification removes the unwanted mass flow activity from the ambient air by isolating the plume region through the presence carbon dioxide. The plume is defined as the region with measurable amounts of carbon dioxide (CO_2) (i.e. above a user-defined threshold). In this manner, the FDS mass flow rate device tracks only the movement of mass if it contains the pre-defined threshold of CO_2. This method is examined with the 5 MW fire simulation explained previously. The results for the new FDS modification are compared to the original FDS device (both utilizing the consistent area method) and the NFPA 92 correlation in Figure 3.10.

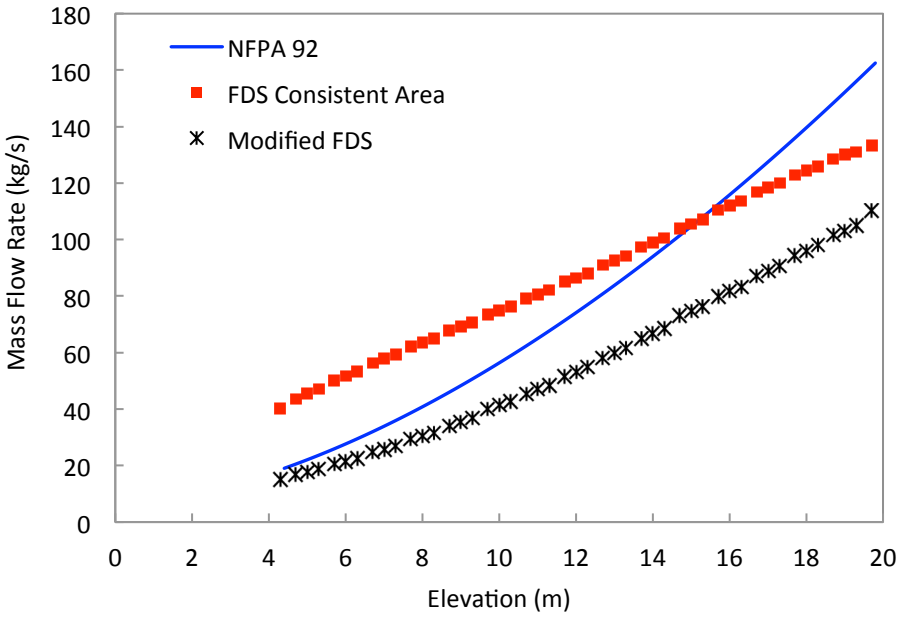

Figure 3.10: Mass Flow Rate method comparisons, 5 MW fire

The modified FDS diagnostic tool shows a closer correlation to the NFPA 92 equation at lower elevations, and underestimated results with increasing elevation. The modified diagnostic shows an exponential increase between 1.2 - 1.3, similar to the NFPA 92 correlation.

It is concluded that when the diagnostic has a varying area centrally lined with the diameter of the plume at each elevation the results compare well with classical engineering correlations. This is not an effective approach. However, the modified tool suitably represents the intent of the diagnostic by isolating the plume to track the movement of mass only in areas with a presence of CO_2. This method is henceforth used as the method to track the mass flow rate of the plume with elevation. The

diagnostic is strictly used as a comparative tool, to examine differences in various simulations with increased makeup air velocities.

3.3 Compartment Design Considerations

In order to determine the optimum FDS results, the configuration of the FDS compartment design is carefully considered. The grid resolution of the configuration must be properly investigated along with additional design factors such as the domain boundary conditions.

3.3.1 Grid Sensitivity Study

A series of simulations were run using three grid cell sizes to determine the optimum grid resolution for subsequent simulations.

A fire centrally located within a 10 m x 10 m x 10 m domain is considered. The fire is a 1 MW propane burner with a 1 m x 1 m burner size. The system is completely open (no walls or obstructions) in order to reduce the possible influence of other variables. The grid resolution study was conducted utilizing the primary diagnostic tools, smoke height, and mass flow rate, outlined in Section 3.2.

The simulations included cell sizes of 0.1 m, 0.2 m and 0.4 m. These values were chosen based on the size of the compartment and fire burner size. The simulation

variables are presented in Table 3.1. The grid layouts for the three simulations are shown in Figures 3.11 – 3.13.

Table 3.1: Sensitivity Study Simulation Variables

Grid Name	Meters	Total Grid Cells (10 x 10 x 10 m compartment)
Fine	0.1	1,000,000
Medium	0.2	125,000
Coarse	0.4	15,625

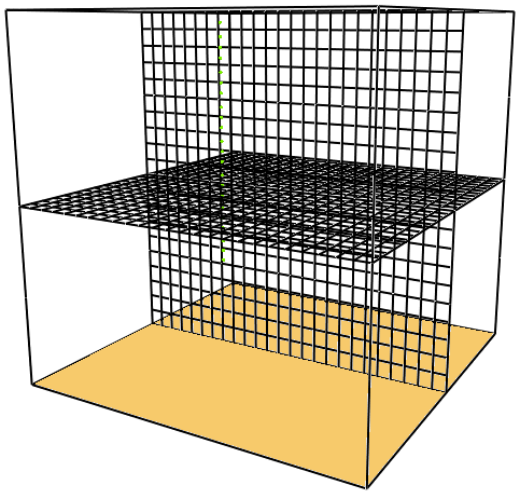

Figure 3.11: Coarse grid: 0.4 x 0.4 x 0.4 m

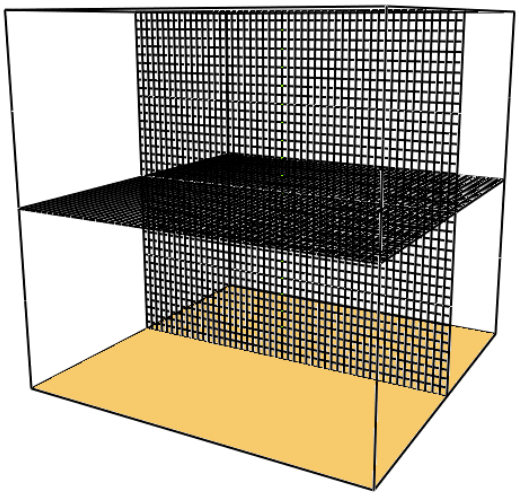

Figure 3.12: Medium grid: 0.2 x 0.2 x 0.2 m

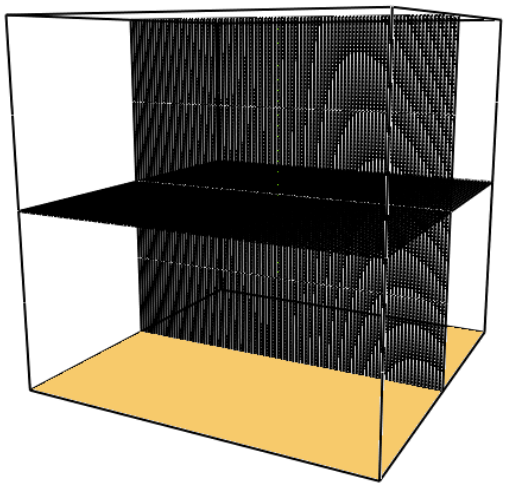

Figure 3.13: Fine grid: 0.1 x 0.1 x 0.1 m

The smoke layer height diagnostic explained in Section 3.2.1 is utilized for the three configurations. The results comparing the smoke layer height for the 0.10 m, 0.20 m, and 0.40 m, grid is shown in Figure 3.14.

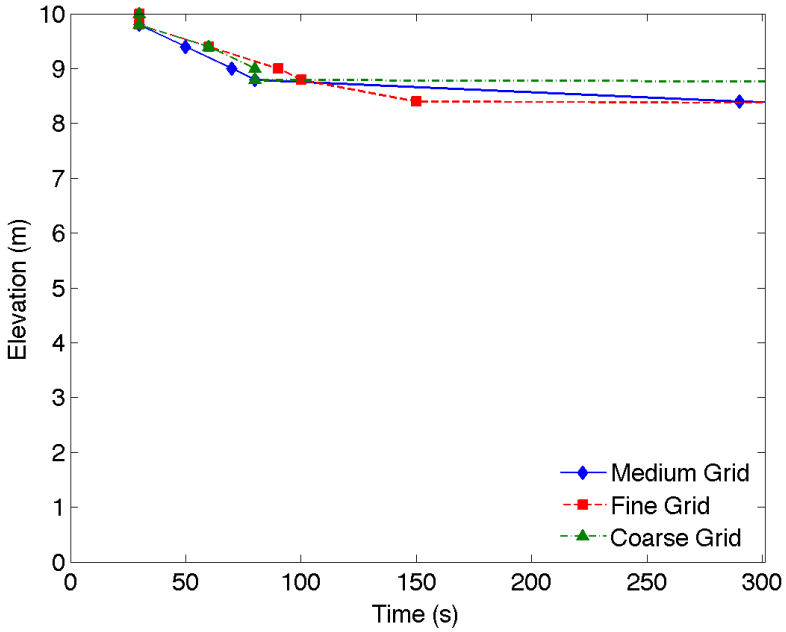

Figure 3.14: Grid Resolution Comparison using Smoke Layer Height Diagnostic

The results indicate that the grid cell size from 0.10 to 0.40 m has very little influence on this smoke layer diagnostic. The data does show a defined layer convergence between the 20 cm and 10 cm grid. However, the discrepancies present on this plot have little significance as they are within the designated $\pm$ 0.8 m error region.

The mass flow rate diagnostic is also utilized to compare the grid sensitivity. The data presented in Figure 3.15 compares the three simulations.

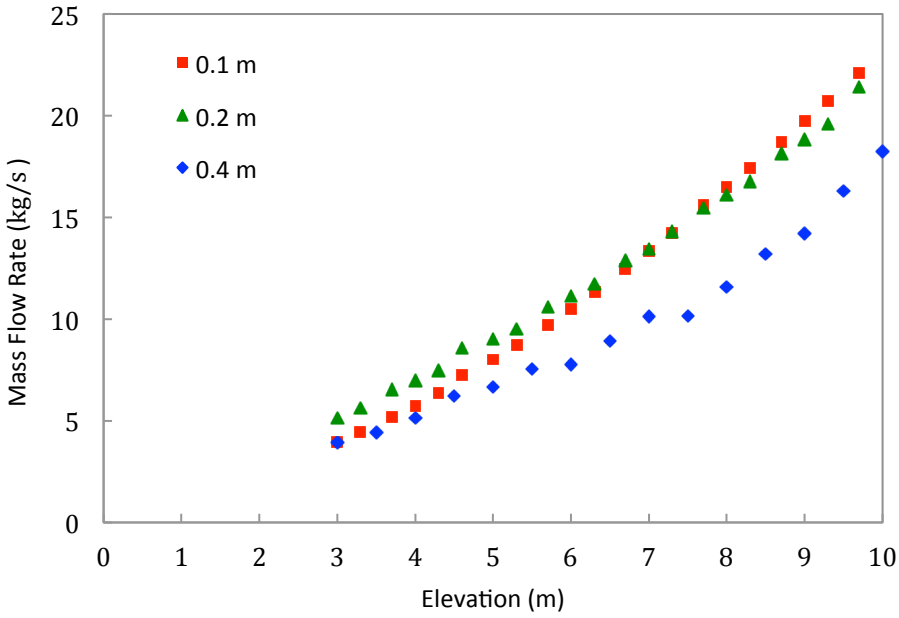

Figure 3.15: Grid Comparison using Mass Flow Rate

It is shown in Figure 3.15 that the 10 cm and 20 cm grid cell size trend in mass flow rate is very similar, while the results of mass flow from the 40 cm grid are appreciably less than those from the 10 cm and 20 cm s at higher elevations. The results from Figure 3.15 indicate that either 10 cm or 20 cm are appropriate to track smoke flow within the plume.

A uniform 20 cm grid cell size is selected for subsequent simulations, as further explained in Section 3.4. The 20 cm grid is 2% of the height of the compartment, with 5 grid cells over the diameter of the smallest fire burner. The results indicate that 20 cm provides optimum detail while maintaining a suitable simulation computation time.

3.3.2 Domain Boundary Conditions - Exterior Makeup Air Vent Domain

When considering an FDS compartment configuration, many design concepts must be investigated. The FDS configuration for this study requires a mechanical smoke exhaust system. In all smoke management systems, makeup air is naturally entrained into the compartment through the exterior walls.

In FDS 6.0, the size of the computational domain defines the location of the boundary conditions. Typically, when running an FDS simulation with one simple compartment, the domain is set to the size of the compartment. To entrain makeup air from the exterior boundary ("the outside"), an open vent must be defined. However, using the FDS exterior mesh boundary as the opening for a makeup air vent creates errors. The pressure boundary condition on such openings is imperfect [4]. To emulate the possible inaccuracies, an example with no fire and a ceiling exhaust rate of 20 m^3/s is simulated. A vent is located on each wall at a low elevation to represent makeup naturally entering through a door. The average volume flow through each

vent should be about 5 m^3/s based on the area of each vent. Figure 3.16 is a plot of the volume flow through the four makeup air vents vs. time.

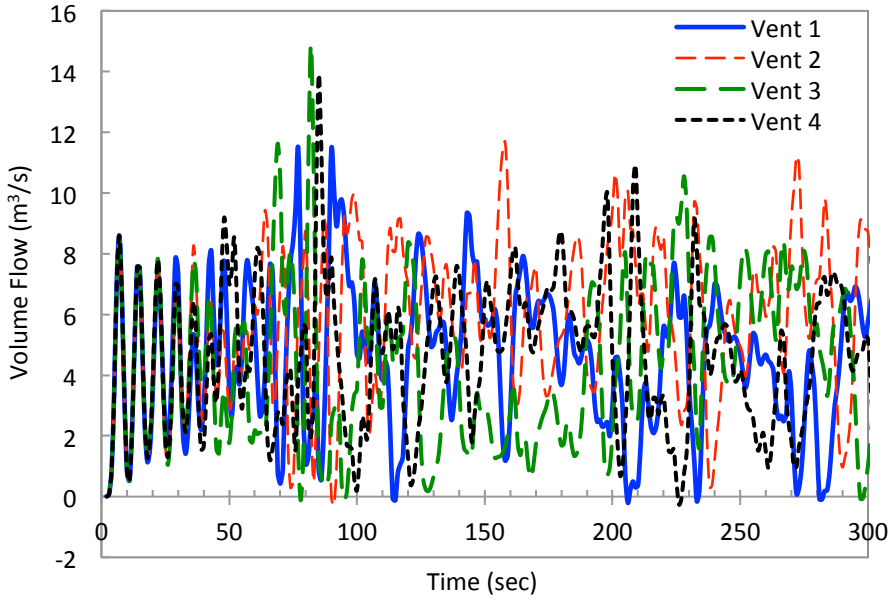

Figure 3.16: Makeup Air Vent defined at the FDS exterior boundary

The pressure boundary condition creates an unrealistic oscillatory flow pattern through the exterior vent that ranges from about 2 to 8 m^3/s. Although the average volume flow is approximately correct, the turbulent nature of the makeup airflow pattern entering the compartment may affect the fire plume dynamics due to potential oscillations in the makeup air.

In order to maintain a more steady flow through the makeup air vents the FDS domain is extended by 2 m. The makeup air vent is then defined as a hole, and the extended sides of the computational domain are defined as open. Figure 3.17 and 3.18 show the two different FDS configurations in Smokeview.

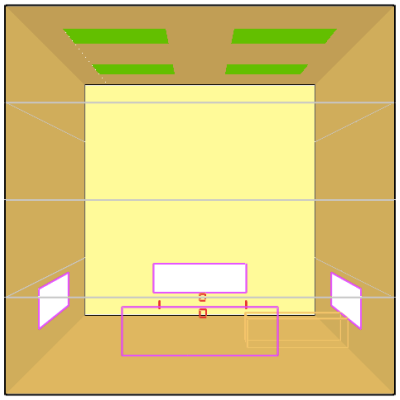

Figure 3.17: FDS Domain defined by compartment size

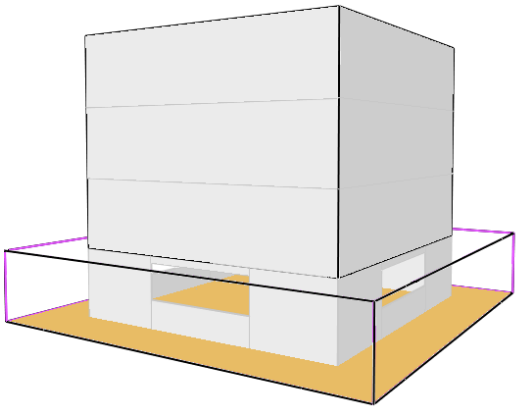

Figure 3.18: FDS Domain Extended

Figure 3.19 is a plot of the volume flow through the makeup air vent with the extended domain as seen in Figure 3.18. The airflow pattern is significantly steadier with an average volume flow of 5 m^3/s.

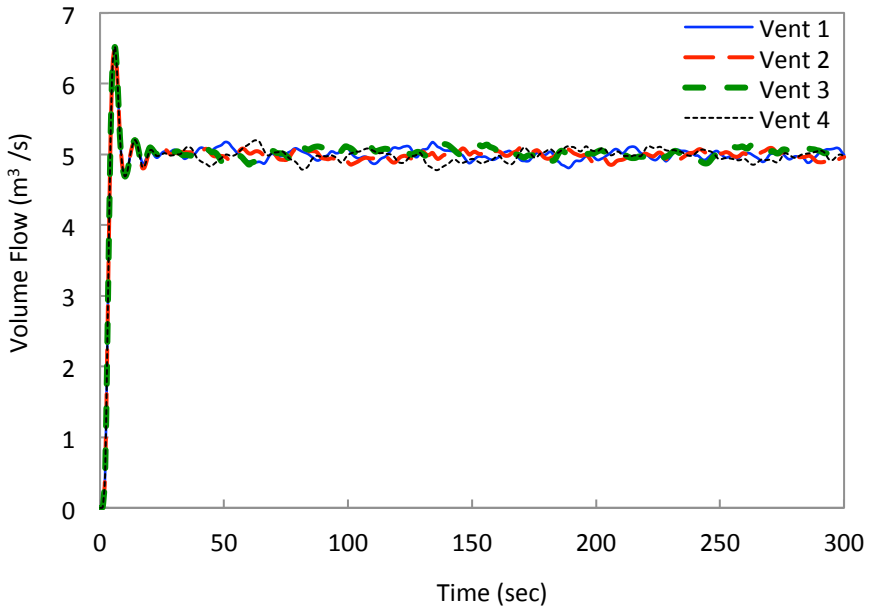

Figure 3.19: Makeup Air Vent defined as hole with Extended FDS Exterior Boundary

The FDS simulations detailed in Section 3.4 utilize an extended boundary domain design around the exterior mounted open makeup air vents in order to reduce significant volume flow oscillations into the compartment.

3.3.3 Flame Tilt Angle

Flame tilt angle calculations are performed to account for potential flame tilt due to increased crosswind at the base of the flame. The results from the calculations are then used to determine the appropriate compartment size due to possible plume tilt. The intent of the study is to observe an axisymmetric plume; therefore, the plume must not interfere with the walls of the compartment.

The following calculations are based on the correlation presented by Thomas shown in Equation 2.11.

The extent of this study measures the conditions on 1 MW, 2.5 MW, 5 MW fire sizes. The maximum makeup air velocity, or cross wind at the base of the flame, that is studied is 1.75 m/s. The following calculations are applied to approximate the flame tilt angle of the following three fire sizes on the maximum velocity makeup air under study. The fire under study is a propane burner, and the heat of combustion is approximated as 50.35 MJ/kg.

Example calculations for a 1 MW fire are:

$$\dot{m}'' = \frac{Q}{\Delta H_c} = \frac{1\ \text{MW}}{50.35\ \text{MJ/kg}} = 0.019\,\frac{\text{kg}}{\text{m}^2\text{s}}$$

$$\cos(\theta) = 0.7\left[\frac{1.75}{\left(\frac{0.019\,\frac{\text{kg}}{\text{m}^2\text{s}}\left(9.81\,\frac{\text{m}}{\text{s}^2}\right)(1.2\text{m})}{1.2\,\frac{\text{kg}}{\text{m}^2}}\right)^{1/3}}\right]^{-0.49} \Rightarrow \theta = 66.14°$$

The same calculations are applied under a 1.75 m/s cross wind for the 2.5 and 5 MW fire; the results are presented in Table 3.2.

Table 3.2: Angle of Tilt under 1.75 m/s crosswind

Fire Size (MW)	Diameter of Burner	Mass Burn Rate $\left(\frac{kg}{m^2 s}\right)$	Angle of Tilt (θ)
1	1.2 m	0.019	66.1°
2.5	2 m	0.049	61.8°
5	2 m	0.099	58.0°

The results conclude that there may be a significant plume tilt with the additional crosswind velocity.

In addition to the following calculations, an FDS study is used to reinforce the results from the algebraic equations. The most significant calculated affect, shown as the 1 MW fire under 1.75 m/s velocity conditions is therefore modeled. The model is configured so that a vent located 1.2 m away from the edge of the burner injects the velocity. The fire is located centrally within the square compartment.

The Smokeview image, shown in Figure 3.20, illustrates a significant flame tilt. However, as the temperature profile is viewed in Figure 3.21, only the lower portion of the plume is affected, with the upper portion of the plume observed to rise vertically.

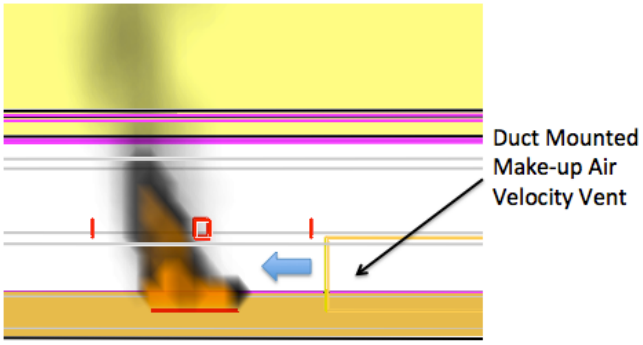

Figure 3.20: Smokeview image of flame tilt with 1.75 m/s velocity

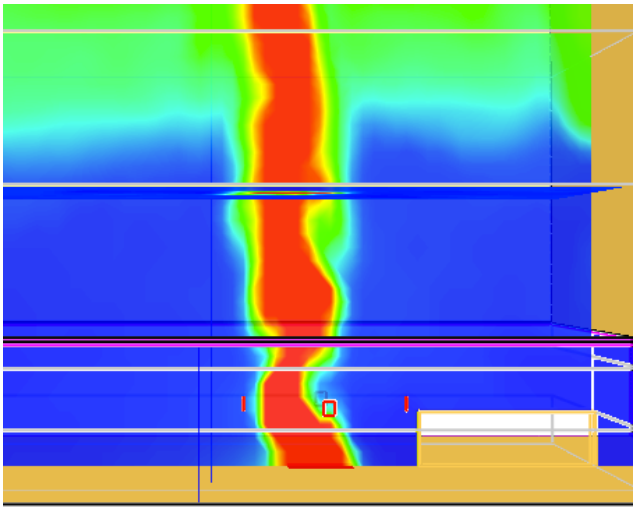

Figure 3.21: Smokeview image of Smoke plume with 1.75 m/s velocity

Overall, with the presence of a visible and empirically calculated flame tilt, the compartment design is altered to increase the distance between the wall and flame. The wall located in line with the increased makeup air velocity is extended by 4 m to ensure the plume does not interact with the compartment walls before reaching the

smoke layer. The compartment size is then increased in the X direction from 10 m to 14 m as shown in Figure 3.22.

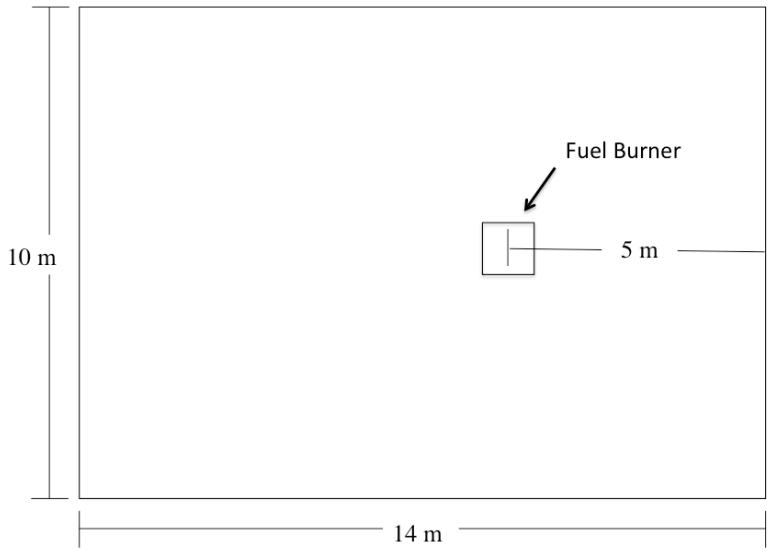

Figure 3.22: Plan View of Compartment Size

3.4 FDS Model Configuration and Simulation Matrix

The system is designed with a mechanical smoke management system. The design intent is to stabilize the smoke layer at 80% of the total height of the compartment. The study considers a rectangular atrium with the fire at ground elevation. The basic FDS design is illustrated in Figure 3.23.

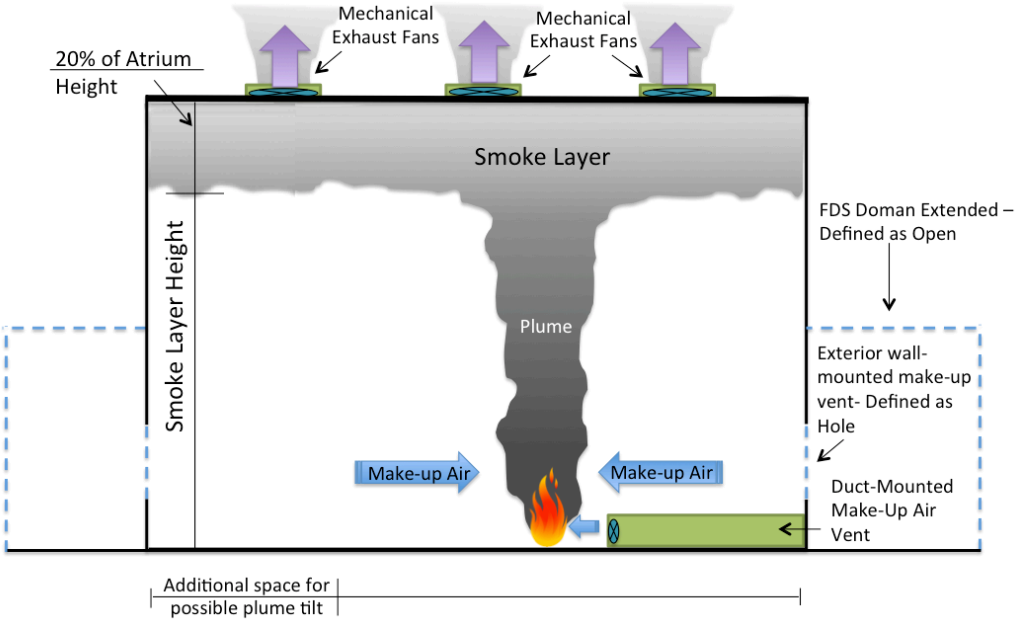

Figure 3.23: Basic FDS Design

3.4.1 Exterior Wall-mounted Makeup Vents

Makeup air is introduced into the system to satisfy the required volume of clean air entrained into a smoke management system. The makeup vents, depicted as the "exterior wall-mounted makeup air vent", are located along the walls close to the floor level.

The exclusive purpose of the exterior wall-mounted vents is to allow for the necessary makeup air to naturally entrain into the system. By setting the makeup air vents as passive holes, air naturally enters the compartment while the ceiling vents exhaust smoke. The configuration is designed so that the wall-mounted makeup air does not impact the air entrainment rate of the fire. In these simulations, the maximum velocity through the exterior wall mounted vents is 0.5 m/s. This velocity is low enough to ensure no interference or increased air entrainment.

3.4.2 Duct Mounted Makeup Air Vent

A rectangular duct protrudes from the wall to create a velocity initiated close to the fire plume. This duct-mounted makeup air vent serves as the makeup air that will produce the maximum interaction between the flame zone and the fire plume. The magnitude of the velocity, as well as the location and size of the duct vary in each simulation configuration.

3.4.3 FDS Atria Model Configurations for Study

In this study, The FDS configurations of the atria are configured under the following conditions.

Fire Source:

- Reaction fuel is defined as propane.
- The fuel burner is centrally located in compartment along the y-direction.
- The fuel burner is square shaped.

Compartment configuration:

- Compartment is 10 m x 14 m.
- The height is 10 m.
- Exterior mounted makeup air vents defined as holes- beginning at 1 m off the base of the compartment (area further detailed in Table 3.3).

Mechanical Exhaust System:

- The volumetric exhaust rate of the compartment is calculated, as described in Section 2.4.3, in order maintain a smoke layer height that stabilizes at approximately 80% of the total height.
- The exhaust vents are located on the ceiling (further described in Section 3.4.3.1).

Boundary Conditions:

- Exterior makeup air vents: The vents are located along the lower level of the each wall, stretching the entire wall. The area of the vents are adjusted per each simulation with varying ceiling exhaust rates, in order to maintain natural velocities through the vents below 0.5 m/s.

- Solid Wall: Every surface (walls/ceiling/floor) is be modeled as a solid gypsum plaster material that is 0.2 m thick.

3.4.3.1 Grid Resolution

The grid resolution study presented in Section 3.3.1 defined an acceptable grid size of 20 cm. The FDS model uses a 0.2 x 0.2 x 0.25 m grid cell size within the compartment. As the extended domain is utilized solely to reduce the effects from the open boundary conditions in FDS the grid in the extended area is coarse, with a 0.4 m x 0.4 m x 0.4 m grid cell size. The grid for the 10 m compartment is shown in Smokeview in Figure 3.24.

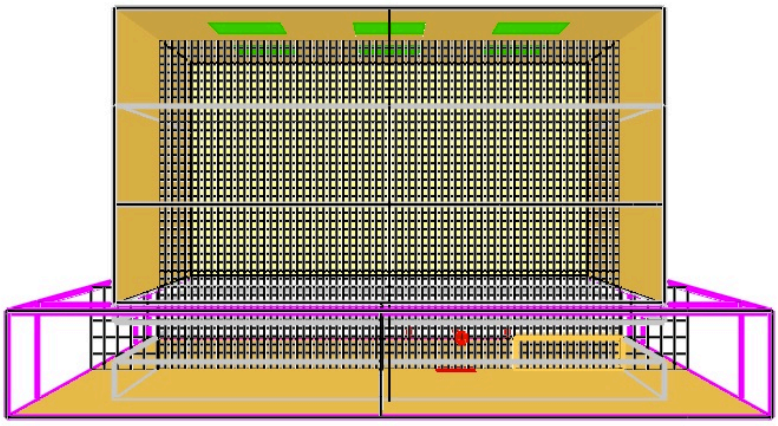

Figure 3.24: Grid for Simulation titled SOA

3.4.3.2 Ceiling Exhaust Vents

For all 10 m high simulations there are 6 ceiling openings defined as the ceiling exhaust vents. The volumetric exhaust required is divided equally among vents.

Figure 3.25 illustrates the ceiling exhaust inlets in Smokeview. In order to avoid plugholing, NFPA 92 defines the minimum distance between vent inlets as:

$$S_{min} = 0.9V_e^{1/2}$$

S_{min} = Minimum distance between vent inlets (m)

V_e = Volumetric exhaust per vent (m^3/s)

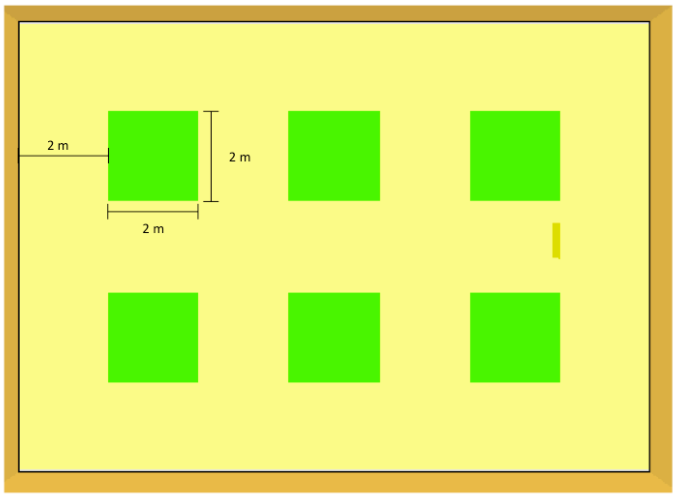

Figure 3.25: Ceiling Exhaust Inlet Locations

For the 1 MW and 2.5 MW cases the S_{min} is less than 2 m. For the 5 MW fire the minimum calculated separation distance is 15% over the 2 m spacing. However, the FDS results do not indicate plugholing characteristics, so the 2 m separation was used to maintain consistency between simulations.

3.4.3.3 Simulation Matrix Configuration

The primary simulations run in FDS 6.0 are outlined in Table 3.3. Each simulation is set with the same parameters as defined in Section 3.4.3. The ceiling volumetric exhaust rate is calculated to stabilize the smoke layer at 8 m. The duct-mounted makeup air vent is run with the velocities of 0 m/s, 1 m/s, 1.25 m/s, 1.5 m/s and 1.75 m/s for every simulation.

Table 3.3: Simulation Matrix Configuration Details

Simulation Name		SOA	STA	SFA	SOB	SOA_rvent	SOA_rdoor
Fire Size (MW)		1	2.5	5	1	1	1
Burner Size (m)		1.2 x 1.2	2 x 2	2 x 2	1.2 x 1.2	1.2 x 1.2	1.2 x 1.2
HRRPUA (kW/m^2)		694.4	625	1250	694.4	694.4	694.4
Total Ceiling Exhaust Rate (m^3/s)		18.66	27.92	39.36	18.66	18.66	18.66
Exterior Wall-mounted Makeup Air Vent Area (m^2)		48	96	120	48	48	48
Duct-mounted Makeup Air Vent	Distance from Edge of Burner (m)	1.2	2	2 m	1.2	1.2	1.2
	Height (m)	1	1.4	1.8	0.5	1	2 m
	Width (m)	0.6	0.6	0.6	0.6	0.6	1 m
	Elevation in z (m)	0 - 1	0 – 1.4	0 – 1.8	0 -0.5	1.3 - 2.3	1.3 – 3.3 m

All simulation titles beginning with “SO” represent 1 MW fires, the principal variations between these simulations are with the duct mounted makeup air vent location. All vents are located a burner diameter distance from the edge of the burner. For the basic simulations, “SOA”, “STA”, and “SFA”, the height of the makeup air vent is approximately half the mean flame elevation and the width is equal to a standard 24-inch (0.6 m) vent.

The simulations presented in Table 3.3 represent the initial cases developed and run for all makeup air velocities chosen. Based off of the results from these simulations, additional configurations are run to extract further relevant data. The additional simulations include shifting the vent so it is not centrally aligned with the fire, rotating the vents height and width, and further elevating the makeup air vents. These configuration descriptions and results are presented in Section 5.2.

3.5 Heat Flux Simulations - Description of Model Configuration

3.5.1 FDS Configuration for Heat Flux Model

The following FDS study applies the same principles from the previous simulations by introducing a duct-mounted makeup air vent at the base of the flame to study the effects of makeup air on radiative heat flux. Radiative heat flux gauges are used in FDS to approximate the appropriate heat flux value at a distance away from the burner. The FDS simulation is configured to include a 1 MW and 5 MW fire located in the center of the space. The incident heat flux produced from the smoke layer is inconsequential as the temperature of the layer is very low compared to the fire temperature. Due to this circumstance, the configuration defined in FDS does not include walls or a smoke layer. Thus, the compartment is completely open i.e., there are no walls or ceilings defined, and a smoke layer does not form. The smaller

configuration allows for a more detailed grid resolution defined around the fire, further explained in Section 3.5.2.

Radiative heat flux gauges are located in line with the prescribed makeup air. Two sets of gauges are used, one set on the floor, and the other set elevated at half the mean flame height. The elevated gauges are oriented to face towards the fire, and have a length, width, and height of 0.001 meters. The floor gauges are oriented upward. The gauges are placed at every 0.5 m beginning at the burner's edge. A total of nine gauges are placed in line with the center of the burner. Both the elevated and floor gauges are considered for comparison. The configuration is illustrated in Figure 3.26, which includes the presence of a 5 MW fire.

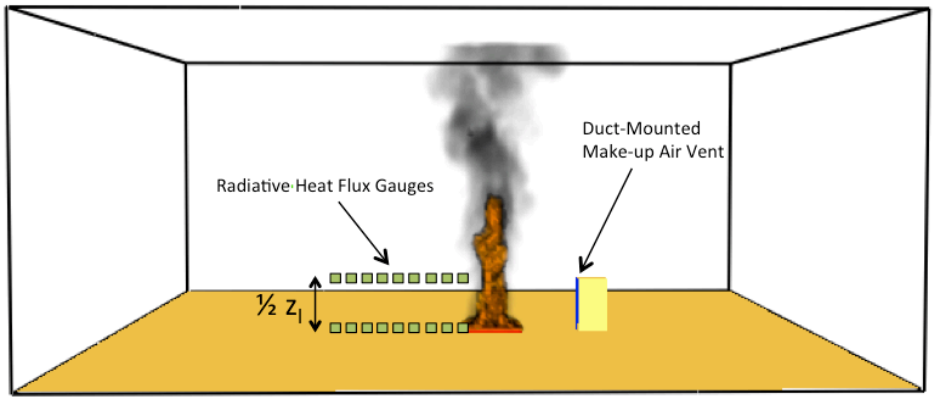

Figure 3.26: FDS simulation configuration for the 5 MW fire case

The configurations between the 1 MW and 5 MW fires vary only slightly. The duct mounted makeup air vent is located on the floor. The height makeup air vent is half the diameter of the plume at the mean flame height. The width of the duct is 0.6 meters and centered with the burner. A more detailed FDS configuration explanation for both the 1 MW and 5 MW fire is shown in Table 3.4.

Table 3.4: FDS Simulation configuration details

Simulation Title	HOA	HFA
Fire Size	1 MW	5 MW
Burner Size	1 x 1 m	2 x 2 m
HRRPUA	1000 kW/m^2	1250 kW/m^2
Duct-mounted Makeup Air Vent Location	1 m from edge of burner	2 m from edge of burner
Height of Makeup Air Vent	1 m	1.8 m
Width of the Makeup Air Vent	0.6 m	0.6 m
Temperature Gauge Elevation	½ z_l = 1.1 m	½ z_l = 2.1 m

Similar to the previous simulations, the makeup air velocities prescribed at the vent are 0 m/s, 1 m/s, 1.25 m/s, 1.5 m/s, and 1.75 m/s.

3.5.2 Grid Resolution

This study includes a 0.1 m grid cell size around the fire, as radiative heat flux values are more sensitive to a finer resolution analysis. The grid sensitivity is increased from the previous simulations, which includes a 0.2 m grid cell size. The total size of the compartment is 24 m by 22 m, however a multi-mesh design is used within the compartment. The finer, 0.1 m, grid cell size is within a mesh that is 12 m long, and 6 m wide. It is centrally located within the compartment to include the fire and all heat flux gauges. The rest of the compartment has a more coarse grid cell size of 0.4 m. An image illustrating the grid cell variation is shown in Figure 3.27.

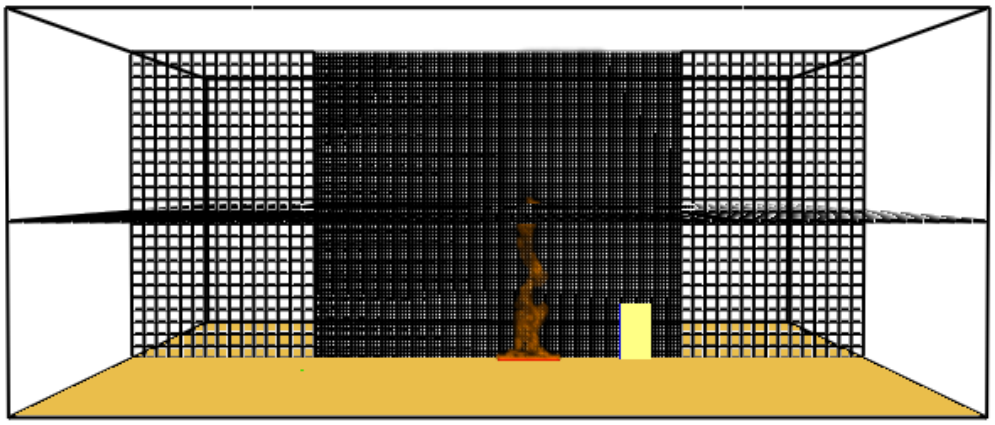

Figure 3.27: Grid Resolution for Heat Flux Simulations

Chapter 4

Past Simulation Verification in 6.0

Fire Dynamic Simulation (FDS) 6.0 presents prominent variations from past versions of the FDS software that may alter results and conclusions. Comprehensive studies were completed by George Hadjisophocleous at Carleton University, and Kerber and Milke at the University of Maryland, regarding the topic of makeup air in atria, using FDS 4.0 [15-16]. The following section outlines similar replications of the past FDS configurations and results completed at Carleton University and the University of Maryland using FDS 6.0. The FDS Model design considerations and diagnostics presented in Chapter 3 are utilized in the following section in order to evaluate and compare the results. The following evaluation is qualitative, and used to compare basic models and confirm similar trends based on the configuration details and model characteristics provided in the reports.

4.1 Carleton University Study

In 2007, Professor George Hadjisophocleous of Carleton University investigated the topic of makeup air in atria [15]. This study considered a configuration corresponding to a simple 10 x 10 x 10 m compartment, with the fire 2.5 meters from the wall with one makeup air vent in the center. The makeup air vent was only located on one side. Hadjisophocleous defined the heat release rate due to convection to be 65% of the

total heat release rate. Using this assumption, along with the assumption that the fraction of energy contained in the smoke layer is defined as 0.5, the exhaust rate was calculated to require 18.3 m^3/s [3]. In order to limit the makeup air supply velocity to approximately 1 m/s, the makeup air vent needed to have a cross-sectional area of about 18.3 m^2. However, a 19.25 m^2 vent size was configured due to the grid size used in this replication. The fire simulated in the FDS 6.0 replication was a steady 1 MW methane burner.

In the Carleton University design, referred to as the CU design, a 0.25 m grid cell size was used [15]. In the FDS 6.0 replication a 0.2 m grid cell size was created (see the FDS 6.0 configuration in Figure 4.1).

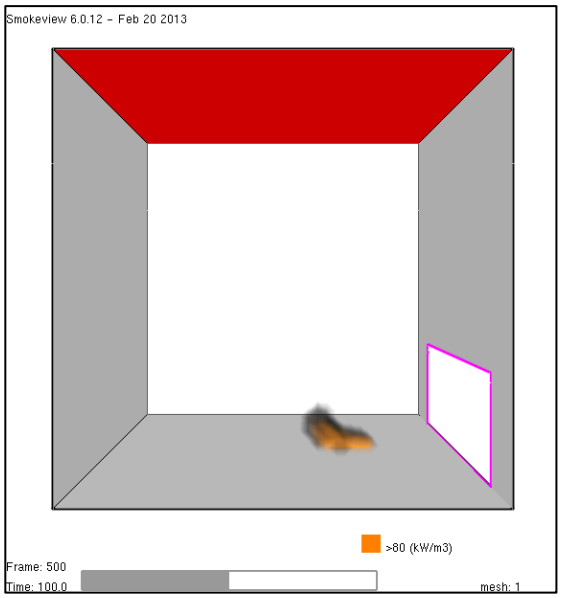

Figure 4.1: CU Design Replication using FDS 6.0

The Smokeview image of the temperature profile at 200 seconds for the CU study and the FDS 6.0 replication are illustrated in Figure 4.2 and 4.3 respectively. Note that the temperature scales appear marginally different, however, they are consistent given the difference in the FDS and Smokeview versions.

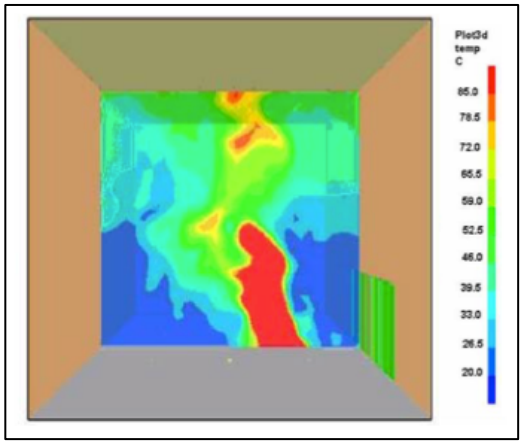

Figure 4.2: CU Model, t = 200 s [15]

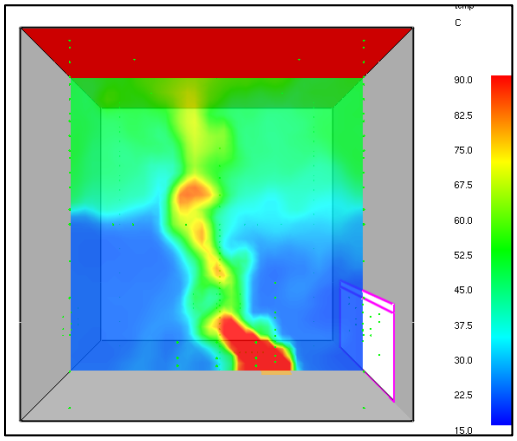

Figure 4.3: FDS 6.0 Model, t = 200 s

The FDS 6.0 replication produced similar results to that obtained by the CU model. The makeup air velocity of 1 m/s created a tilt in the fire plume, which caused turbulence within the smoke layer region. The FDS 6.0 model uses a steady 1 MW methane fire, while the CU report does not define what is used. The disparity in the height of the flame may relate to the difference in the burner, however, both models specify the same steady heat release rate so the smoke production should be properly comparable. The CU Smokeview model illustrates a more turbulent temperature profile throughout the lower region of the compartment. The FDS 6.0 result shows a smoother temperature profile defining the smoke layer height.

The smoke layer interface height diagnostic is used, as defined in Chapter 3. In this example, the cold lower layer is at an ambient temperature of 20°C, and the average

temperature within the layer is approximately 52°C. The values of C_n defined in NFPA 92 for modeling are an average of 0.85 to identify the smoke layer interface and 0.15 for the first indication of smoke [3].

$$T_n = 0.85(52°C - 20°C) + 20°C$$

$$T_n = 0.15(52°C - 20°C) + 20°C$$

Figure 4.4 is a plot of the elevation vs. time using this diagnostic tool. The graph shows that the smoke layer interface height is approximately 7 m, and the first indication of smoke height is approximately 5 m.

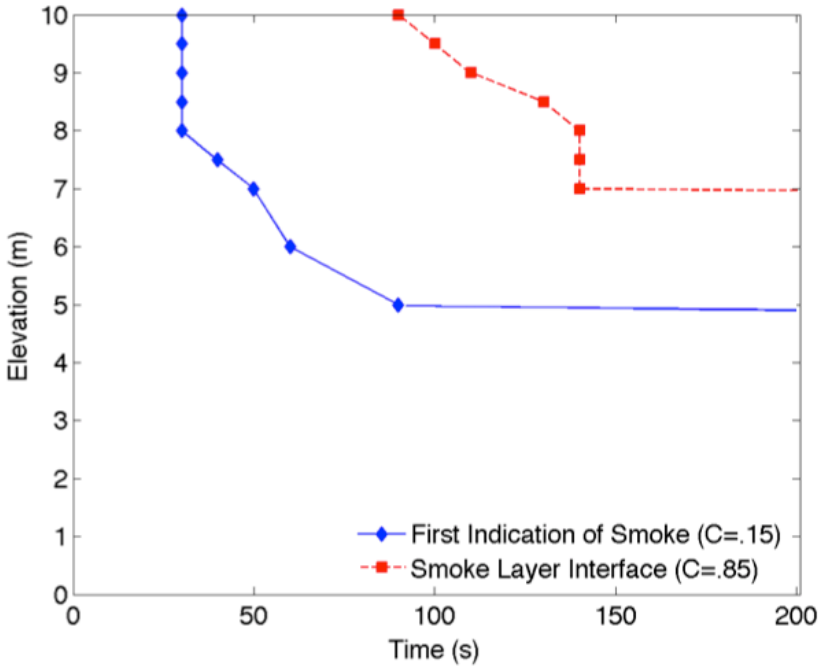

Figure 4.4: FDS 6.0 results of Elevation vs. Tau (time)

In the CU report, the smoke layer height for this 1.0 m/s makeup air velocity case is never defined but the report does conclude that even the 1.0 m/s makeup air velocity

causes the plume to tilt and the hot layer to descend [15]. Overall the results show very similar trends between FDS 4.0 and FDS 6.0 with consideration to the various differences in the FDS configuration and inputs.

4.2 University of Maryland Study

In 2007 a study by Kerber and Milke was completed to analyze the effect of makeup air on smoke layer height in an atrium in the shape of a 30.5 m cube [16]. A similar study with an example configuration taken from this report was conducted using FDS 6.0.

The FDS 6.0 design was created to closely simulate Kerber's first simulation with makeup air vents close to the floor on every vertical wall. The design, referred to as the UMD design, was a 30 x 30 x 30 m compartment with a fire located in the center [16]. The UMD design used 0.1 m grid cell size located in a sub-domain 6.7 x 6.7 x 7.6 m around the fire and a 0.3 m cell size in the rest of the compartment. There were four square exhaust vents on the ceiling with a 1.2 m length [16]. In the FDS 6.0 simulation a 0.5 m grid cell size was created, so a 1.5 m exhaust vent length was used to satisfy the grid cell size. This slightly increased the area of the vent, however, the same volume flow of 45.6 m^3/s per vent was still specified.

The UMD design had a fast growing wood crib fire with a maximum heat release rate of approximately 5 MW. The average heat release rate was about 3.5 MW (a graph of

the UMD design heat release rate history is presented in Figure 4.5). In the FDS replication a methane fire was used, with a t^2 fire growth that became steady at 3.5 MW after approximately 250 seconds. Figure 4.6 illustrates an approximation of the heat release rate curve that is used for the FDS 6.0 replication.

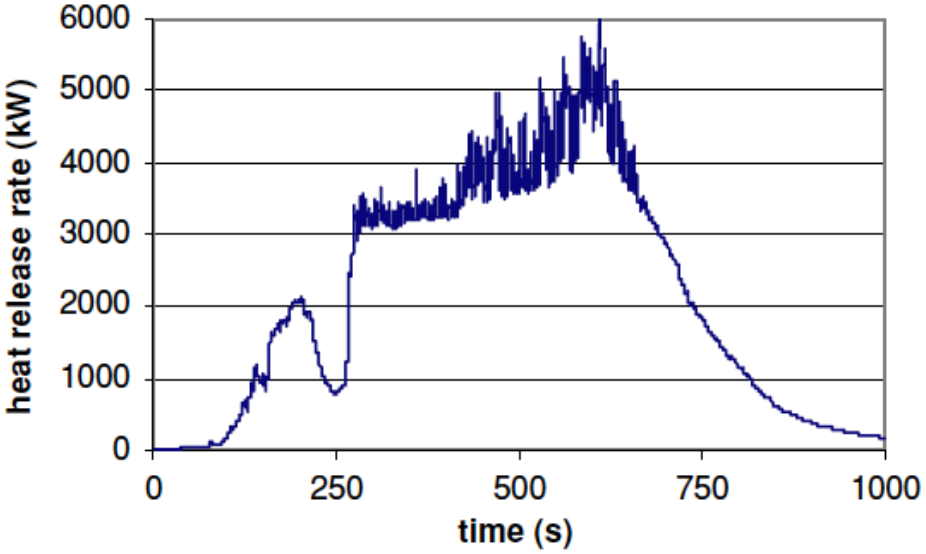

Figure 4.5: UMD Design HRR vs. Time [16]

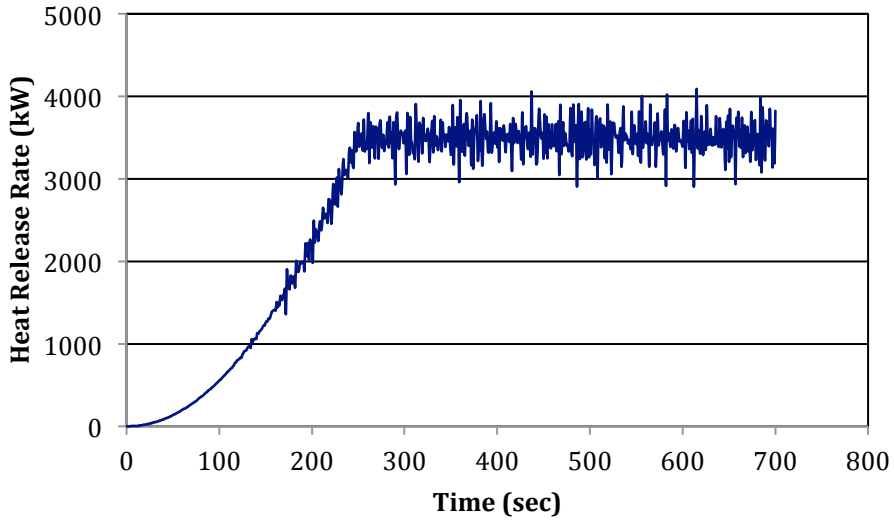

Figure 4.6: FDS 6.0 Replication Design HRR vs. Time

Due to the grid resolution of the FDS 6.0 replication, a larger burner diameter is used to properly resolve the component. A 1.25 x 1.25 m burner was prescribed as opposed to the 0.5 x 0.5 m in the UMD design. However, as shown in Figure 4.5 and 4.6 the heat release rate values are comparable, thereby creating similar smoke conditions.

The results show similar trends. Kerber's report states that the smoke layer stabilizes at approximately 24 m [16].

The smoke layer interface height diagnostic is used to further analyze these results. The diagnostic is explained in detail in Section 2.3. In this example the cold lower layer is at an ambient temperature of 20°C, and the average temperature within the layer is approximately 31°C. The values of C_n defined in NFPA 92 for modeling are an average of 0.85 for smoke layer interface and 0.15 for the first indication of smoke [3].

$$T_n = 0.85(52°C - 20°C) + 20°C$$

$$T_n = 0.15(52°C - 20°C) + 20°C$$

The FDS 6.0 replication results shows a stabilized smoke layer interface at approximately 21.5 m, as illustrated in Figure 4.7.

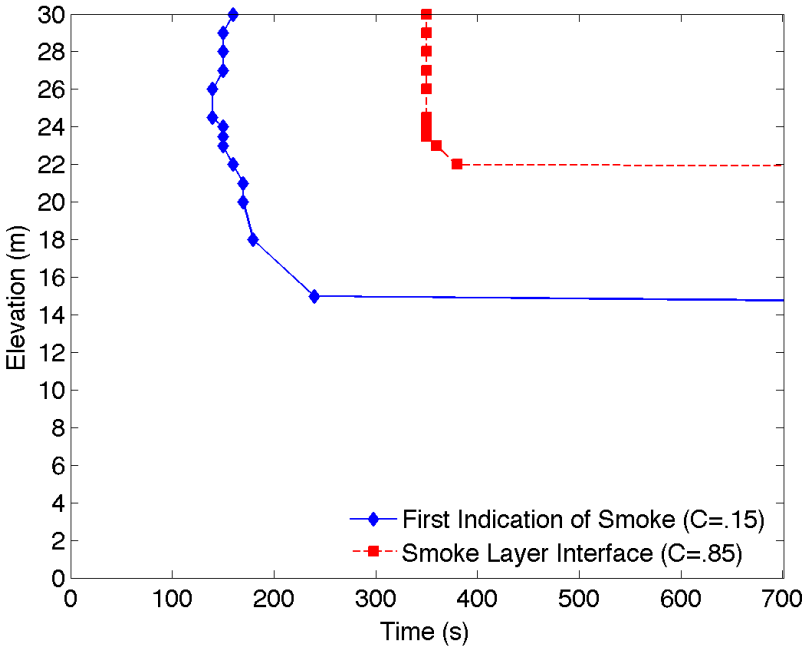

Figure 4.7: Smoke Layer Stabilization
Elevation vs. Tau (time)

The Smokeview images produced by Kerber, and the FDS 6.0 replication are shown in Figures 4.8 and 4.9, respectively. In Kerber's report the results are presented using the 3D smoke tool in FDS 4.0, however, the FDS 6.0 replication utilizes the temperature plot through the center of the fire [16].

Note that the Smokeview image shows the entire FDS domain. The FDS 6.0 replication has an extended domain around the open vents.

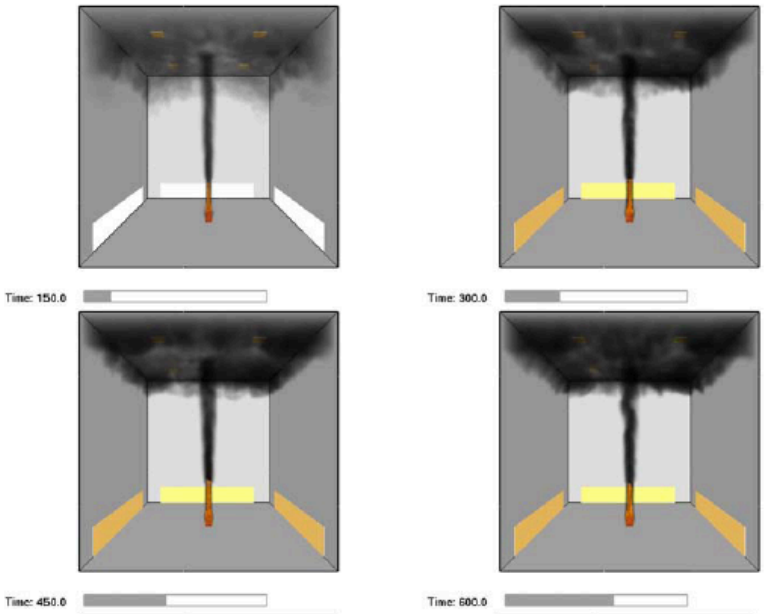

Figure 4.8: UMD Design Smokeview Results [16]

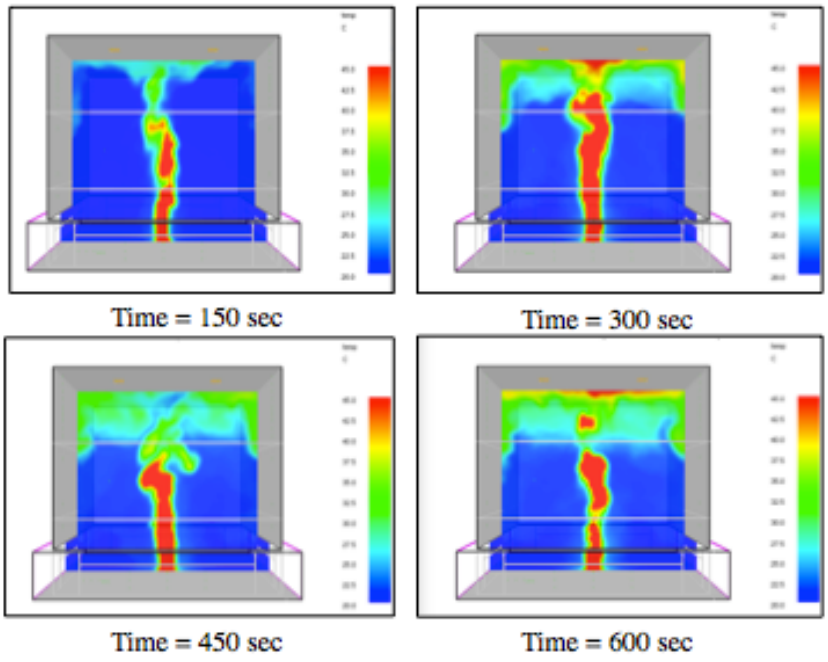

Figure 4.9: FDS 6.0 Replication Smokeview Results

The Smokeview images show a stabilization in the smoke layer height over the 700 sec in the FDS 6.0 results. The smoke layer temperature diagnostic better illustrates

the true smoke layer height. Overall the results are similar when the variations used in the FDS 6.0 configuration replication are considered.

Chapter 5

Smoke Production - Results and Design Tool

This chapter presents and discusses the results from various FDS simulations. These simulations include the main simulation matrix explained in Section 3.4.3.3. Additional simulations were run as special cases, in order to further evaluate the smoke layer and mass flow rate of the plume under different vent location and size configurations. All results are presented using the diagnostic tools explained in Chapter 3.

The results are used to determine the impact of the makeup air velocity on the rate of smoke production and consequent smoke layer position. Further the results are used to develop an engineering tool that assists in accounting for the impact of makeup air velocities exceeding 1 m/s.

5.1 FDS Simulation Matrix Results and Discussion

The following simulation configurations are detailed in Section 3.4.3. The basic configuration changes are highlighted briefly and each new simulation's results are presented. However, Section 3.4.3 should be referred to for more detail of any of the simulations. The range of all simulation configurations addresses the impact of the vent providing an airflow velocity of 0 m/s, 1 m/s, 1.25 m/s, 1.5 m/s and 1.75 m/s

toward the fire.

5.1.1 Analysis Method defined for Alpha

In addition to the smoke layer height and mass flow rate graphs defined in Section 3.2, an analysis of the increase in smoke production is presented. In the mass flow rate diagnostic the mass flow rate vs. elevation is presented for all velocities. In order to account for the increase in smoke production provided by the makeup air velocities, the simulation results for velocities exceeding 0 m/s are compared to the 0 m/s results. The ratio of the mass flow rate at a particular elevation (z) at the velocity prescribed to the mass flow rate of the 0 m/s simulation is defined as alpha (α), shown in Equation 5.1.

$$\alpha(\mathrm{z}) = \frac{\text{Mass Flow Rate @ 1,1.25,1.5,1.75 m/s}}{\text{Mass Flow Rate @ 0 m/s}} \tag{5.1}$$

The α value per elevation within the plume region is also graphed vs. elevation to further compare and discuss the results. As presented in the following section, the alpha values show consistent values as elevation increases for of the main simulations. An average value is taken for the alpha values for each velocity, and the standard deviation is presented. This average alpha value represents the increase in the rate of smoke production with the additional airflow velocity of the duct mounted makeup air vent. The significance of the average alpha value is explained Section 5.3, as it is utilized for the proposed engineering tool.

5.1.2 Main Simulation Results and Discussion

For the 1 MW fire titled SOA, the vent is placed on the floor level and is 1 m high by 0.6 meters wide. The vent is aligned in the center of the burner and placed 1.2 m away from the edge of the burner. The smoke layer height and mass flow rate results are shown in Figures 5.1 and 5.2, respectively.

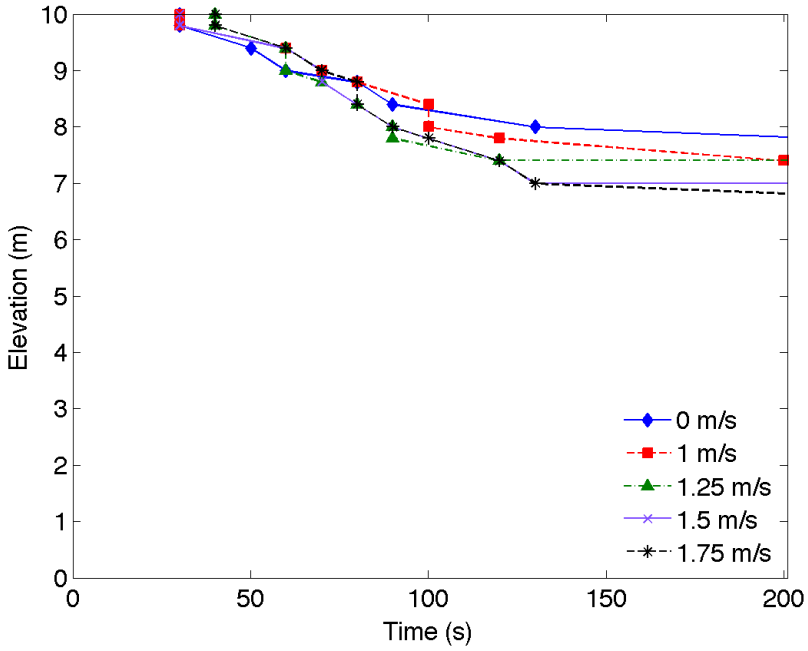

Figure 5.1: SOA Smoke Layer Height

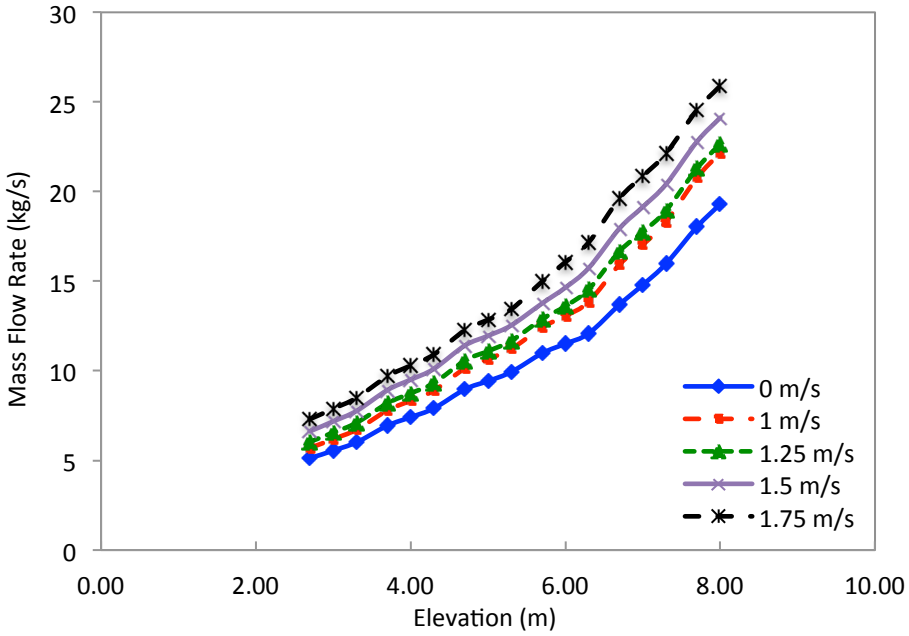

Figure 5.2: SOA Smoke Layer Height

The smoke layer heights presented in Figure 5.1 show that as the velocity of the makeup air increases, the smoke layer height descends. The results presented in Figure 5.2 show that the mass flow rate of smoke in the plume also increases with increased makeup air velocity. Smokeview images of the temperature profile taken at 200 seconds are presented in Figure 5.3 and 5.4 of the 0 m/s and 1.75 m/s makeup air velocity simulations, respectively. The images visually illustrate that the smoke layer height for the 1.75 m/s case is lower than the smoke layer height with a 0 m/s velocity makeup air.

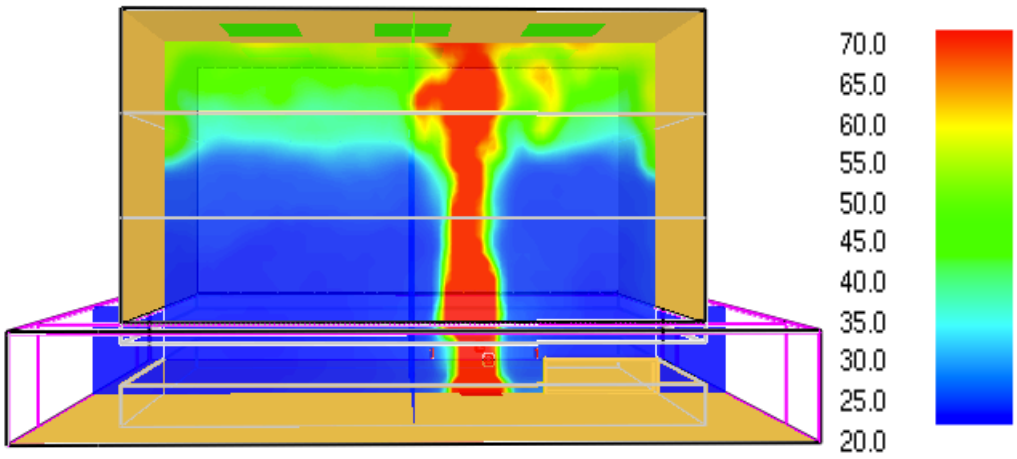

Figure 5.3: Temperature Profile for 0 m/s

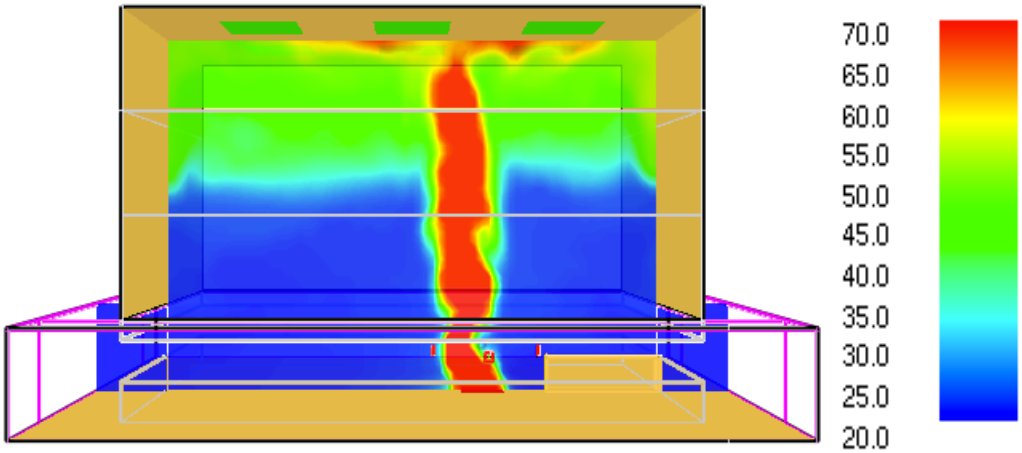

Figure 5.4: Temperature Profile for 1.75 m/s

The alpha value comparing the mass flow rate to the 0 m/s mass flow rate value is graphed vs. elevation in Figure 5.5. Table 5.1 presents the smoke layer height at 200 seconds, the average and the standard deviation of the alpha value within the plume taken at steady state.

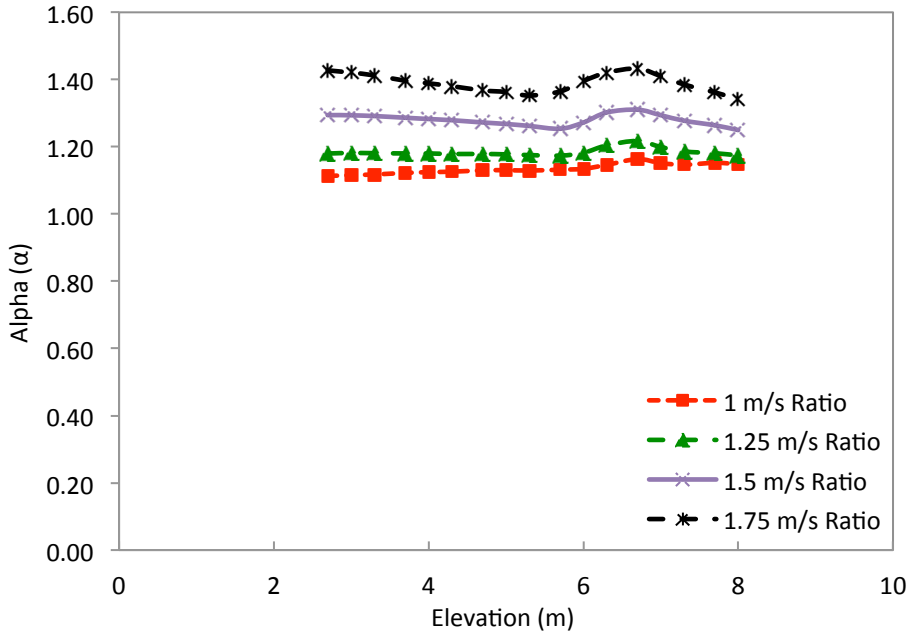

Figure 5.5: SOA Alpha Ratio

Table 5.1: SOA Results Comparisons

Makeup Air Velocity	**Smoke Layer Height @ 200 seconds**	**Average Alpha (α_{avg})**	**Standard Deviation (σ) of α_{avg}**
0 m/s	7.8 m	-	-
1 m/s	7.6 m	1.13	0.01
1.25 m/s	7.4 m	1.18	0.01
1.5 m/s	7.0 m	1.28	0.02
1.75 m/s	6.8 m	1.39	0.03

As anticipated, the mixing of makeup air at the base of the flame creates more smoke production and a deeper smoke layer. The results show that a 1.75 m/s makeup air velocity increases the mass of smoke production by 39% and drops the smoke layer by 1 m. The velocities below the maximum 1.75 m/s makeup air velocity also affect the smoke production, but to a lesser degree.

For the simulation involving the 2.5 MW fire, titled STA, the vent is placed on the floor level and is 1.4 m high by 0.6 m wide. The vent is aligned in the center of the burner and placed 2 m away from the edge of the burner. The smoke layer height and mass flow rate results are shown in Figures 5.6 and 5.7, respectively.

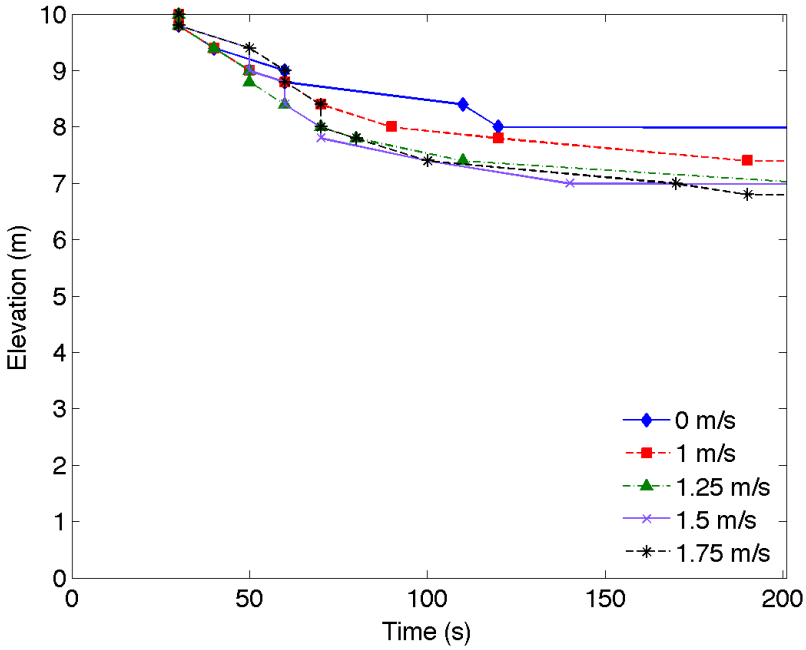

Figure 5.6: STA Smoke Layer Height

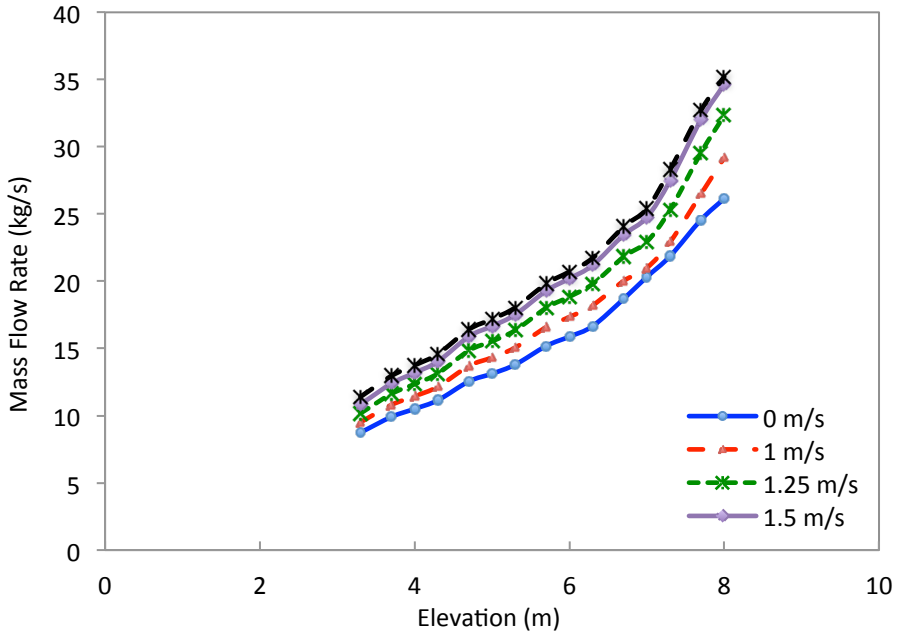

Figure 5.7: STA Mass Flow Rate

The results follow a similar trend as in the 1 MW fire results. The alpha value is graphed vs. elevation in Figure 5.8. Table 5.2 presents the smoke layer height at 200 seconds, the average alpha value within the plume take at steady state and the standard deviation of the average alpha value.

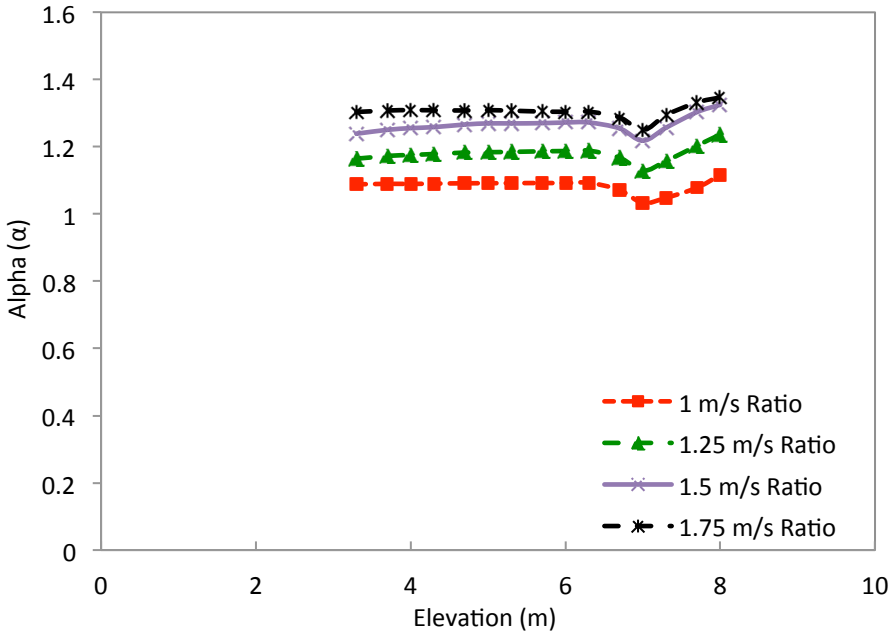

Figure 5.8: STA Alpha Ratio

Table 5.2: STA Results Comparisons

Makeup Air Velocity	**Smoke Layer Height @ 200 seconds**	**Average (α_{avg})**	**Standard Deviation (σ) of α_{avg}**
0 m/s	8 m	-	-
1 m/s	7.4 m	1.08	0.02
1.25 m/s	7.0 m	1.18	0.02
1.5 m/s	7.0 m	1.27	0.02
1.75 m/s	6.8 m	1.31	0.02

The overall results show a similar trend, i.e. as the makeup air velocity increases the smoke layer descends. The alpha value as shown in Figure 5.8 is very steady over each elevation within the plume, and the standard deviation does not exceed 2%. At a 1.75 m/s makeup air velocity, the average alpha value is approximately 1.31. This value is less than the 39% increase for the 1 MW fire. The makeup air velocity is the same for both examples, yet the volume of makeup air is slightly increased in the 2.5

MW fire case. The height of the vent is 40% larger in the 2.5 MW fire case in order to have the top of the vent reach half the mean flame height.

The results indicate that the 1.75 m/s makeup air velocity has less of an effect on the 2.5 MW fire than the 1 MW fire. The momentum of the makeup air striking the fire has less of an effect with the larger fires source strength. This phenomenon is further explained in Section 5.3, and a ratio between the strength of the makeup air flow and fire source is determined for each example.

For the 5 MW fire titled SFA, the vent is placed on the floor level and is 1.8 m high by 0.6 m wide. The vent is aligned in the center of the burner and placed 2 m away from the edge of the burner. The smoke layer height and mass flow rate results are shown in Figures 5.9 and 5.10, respectively.

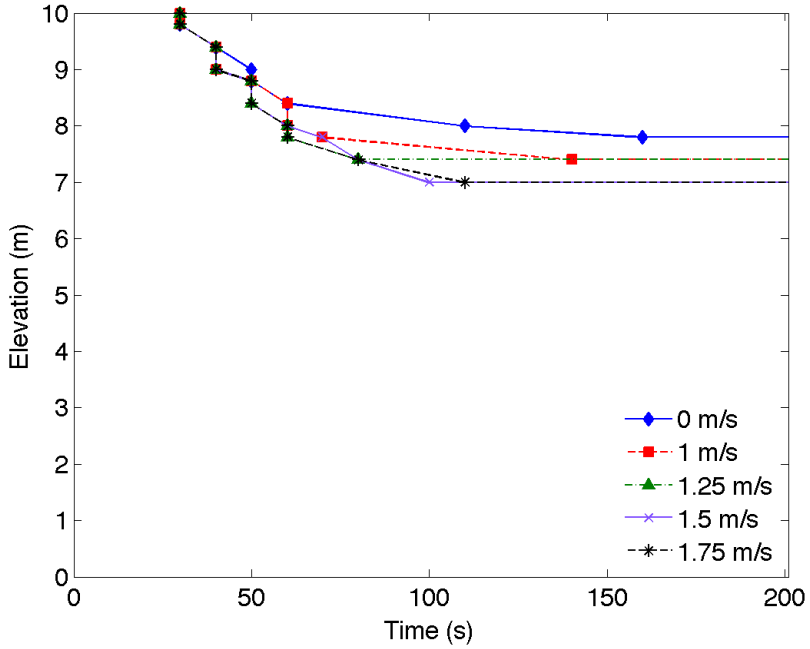

Figure 5.9: SFA Smoke Layer Height

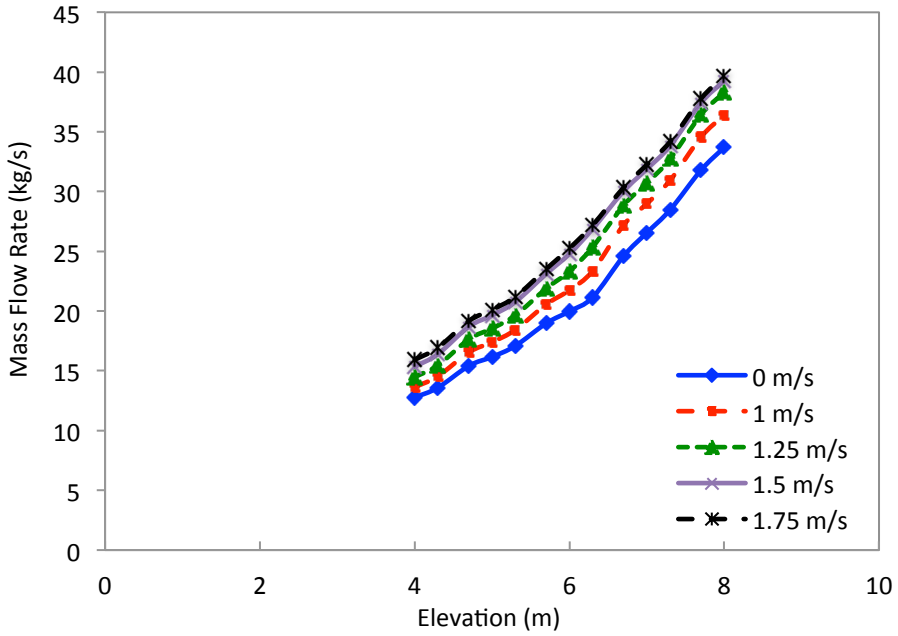

Figure 5.10: SFA Mass Flow Rate

The results show similar affects to the 1 and 2.5 MW fire results. The alpha value is graphed vs. elevation in Figure 5.11. Table 5.3 presents the smoke layer height at 200 seconds, the average and the standard deviation of the alpha value within the plume are taken at steady state.

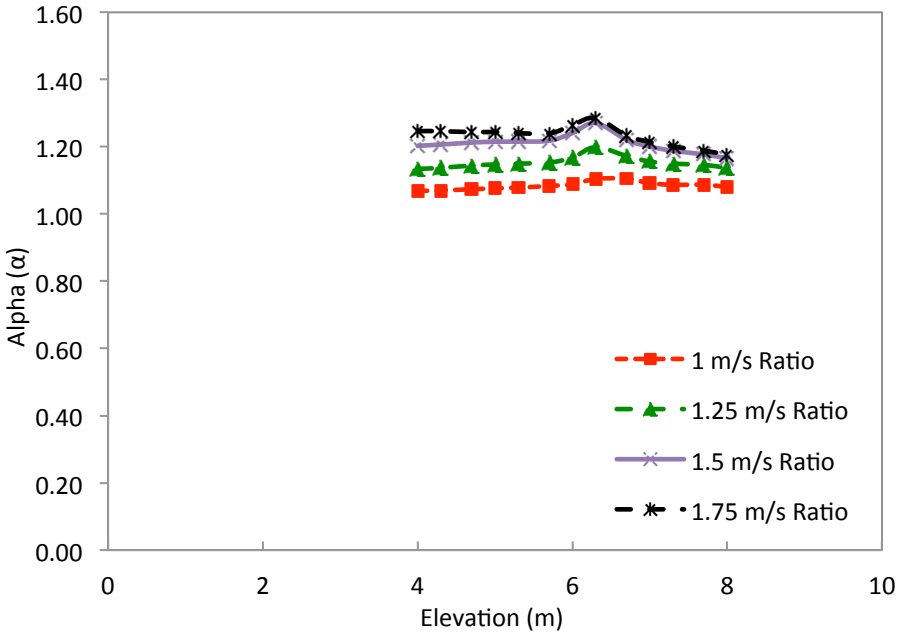

Figure 5.11: SFA Alpha Value Ratio

Table 5.3: SFA Results Comparisons

Makeup Air Velocity	**Smoke Layer Height @ 200 seconds**	**Average (α_{avg})**	**Standard Deviation (σ) of α_{avg}**
0 m/s	7.8 m	-	-
1 m/s	7.4 m	1.08	0.01
1.25 m/s	7.4 m	1.15	0.02
1.5 m/s	7.0 m	1.21	0.03
1.75 m/s	7.0 m	1.24	0.03

The results for the 5 MW fire again show a similar trend to the 1 and 2.5 MW fire. The 1.75 m/s case results in an approximate 24% increase in mass flow rate. The source strength of the fire is double the 2.5 MW fire, and the vent is about 28% larger. Again the vent has less of an effect as the fire size increases.

For the 1 MW fire titled SOB, the vent is placed on the floor level and is 0.5 m high by 0.6 m wide. The vent is aligned in the center of the burner and placed 1.2 m away

from the edge of the burner. The smoke layer height and mass flow rate results are shown in Figures 5.12 and 5.13, respectively.

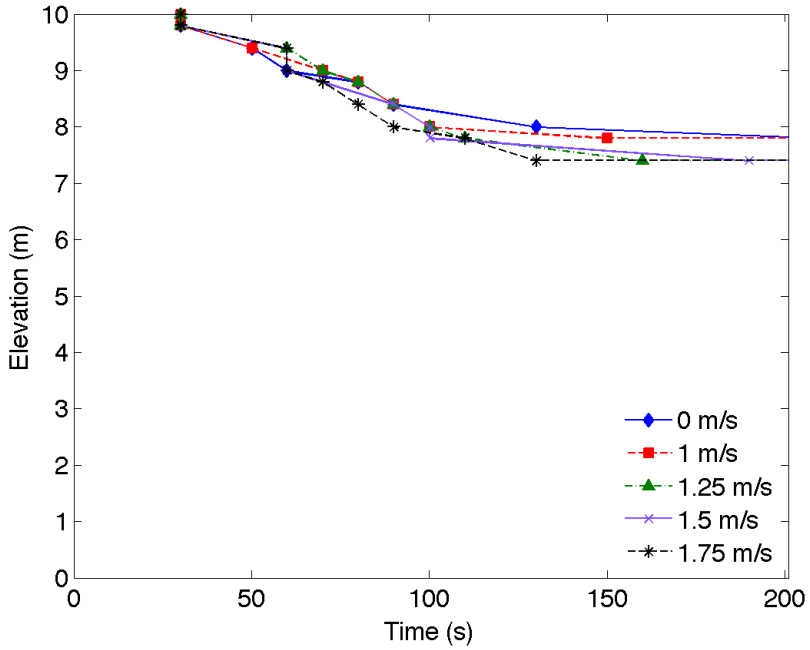

Figure 5.12: SOB Smoke Layer Height

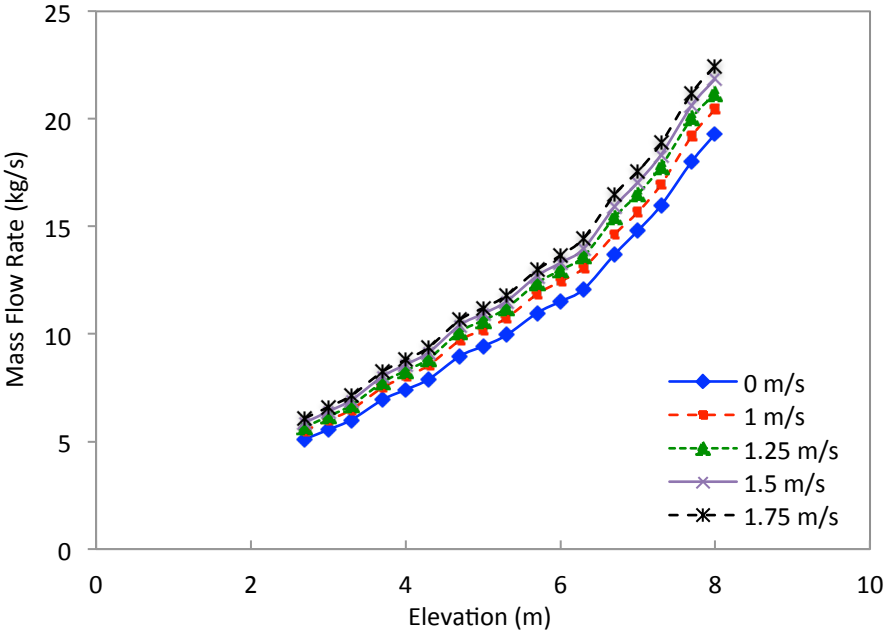

Figure 5.13: SOB Mass Flow Rate

As expected, the smoke layer and mass flow rates are less affected with a smaller vent area of makeup air. The alpha value is graphed vs. elevation in Figure 5.14. Table 5.4 presents the smoke layer height at 200 seconds, the average and the standard deviation of the average alpha value within the plume are taken at steady state.

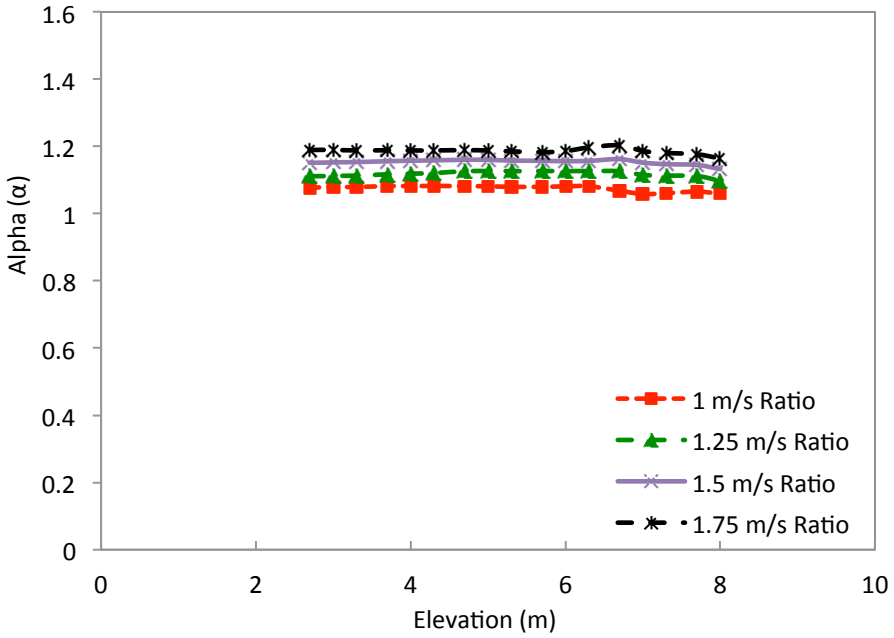

Figure 5.14: SOB Alpha Ratio

Table 5.4: SOB Results Comparisons

Makeup Air Velocity	**Smoke Layer Height @ 200 seconds**	**Average (α_{avg})**	**Standard Deviation (σ) of α_{avg}**
0 m/s	7.8 m	-	-
1 m/s	7.8 m	1.07	0.01
1.25 m/s	7.4 m	1.11	0.01
1.5 m/s	7.4 m	1.14	0.01
1.75 m/s	7.4 m	1.18	0.01

With a vent 50% smaller than the SOA, 1 MW fire case, the results show the makeup air has less of an effect on the fire. The alpha value at 1.75 m/s makeup air is 18% compared to the 39% SOA simulation. This is close to double the percentage increase

in smoke production and aligns with double the vent size. Overall, the smoke layer does not descend more than 0.4 m with the smaller vent. It is concluded that this small of a vent has very little significance in the smoke layer clear height.

For the 1 MW fire titled SOA_rvent, the vent is raised by half the mean flame height, and begins at an elevation of 1.3 m. The vent is 1 m tall (extends from 1.3 to 2.3 m in the z-direction), and is 0.6 m wide. The vent is aligned in the center of the burner and placed 1.2 m away from the edge of the burner. The only difference between this simulation and the SOA simulation is that the vent is raised by 1.3 m. The smoke layer height and mass flow rate results are shown in Figures 5.15 and 5.16, respectively.

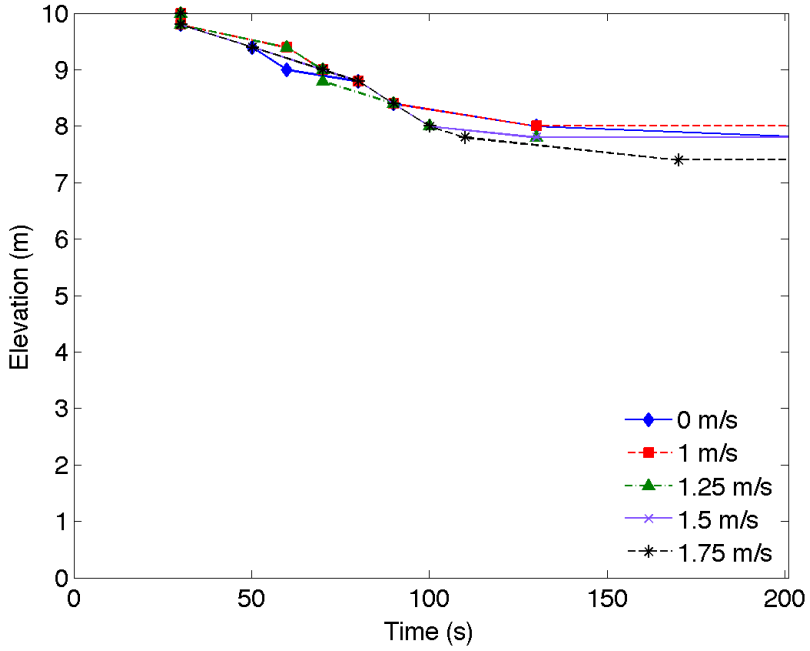

Figure 5.15: SOA_rvent Smoke Layer Height

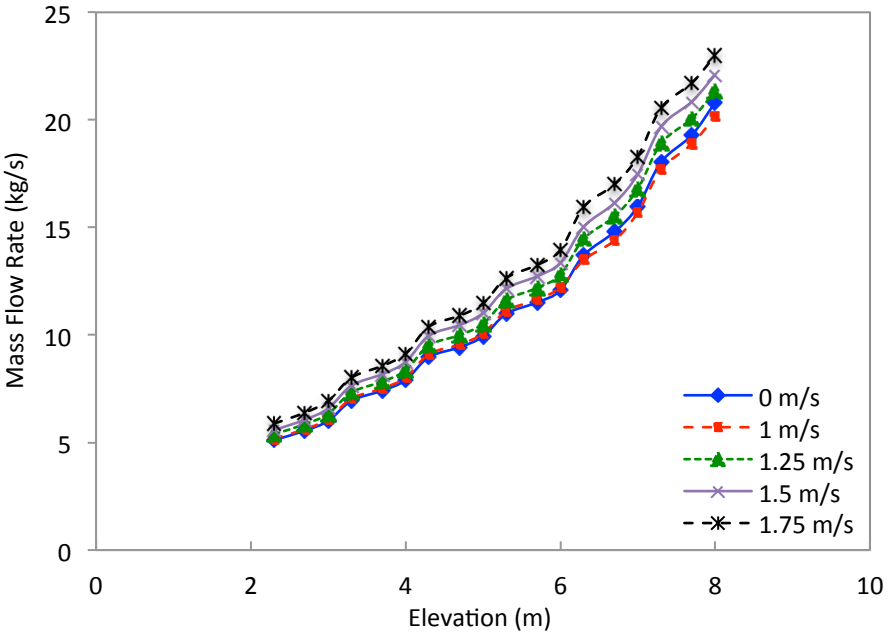

Figure 5.16: SOA_rvent Mass Flow Rate

The alpha value is graphed vs. elevation in Figure 5.17. Table 5.5 presents the smoke layer height at 200 seconds, the average and the standard deviation of the alpha value within the plume are taken at steady state.

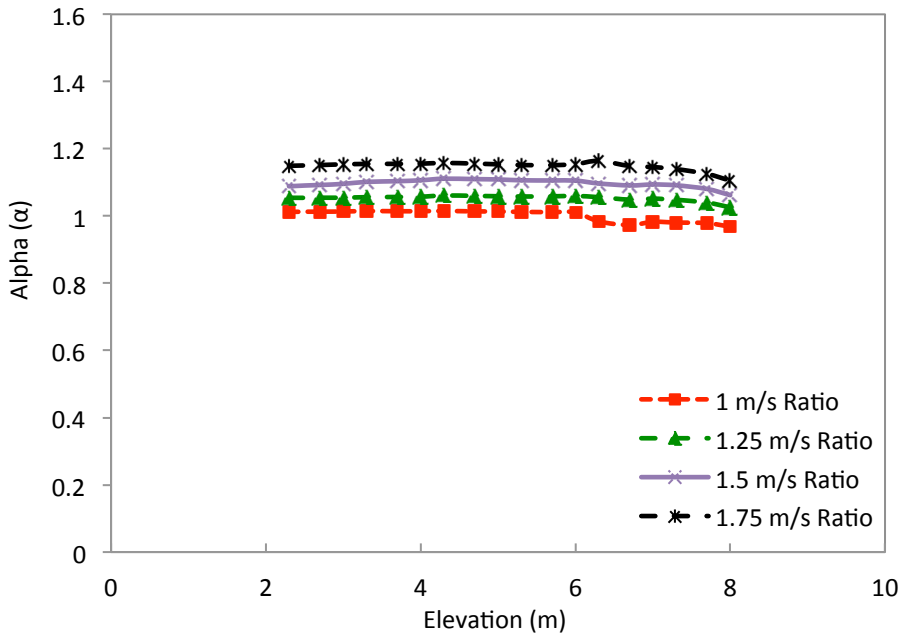

Figure 5.17: SOA_rvent Alpha Ratio

Table 5.5: SOA_rvent Results Comparisons

Makeup Air Velocity	**Smoke Layer Height @ 200 seconds**	**Average (α_{avg})**	**Standard Deviation (σ) of α_{avg}**
0 m/s	7.8 m	-	-
1 m/s	8.0 m	1.00	0.01
1.25 m/s	7.8 m	1.05	0.008
1.5 m/s	7.8 m	1.09	0.01
1.75 m/s	7.4 m	1.14	0.01

When compared to the SOA 1 MW case, it Figure 5.26 Standard Vent Shifted is clear that the raised vent has much less of an effect on the smoke layer height and mass flow rate. For the 1 m/s makeup air velocity, the smoke layer stabilizes at 8 m and the smoke production rate is the same as that for the 0 m/s velocity case. Thus, the raised vent with a 1 m/s makeup air velocity does not affect the fire significantly. The 1.75 m/s velocity causes the smoke layer to descend 0.6 m from its designed stabilization

height, and has an average alpha value of 1.14. The results indicate that the elevation of the vent significantly affects the smoke production increase.

If the makeup air strikes the flame above the half the flame height less smoke production results than for cases where the makeup air strikes the flame at its base. The alpha value of 1.75 m/s case varies from 39% for the vent on the floor, opposed to the 14% with the vent raised to half the mean flame height.

For the 1 MW fire titled SOA_rdoor, the vent is larger than the other cases. In this case the simulation title refers to the vent as a door because its size is comparable to a door, however, the door performs the same function as the other vents. The door is raised by half the mean flame height, and begins at 1.3 m. The door is 2 m tall (extends from 1.3 to 2.3 m in the z-direction), and is 1 m wide. The door is aligned in the center of the burner and placed 1.2 m away from the edge of the burner. The smoke layer height and mass flow rate results are shown in Figures 5.18 and 5.19, respectively.

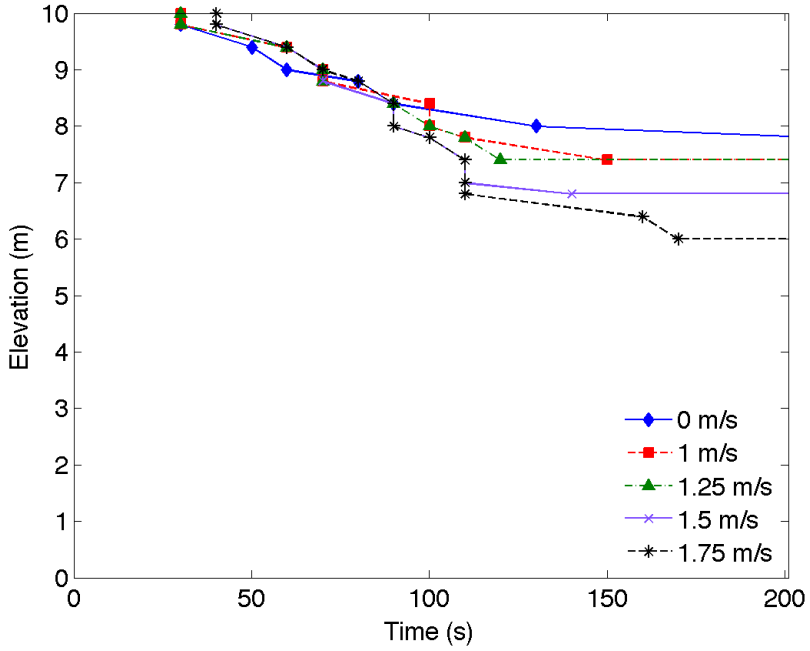

Figure 5.18: SOA_rdoor Smoke Layer Height

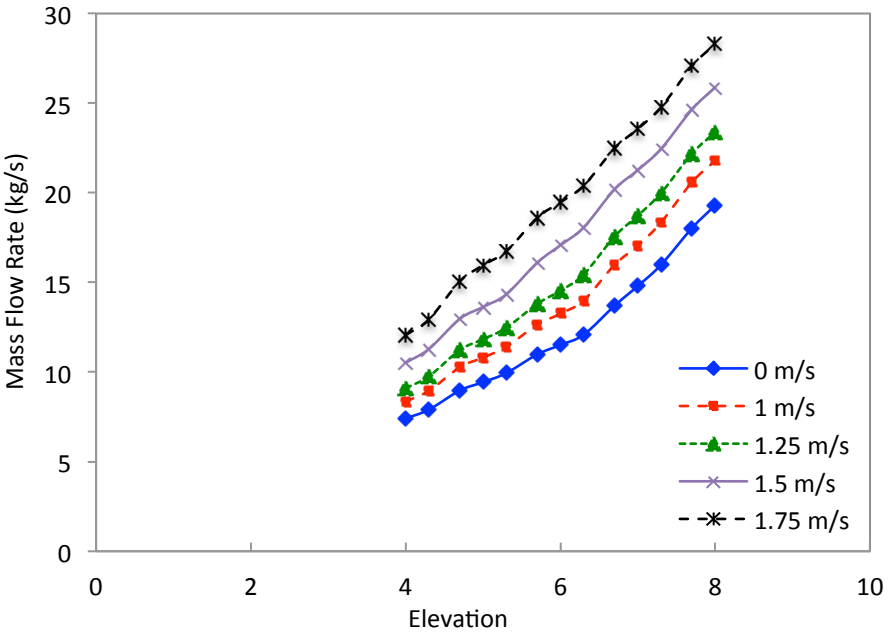

Figure 5.19: SOA_rdoor Mass Flow Rate

The results in Figure 5.18 and 5.19 show that the large volume of makeup air has a significant effect on the smoke layer height and the mass flow rate. However, this

significant increase still shows that the mass flow rate increase is relatively steady when compared to the 0 m/s velocity case. The alpha value is graphed vs. elevation in Figure 5.20. presents the smoke layer height at 200 seconds, the average and the standard deviation of the alpha value within the plume are taken at steady state.

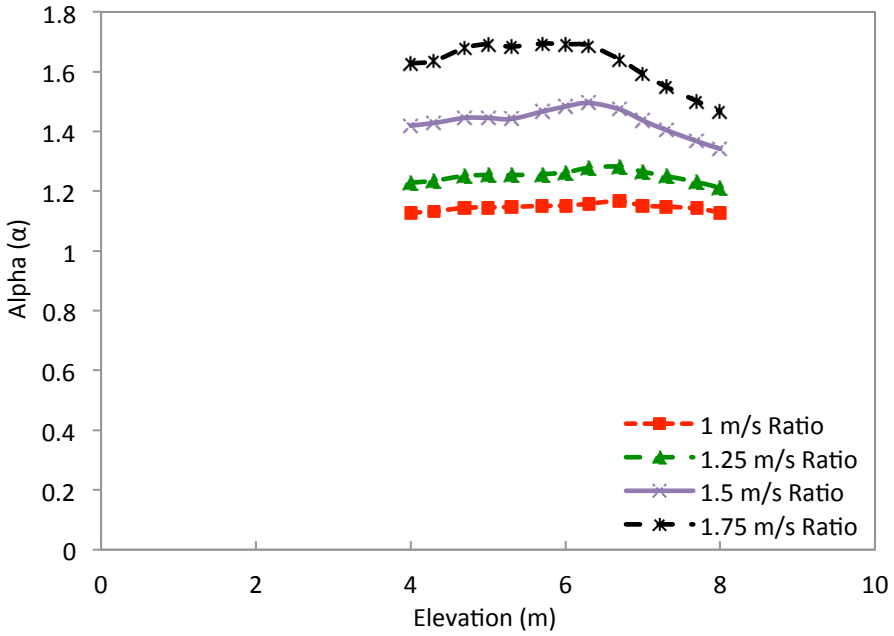

Figure 5.20: SOA_rdoor Smoke Layer Height

Table 5.6: SOA_rdoor Results Comparisons

Makeup Air Velocity	**Smoke Layer Height @ 200 seconds**	**Average (α_{avg})**	**Standard Deviation (σ) of α_{avg}**
0 m/s	7.8 m	-	-
1 m/s	7.4 m	1.15	0.01
1.25 m/s	7.4 m	1.25	0.02
1.5 m/s	6.8 m	1.43	0.04
1.75 m/s	6.0 m	1.62	0.07

The results in Figure 5.20 show that the alpha values for the greater velocities are not as steady as elevation increases. For both the 1.5 and 1.75 m/s velocity values the alpha value decreases during the last 2 meters of the plume, before the formation of the smoke layer, and the standard deviation is higher than in most other simulations

with a value of 4 and 7% respectively. The validity of taking an average value for this simulation will further be discussed in Section 5.3.

Overall the results show that the raised door had a large effect on the smoke layer and mass flow rate. However, the smoke layer tool, and the smoke view file, both indicate that this significant effect does not destroy the formation of a smoke layer. The Smokeview images of Temperature and Smoke at 200 seconds are shown in Figure 5.21 and Figure 5.22, respectively.

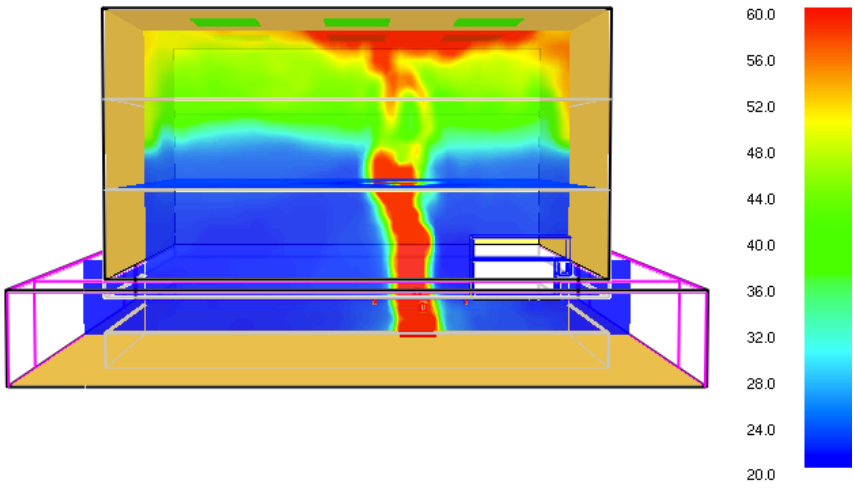

Figure 5.21: Smokeview Temperature Profile taken at 200 seconds

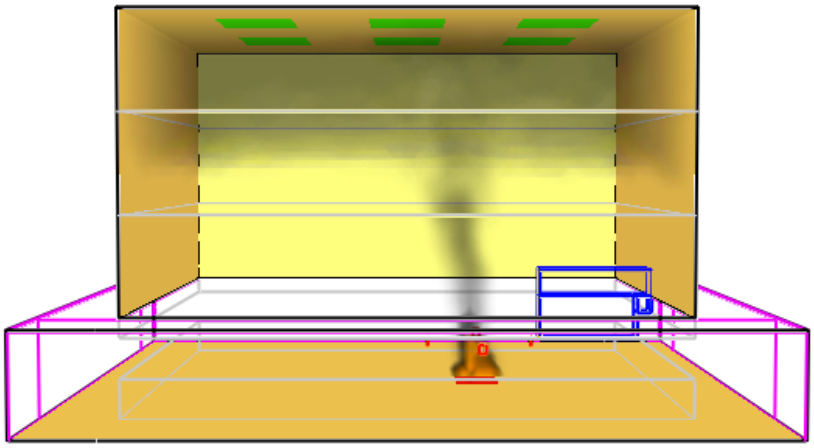

Figure 5.22: Smokeview Profile of Soot Mass Fraction (smoke) taken at 200 seconds

With the results presented in Section 5.1, and additional cases presented in section 5.2, an engineering tool is developed and explained in Section 5.3.

5.2 Special Cases

Additional simulations are run in order to evaluate the effects of the duct mounted makeup air vent location with respect to the fire.

5.2.1 Additional Simulations - Vent located on the floor

The vent configuration for the simulations titled SOA, STA and SFA all have similar characteristic configurations as the duct mounted makeup air vent located on the floor. The height of the vent is equal to half the mean flame height, and the width is equal to 0.6 meters. In order to assess if the orientation of the vent has a major influence on smoke production, an additional simulation is run to compare the same size vent with the height and width length switched in both directions. The new simulation is run for the 1 MW case, the vent is 0.6 m tall and 1 m wide. The velocity induced by the vent for both simulations is 1.75 m/s. The smoke layer height and mass flow rate results are shown in Figure 5.23 and 5.24. The new simulation is labeled “Standard vent flip”, while the original SOA simulation is labeled “Standard Vent” in the legend of the following figures.

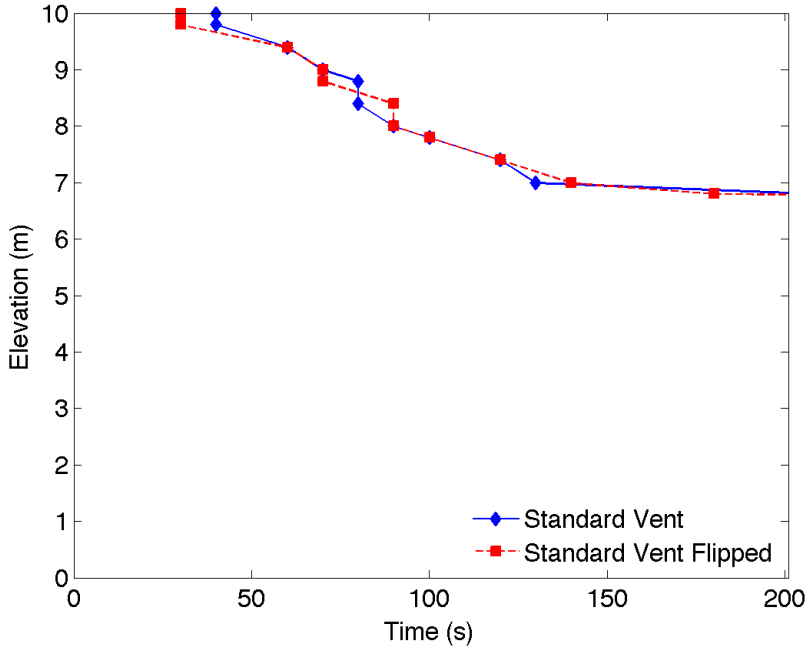

Figure 5.23: Smoke Layer Height of Vent Orientation 1 MW fire

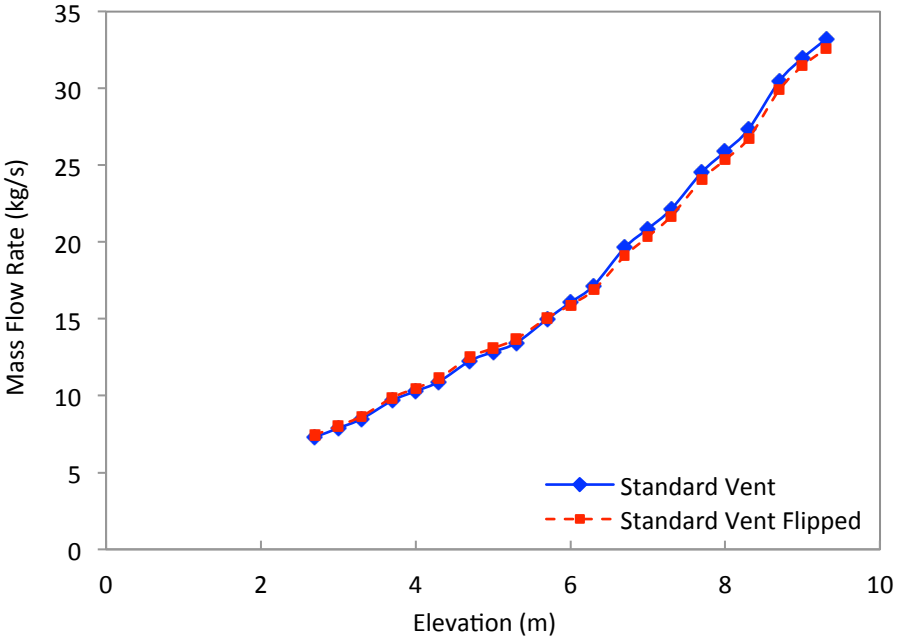

Figure 5.24: Mass Flow Rate of Vent Orientation for 1 MW fire

The results from Figure 5.23 and 5.24 indicate that there is no significant difference between the two simulation configurations.

Another simulation is also run to compare the location of the duct-mounted makeup air vent in regards to its alignment with the fire burner. In all of the simulations previously discussed, the vent is centrally aligned with the burner. An additional simulation is run which shifts the edge of the vent so that the edge of the vent is approximately aligned with the center of the burner. The size of the vent is consistent between the two simulations, and are both run with a 1.75 m/s velocity. Figures 5.25 and 5.26 compare the Smokeview image of original configuration SOA, with the new simulation with the shifted vent.

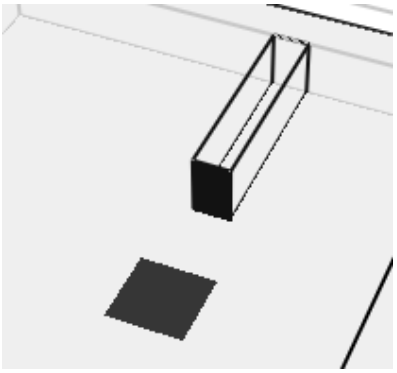

Figure 5.25 Standard Vent centrally Aligned

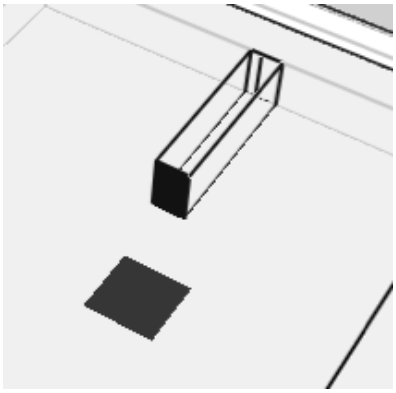

Figure 5.26 Standard Vent Shifted

The smoke layer height and mass flow rate results are shown in Figure 5.27 and 5.28. The new simulation is labeled “Standard vent shift”, while the original SOA simulation is labeled “Standard Vent” in the legend of the following figures.

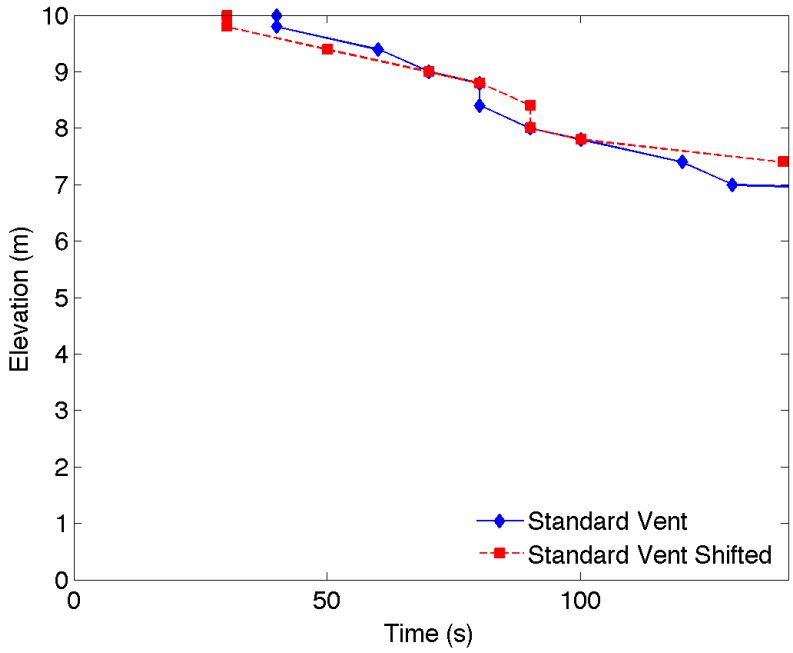

Figure 5.27: Smoke Layer Height of Vent Alignment for 1 MW fire

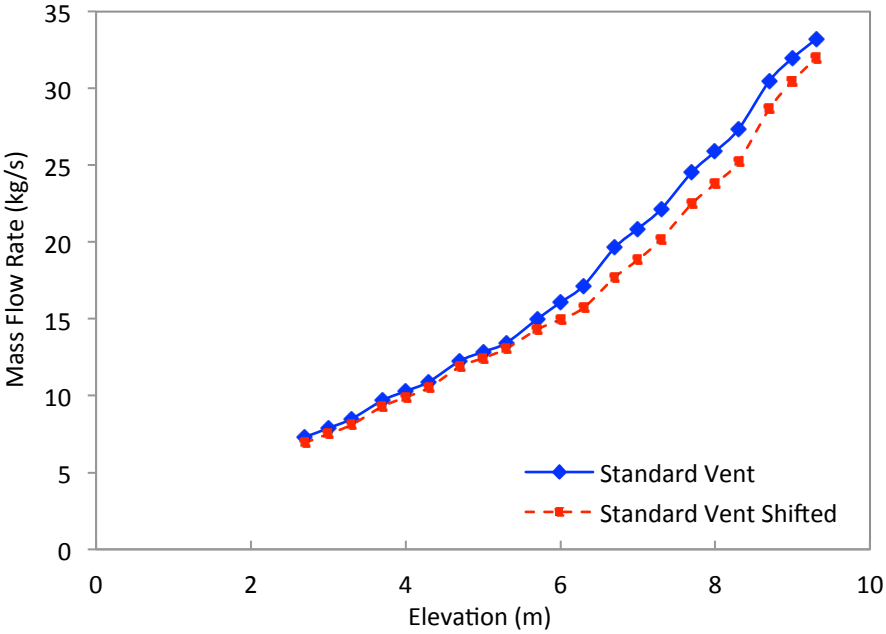

Figure 5.28: Mass Flow Rate of Vent Alignment for 1 MW fire

When the vent is shifted in this manner, the forced mixing of the makeup air with the fire is reduced. This mixing causes less of an effect on the volume of smoke production, evident in Figure 5.28. As this effect is small the smoke layer height does

not descend significantly. The results conclude that center alignment, creates a worse case scenario.

5.2.2 Additional Simulations - Vent located at Various Elevations

The simulations discussed in Section 5.1.2 include configurations where the vent and door are raised in elevation, and strike the flame at different reference elevations. In order to determine which scenario leads to more smoke production and a deeper smoke layer, the following simulations are run. The following simulations are run with a makeup air velocity of 1.75 m/s.

The simulation titled SOA_rvent in Section 5.1.2 refers to a 1 MW fire with the vent raised by half the mean flame height, which is approximated as 2.2 m. In this case the vent is the same size as the original 1 MW simulation titled SOA, with a height of 1 m and a width of 0.6 m. The simulation titled SOA strikes the flame from 0 m – 1 m in elevation and while the simulation titled SOA_rvent strikes the flame 1.3 m – 2.3 m in elevation. Both vents strike the flame region with the same volume flow. An additional simulation is run so the same size vent strikes the plume region, above the approximate mean flame height, from 2.3 to 3.3 m, titled SOA_rvent2. The smoke layer height and mass flow rate results are compared in Figures 5.29 and 5.30 respectively. Table 5.7 summarizes the configuration differences and smoke layer height results.

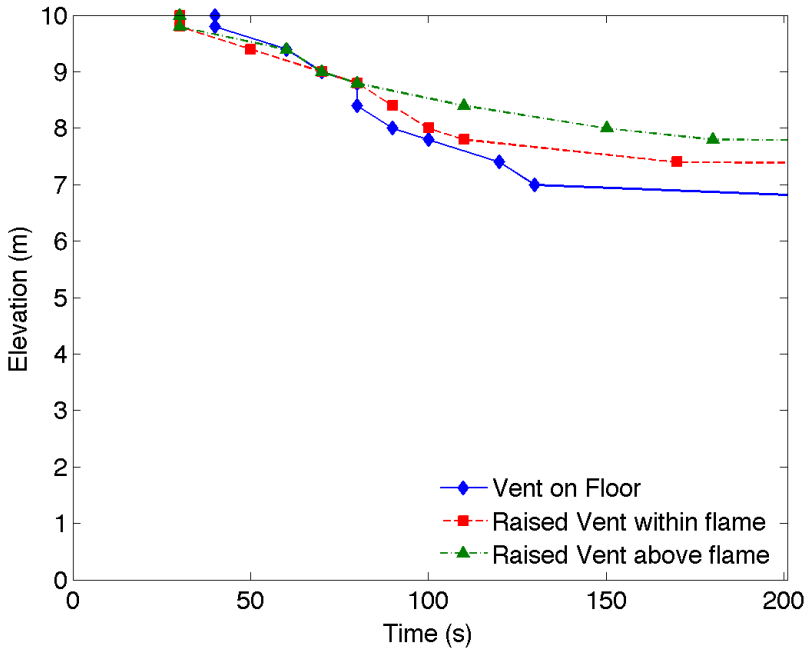

Figure 5.29: Smoke Layer Height of Vent elevation modifications for 1 MW fire

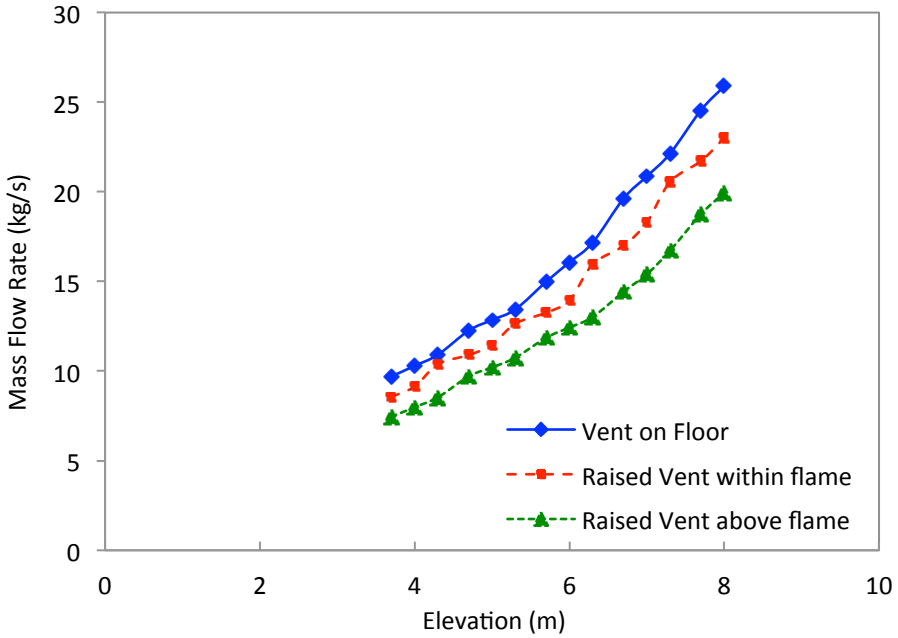

Figure 5.30: Mass Flow Rate of Vent Elevation Modifications for 1 MW fire

Table 5.7: Results for Vent Elevation Modifications

Simulation Reference Title	Simulation Title	Elevation in Z	Vent Area	Smoke Layer Height
Vent on Floor	SOA	0 – 1 m	0.6 m^2	6.8
Raised Vent Within Flame	SOA_rvent	1.3 – 2.3 m	0.6 m^2	7.4
Raised Vent Above Flame	SOA_rvent2	2.3 – 3.3 m	0.6 m^2	7.8

The results indicate that the smoke layer height and mass flow rate are affected significantly by the elevation of the makeup air vent. The volume of smoke production, and therefore the smoke layer height, show the most substantial effects when the vent is located on the floor.

With the vent located on the floor, the smoke layer stabilizes at approximately 6.8 m, while the smoke layer stabilizes at 7.4 and 7.8 m for the raised vents. The raised vent with the vent still within the flame region produces about 10% less mass flow rate, while the raised vent above the flame region produces about 30% less mass flow rate compared to the vent on the floor. This suggests that when the makeup air strikes the fire from 0-1 m above the base, i.e. in the lower half of the flame height, the volume of smoke is increased most drastically.

5.2.3 Additional Simulations - Door located at Various Elevations

A similar set of simulations is run with a larger vent referred to as a 'door' in Section 5.2.1. The simulations are referenced by the simulation titled "SOA_rdoor" in Section 3.4.3. In the following simulations the fire size is 1 MW, and the vent is run with a 1.75 m/s velocity of makeup air.

The door is 1 m wide, and 2 m tall. The simulation SOA_rdoor refers to a simulation where the vent is raised to from 1.3 m to 3.3 m in elevation. This vent configuration therefore strikes half the flame region and half the plume region. Additional simulations are run where the door is set on the floor from 0 – 2 m in elevation, and also above the mean flame height from 2.3 to 4.3 m, titled SOA_door and SOA_rdoor2, respectively. The three simulations strike the flame or plume at different elevations, but retain the same volume flow rate of makeup air. The smoke layer height and mass flow rate results are compared in Figures 5.31 and 5.32, respectively. Table 5.8 summarizes the configuration differences and smoke layer height results.

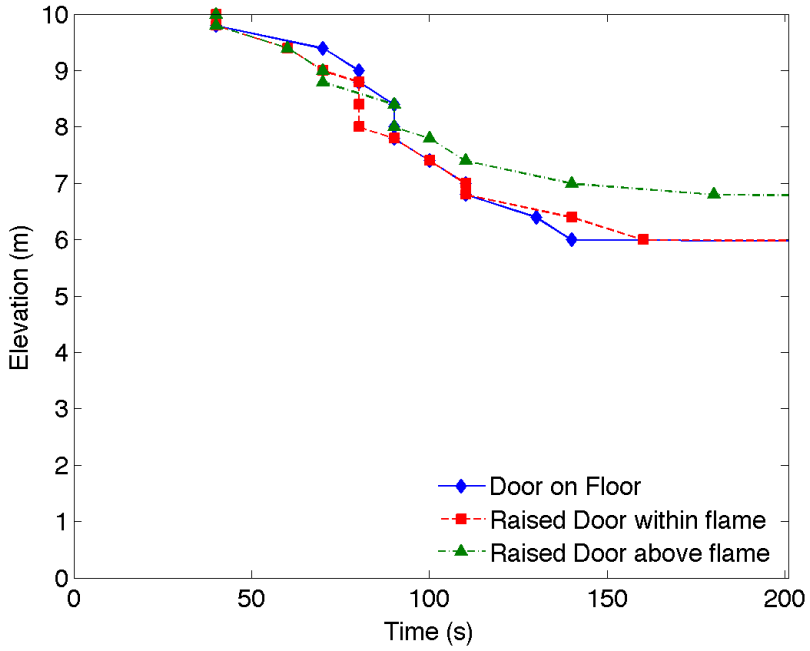

Figure 5.31: Smoke Layer Height for Door Elevation Modifications for 1 MW fire

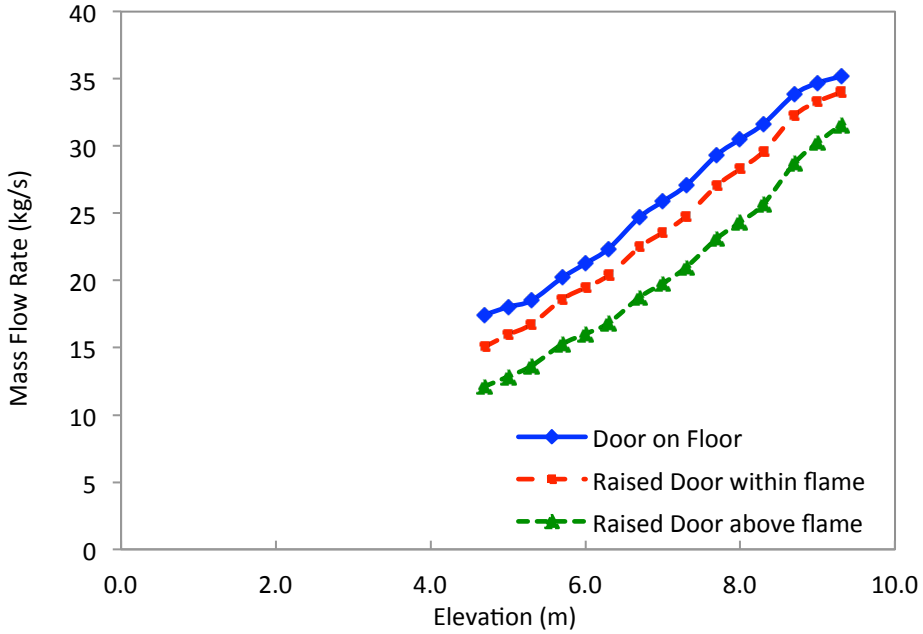

Figure 5.32: Mass Flow Rate for Door Elevation Modifications for 1 MW fire

Table 5.8: Results for Door Elevation Modifications

Simulation Reference Title	Simulation Title	Elevation in Z	Vent Area	Smoke Layer Height
Door on Floor	SOA_door	0 – 2 m	2 m^2	6.0
Raised Door within flame	SOA_rdoor	1.3 – 3.3 m	2 m^2	6.0
Raised Door above flame	SOA_rdoor2	2.3 – 4.3 m	2 m^2	6.8

The raised door modification results conclude similar trends compared to the raised vent. The door located on the floor striking the entire flame region creates a considerable increase in mass flow rate when compared to the door striking both the flame region and plume region. The smoke layer height results show the smoke layer stabilizes at 6 m for the door on the floor and raised 1.3 m. The Smokeview file illustrating the temperature profile within the compartment at 200 seconds is shown in Figures 5.33 and 5.34.

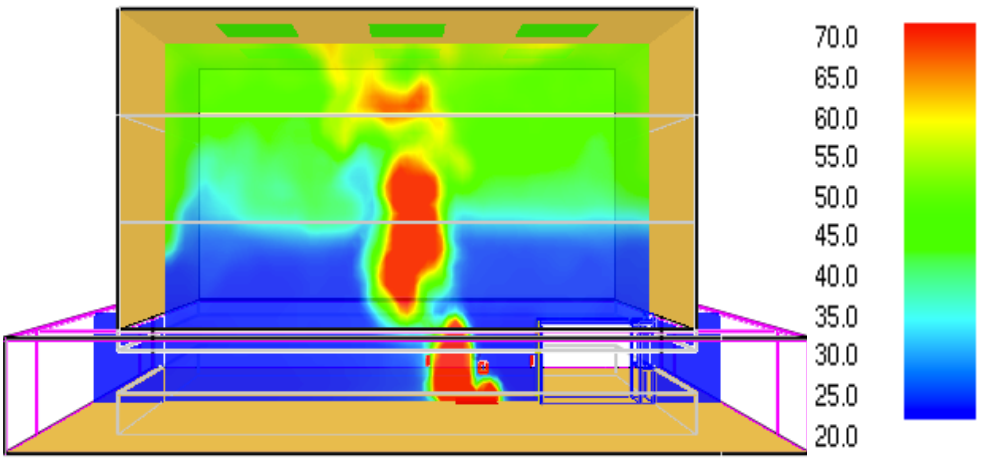

Figure 5.33: Door on Floor

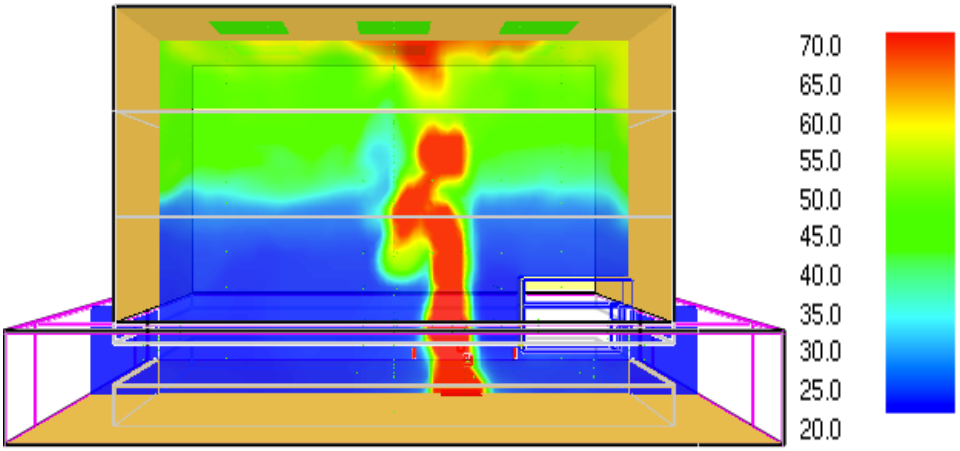

Figure 5.34: Raise Door within flame region

The smoke layer descends a considerable 2 m for these two simulations, however, the Smokeview images indicates that the smoke layer is not destroyed and still holds a stabilized layer.

5.3 Exhaust Modification Engineering Tool

The following section explains the process of creating, and using the exhaust modification engineering tool. The objective of this tool is to create a method that quantifies the excess smoke production from increased makeup air to a modified ceiling exhaust rate. The results in Section 5.2 indicate that the smoke layer descends with increased makeup air. Therefore, the proposed modification to the smoke management system is to increase the volumetric exhaust rate to correct for the excess smoke. The intent of the modified exhaust rate is to stabilize the smoke layer at the original design height despite the increased makeup air velocity.

An engineering design tool is developed to create a method to obtain a modified exhaust rate for a know configuration. The results are scaled so a modified exhaust rate can be found for various makeup air velocities and fire sizes.

5.3.1 Momentum Parameter ($u^*a^*z^*$)

In order to evaluate both the makeup air velocity and fire size, a momentum ratio is created. This parameter measures the strength of the forced horizontal airflow with respect to the buoyant vertical flow generated by the combustion process. The ratio quantifies the energy of air from the duct mounted makeup air towards the flame or plume in the horizontal direction, to the energy provided by the fire source in the vertical direction. This concept is illustrated in Figure 5.35. The image shows a makeup air duct located on floor level and extending to half the mean flame height, as defined in simulations titled SOA, STA, and SFA.

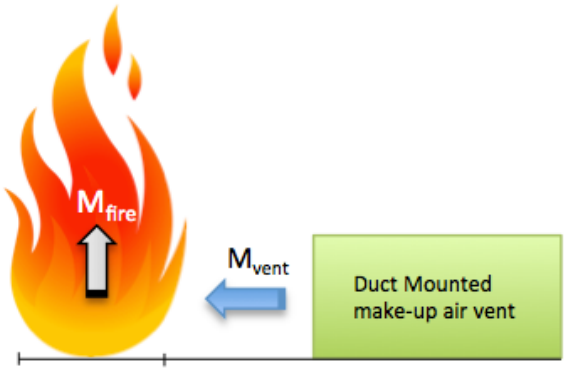

Figure 5.35: Makeup air Rate of Momentum effect on Fire Size

The following equations discuss the assumptions and illustrate the methodology of scaling used to create the characteristic, dimensionless parameter defined as $u^*a^*z^*$.

Momentum is defined as the product of the velocity and mass of an object. In this case, the momentum of makeup air simply translates to the strength of the airflow provided by the duct mounted makeup air and the fire source. The momentum is expressed in time, and further referred to as the rate of momentum. The following scaling methodology defines the characteristic momentum ratios which includes the geometry of the vent and burner. The basic equation of momentum is utilized, however, various assumptions and proportionality constants are included to isolate distinctive design variables. These variables are defined by the configuration of the makeup air vent and fire source.

The components that define the horizontal momentum are shown in Equation 5.2. This equation further defines the mass flow rate of air by the density of ambient air and the volume flow provided by the duct mounted makeup air. The volume flow is equal to the area of the duct-mounted makeup air vent multiplied by the velocity provided by the duct-mounted makeup air vent.

$$\dot{M}_{vent} \sim \dot{m}_{vent} \text{ x } u_{vent}$$

$$\dot{M}_{vent} \sim (u_{vent}\rho_{\infty}A_{vent}) \text{ x } u_{vent} \quad (5.2)$$

$\dot{M}_{vent}$ = horizontal rate of momentum of airflow provided by the duct mounted makeup air vent (kg-m/s^2)

$\dot{m}_{vent}$ = mass flow rate from duct mounted makeup air vent (kg/s)

u_{vent} = velocity of makeup air prescribed by the duct mounted makeup air vent (m/s)

A_{vent} = free area of the duct mounted makeup air vent (m^2)

ρ_{air} = density of ambient air (T_0 = 20°C, ρ= 1.2 m^3/kg)

Although this equation does not consider the distance between the fire and the duct mounted makeup air vent, it assumes the worst-case scenario by setting the fire close to the makeup air duct, as simulated in the FDS configurations.

The vertical rate of momentum is defined by the mass and velocity components of the fire source. The same equation is used to define this vertical momentum, with an additional density differential element. The momentum equation is first stated as Equation 5.3.

$$\dot{M}_{vent} \sim \dot{m}_{fire} \text{ x } u_{vent}$$

$$\dot{M}_{fire} \sim (u_{fire} A_{fire} \rho_{\infty})\, u_{fire} \sim (u_{fire}^2 A_{fire} \rho_{\infty}) \qquad (5.3)$$

$\dot{M}_{fire}$ = vertical rate of momentum of airflow provided by fire source (kg-m/s^2)

$\dot{m}_{fire}$ = mass flow rate of fire source (kg/s)

u_{fire} = velocity of fire source (m/s)

A_{fire} = area of fire (m^2)

ρ_∞ = density of ambient air (ρ= 1.2 m^3/kg)

The fundamental force dominating the vertical flow is the buoyancy force. This force is driven by the density differential between the hot combustion products and ambient air. This differential is relative to the gravitational force dependent on height. In order to approximate the density differential, the ideal gas law assumption is presented. This assumption is used to isolate the relationship between density and temperature. This idea gas law for constant volume and mass, defines the density of the fire proportional to the temperature differential shown in Equation 5.4. The characteristic velocity of the fire, u_{fire}, is defined by an acceleration and length scale, shown in Equation 5.5. The length scale is the height, h, from the base of the fire source.

$$\left(\frac{\rho_{fire}-\rho_\infty}{\rho_\infty}\right) \sim \left(\frac{T_{fire}-T_\infty}{T_\infty}\right) \tag{5.4}$$

T_{fire} = temperature within flame region (℃)

T_∞ = temperature of ambient air (℃)

$$u_{fire} \sim \sqrt{gh\left(\frac{\rho_{fire}-\rho_\infty}{\rho_\infty}\right)} \tag{5.5}$$

The temperature and density relationship in Equation 5.5 is applied to Equation 5.5 to relate the characteristic velocity. The temperature differential between ambient air

and the combustion zone is significant, however, the temperature within the flame region is significant for all strong plumes. The temperature differential divided by the ambient temperature is, therefore, a constant of proportionality` and is assumed the same for all fire sizes and neglected from Equation 5.5, as shown in Equation 5.6.

$$u_{fire} \sim \sqrt{gh\left(\frac{T_{fire}-T_{\infty}}{T_{\infty}}\right)} \tag{5.6}$$

$$u_{fire} \sim \sqrt{gh} \tag{5.7}$$

Equation 5.8 defines the rate of momentum ratio comparing the horizontal to the vertical flow. The ambient density term in both the numerator and denominator reduce the expression. The area of the fire, A_{fire}, is approximated by the known area of the fuel source.

$$\frac{\dot{M}_{vent}}{\dot{M}_{fire}} \sim \frac{(u_{vent}{}^2 \rho_{\infty} A_{vent})}{(u_{fire}{}^2 \rho_{\infty} A_{fire})} \sim \frac{(u_{vent}{}^2 A_{vent})}{(u_{fire}{}^2 A_{fire})} \sim \left(\frac{u_{vent}}{u_{fire}}\right)^2 \left(\frac{A_{vent}}{A_{fire}}\right) \tag{5.8}$$

The velocity and area terms are further defined as a^* and u^* for reference.

$$u^* = \left(\frac{u_{vent}}{u_{fire}}\right)^2, \quad a^* = \left(\frac{A_{vent}}{A_{fire}}\right)$$

As described by Equation 5.6, the characteristic velocity is dependent on gravitational acceleration and height. The reference height (h) is defined at half the mean flame height for all fire sizes. The mean flame height expression defined NFPA 92 is shown in Equation 5.9.

$$z_l = 0.166 Q_c^{2/5} \tag{5.9}$$

The characteristic velocity referenced at half the mean flame height is therefore expressed by Equation 5.10.

$$u_{fire} = \sqrt{g\left(\frac{z_l}{2}\right)} = \sqrt{g\left(\frac{0.166 Q_c^{2/5}}{2}\right)} = \sqrt{g(0.083 Q_c^{2/5})} \tag{5.10}$$

An additional dimensionless parameter is defined in order to account for the elevation of the duct mounted makeup air in relation to the flame height. As established in the 5.2.2, the elevation of the duct and the location at which the air strikes the flame or plume region is a significant factor in the smoke production increase. In order to incorporate this parameter the mid-elevation of the vent defined by Equation 5.11, is referenced over the flame height z_l.

$$z_{mid} = \left(\frac{z_1 + z_2}{2}\right) \tag{5.11}$$

z_{mid} = mid elevation of the makeup air vent

z_1= lowest elevation of the vent

z_2= highest elevation of the vent

This dimensionless elevation parameter is referred as z^*.

$$z^* = \left(\frac{z_{mid}}{z_1}\right)$$

The z^* parameter is multiplied by the momentum ratio in Equation 5.8, to create the scaled momentum ratio parameter defined by the product of $u^*a^*$and z^*.

5.3.1.1. Power Law Curve Fit Method

The parameter $u^*a^*z^*$ is used as the X-axis scale for the engineering tool described in Section 5.3.2. In order to collapse the data that is presented in Section 5.3.2. the $u^*a^*z^*$ parameter is curve fit for a typical power law correlation expressed as:

$$(u^*)^i(a^*)^j(z^*)^k$$

The dimensionless correlating variables are each fit with exponential variables, i, j, and k, that apply to the important physical phenomenon observed. After a trial and error, the best fit function is described as:

$(u^*)^1(a^*)^1(z^*)^{-0.5}$

The velocity and area ratio between the vent and fire are best correlated with an exponential value of 1. The vent elevation factor, z^*, is dependent on the location of the vent relative to the flame height as discussed in Section 5.3.1. The results from Section 5.1 indicate that as the elevation of the vent increases and strikes the flame at higher elevations the average alpha value decreases. It is therefore appropriate that z is related to alpha such that:

$$\alpha \sim \frac{1}{z^*}$$

Therefore a negative exponent value is consistent with the observed trends of alpha. Further, the value of 0.5 best collapsed the data to fit a linear trend further described in Section 5.4. Overall, the values chosen for i, j, and k are consistent with scaling laws and observed physics.

The X-axis is ultimately defined by the following parameters expressed in Equation 5.12.

$$u^*a^*z^* = \left(\frac{u_{vent}{}^2}{g\left(0.083Q_c{}^{\frac{2}{5}}\right)}\right)\left(\frac{A_{vent}}{A_{fire}}\right)\left(\frac{\left(\frac{z_1+z_2}{2}\right)}{0.166Q_c{}^{2/5}}\right)^{-0.5} \quad (5.12)$$

This parameter easily defines the characteristic configuration details into six variables. The equation requires that the fire size and burner area are known, along with the makeup air vent size, elevation, and makeup air velocity. These six configuration variables are illustrated in Figure 5.36.

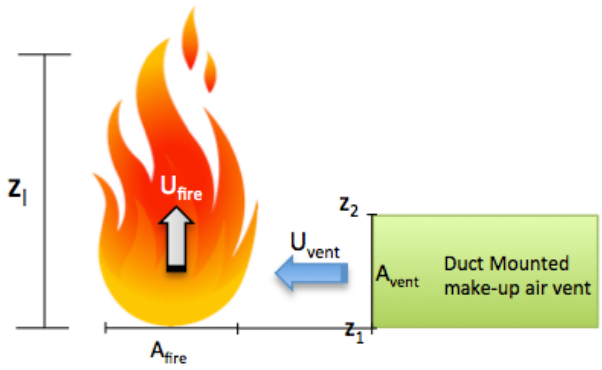

Figure 5.36: Configuration Variables

5.3.2 Smoke Production Design Tool

The results presented in Section 5.1 and 5.2, are compiled and an engineering tool is developed. The engineering tool compares the momentum ratio parameter, $u^*a^*z^*$, to the average alpha value. This comparison quantifies the configuration of the fire and makeup air vent to the increase in smoke production rate numerically determined in the FDS study.

A configuration simulation matrix with all relevant simulations applied to the engineering tool is shown Table 5.9 and 5.10. Table 5.9 identifies the original cases presented in Chapter 3, and include the data for makeup air velocity of 0 m/s, 1 m/s, 1.25 m/s, 1.5 m/s, and 1.75 m/s. Table 5.10 presents the data extracted from the

special cases detailed in Section 5.2 which were run with a makeup air velocity of 1.75 m/s.

Table 5.9: Simulation Matrix Configuration Details (also Table 3.3)

Simulation Name		SOA	STA	SFA	SOB	SOA_rvent	SOA_rdoor
Fire Size (MW)		1	2.5	5	1	1	1
Burner Size (m)		1.2 x 1.2	2 x 2	2 x 2	1.2 x 1.2	1.2 x 1.2	1.2 x 1.2
HRRPUA (kW/m^2)		694.4	625	1250	694.4	694.4	694.4
Total Ceiling Exhaust Rate (m^3/s)		18.66	27.92	39.36	18.66	18.66	18.66
Exterior Wall-mounted Makeup Air Vent Area (m^2)		48	96	120	48	48	48
Duct-mounted Makeup Air Vent	Distance from Edge of Burner (m)	1.2	2	2 m	1.2	1.2	1.2
	Height (m)	1	1.4	1.8	0.5	1	2 m
	Width (m)	0.6	0.6	0.6	0.6	0.6	1 m
	Elevation in z (m)	0 - 1	0 – 1.4	0 – 1.8	0 -0.5	1.3 - 2.3	1.3 – 3.3 m

Table 5.10: Simulation Matrix Configuration Details for Special Cases

Simulation Name		SOA_rvent2	SOA_rdoor2	SOA_door
Fire Size (MW)		1	1	1
Burner Size (m)		1.2 x 1.2	1.2 x 1.2	1.2 x 1.2
HRRPUA (kW/m^2)		694.4	694.4	694.4
Total Ceiling Exhaust Rate (m^3/s)		18.66	18.66	18.66
Exterior Wall-mounted Makeup Air Vent Area (m^2)		48	48	48
Duct-mounted Makeup Air Vent	Distance from Edge of Burner (m)	1.2	1.2	1.2
	Height (m)	1	2	2
	Width (m)	0.6	1	1
	Elevation in z (m)	2.3 – 3.3	2.3 – 4.3	0 - 2

Using the configuration details for each simulation, the $u^*a^*z^*$ value is determined for each FDS simulation. This parameter, along with the corresponding alpha value, is presented in Table 5.11. As explained in Section 5.1.2 the alpha value is taken as an average, and the standard deviation is presented for each point. In addition, to the average value the minimum and maximum alpha values are presented in Table 5.11.

Table 5.11: Simulation Data for Smoke Production Design Tool

Simulation Title	Velocity (m/s)	$\mathbf{u^*a^*z^*}$ **(X-Axis)**	**Average Alpha** ($\boldsymbol{\alpha_{avg}}$) **(Y-Axis)**	Min Alpha (α_{min})	Max Alpha (α_{max})	Standard Deviation (σ) of α_{avg}
SOA	1.00	**0.08**	**1.13**	1.11	1.16	0.01
	1.25	**0.13**	**1.18**	1.17	1.22	0.01
	1.50	**0.18**	**1.28**	1.25	1.31	0.02
	1.75	**0.25**	**1.39**	1.35	1.43	0.03
STA	1.00	**0.03**	**1.08**	1.03	1.12	0.02
	1.25	**0.04**	**1.18**	1.13	1.24	0.02
	1.50	**0.06**	**1.27**	1.22	1.32	0.02
	1.75	**0.09**	**1.31**	1.25	1.35	0.02
SFA	1.00	**0.03**	**1.07**	1.07	1.11	0.01
	1.25	**0.04**	**1.14**	1.14	1.20	0.02
	1.50	**0.06**	**1.19**	1.17	1.27	0.03
	1.75	**0.09**	**1.22**	1.19	1.29	0.03
SOB	1.00	**0.06**	**1.08**	1.06	1.08	0.01
	1.25	**0.09**	**1.12**	1.10	1.13	0.01
	1.50	**0.13**	**1.15**	1.13	1.16	0.01
	1.75	**0.17**	**1.19**	1.16	1.20	0.01
SOA_rvent	1.00	**0.04**	**1.00**	0.97	1.01	0.01
	1.25	**0.07**	**1.05**	1.03	1.06	0.01
	1.50	**0.10**	**1.10**	1.06	1.11	0.01
	1.75	**0.13**	**1.15**	1.11	1.16	0.01
SOA_rdoor	1.00	**0.13**	**1.15**	1.11	1.17	0.01
	1.25	**0.20**	**1.25**	1.19	1.28	0.02
	1.50	**0.28**	**1.43**	1.31	1.50	0.04
	1.75	**0.38**	**1.63**	1.42	1.69	0.07
SOA_rvent2	1.75	**0.10**	**1.06**	1.02	1.08	0.01
SOA_rdoor2	1.75	**0.32**	**1.35**	1.26	1.39	0.04
SOA_door	1.75	**0.58**	**1.76**	1.52	1.86	0.13

The average alpha value is plotted versus $u^*a^*z^*$ in Figure 5.37 for all simulations data sets, and also plotted in Figure 5.38 as one data set with a linear best fit trend line. Each data point is shown with the minimum and maximum value as an error bar.

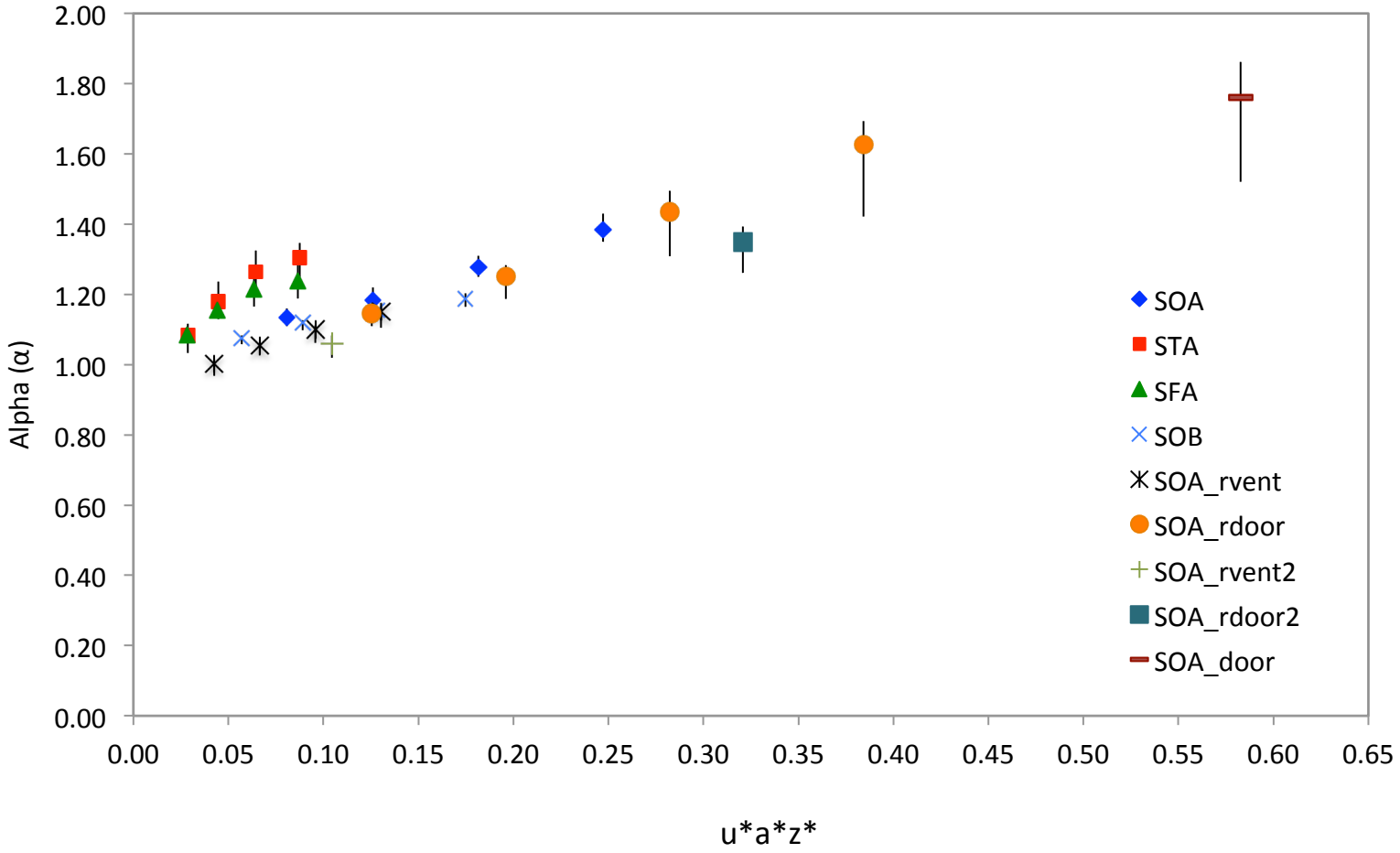

Figure 5.37: Alpha values presented for all data sets

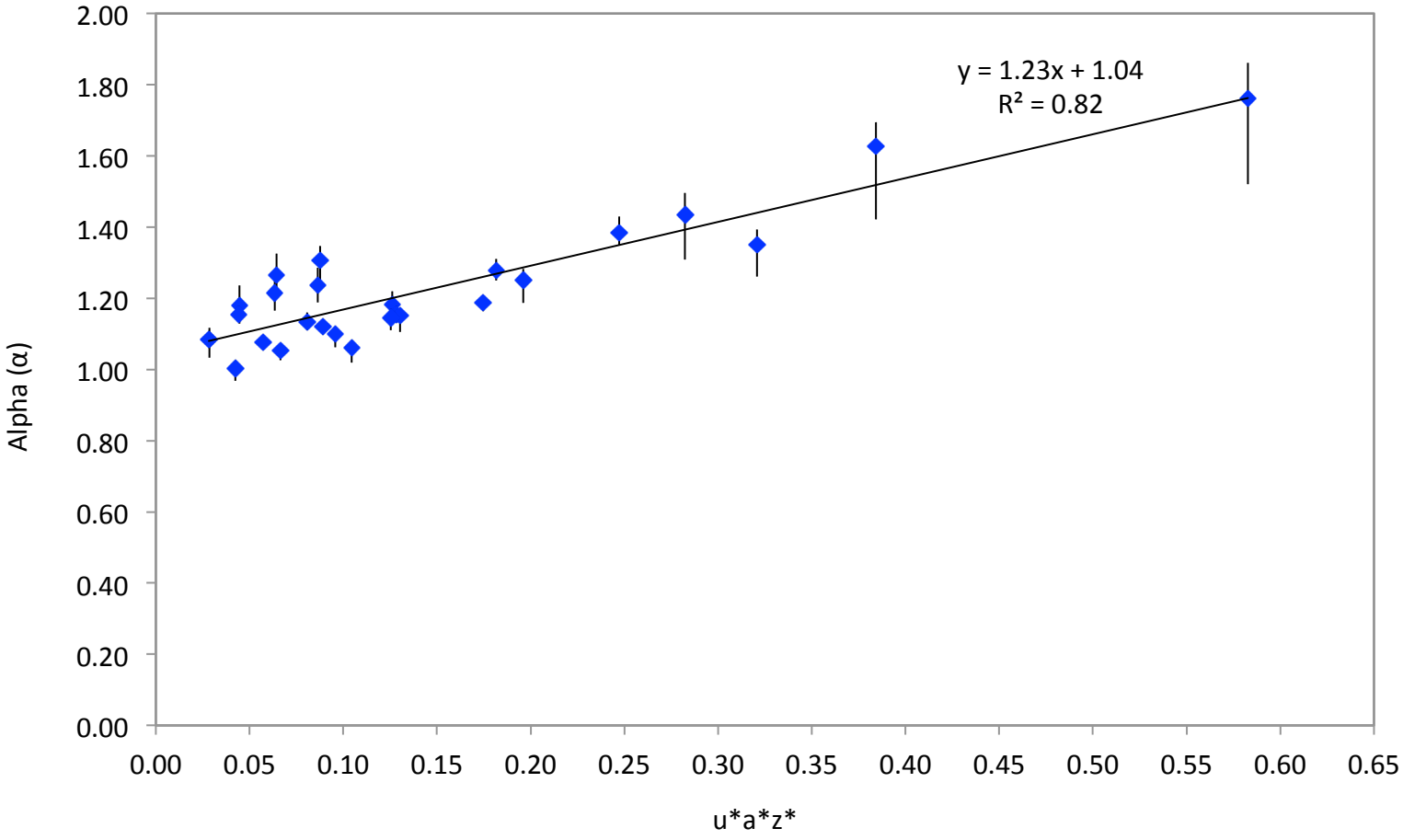

Figure 5.38: Alpha Values for all simulations

The alpha vs. $u^*a^*z^*$ plot shows an established trend for each simulation. As the makeup air velocity increases the momentum ratio parameter, $u^*a^*z^*$, also increases. The relationship for this increase is linear for each simulation configuration. The data is compiled to present a linear best-fit line for the 1 MW, 2.5 MW, and 5 MW fire. The best-fit line also includes the coefficient of determination value, denoted as R-squared on the graph. This value indicates how well the data points fit the correlation.

The results in Figure 5.38 indicate that all fire sizes with multiple simulations detailing different vent configurations align to fit one linear line, with an R-squared value of 0.82. The best-fit line, given by Equation 5.13, is then be used to determine the appropriate alpha value for a given configuration and fire size.

$$\text{Alpha} = 1.23(u^*a^*z^*) + 1.04 \qquad (5.13)$$

The engineering tool therefore requires the calculation of parameter $u^*a^*z^*$, detailed in Equation 5.12, to determine the alpha value for the given characteristic configuration. Section 5.3.3 explains how the alpha value is used to calculate the modified exhaust rate.

5.3.3 Modified Exhaust Rate Calculation

The average alpha value directly defines the modified exhaust rate value by defining it as the percent increase in mass flow rate. The original methodology to determine

the necessary exhaust rate to stabilize a smoke layer at a design elevation is explained in Section 2.4.3. The same process is used to determine the modified exhaust rate, however, the alpha value is introduced to the calculation method. The average alpha value is applied to the simplified axisymmetric mass flow rate equation defined in Equation 5.16, for z greater than or equal to z_l.

$$m_p = 0.071{Q_c}^{1/3}z^{5/3} + 0.0018Q_c \quad (5.16)$$

z_l= limiting elevation (m)

z = distance above base of fire to the smoke layer interface (m)

Q_c= convective portion of the heat release rate (kW)

The alpha average value is multiplied by the original mass flow rate at the z elevation of the intended smoke layer interface, illustrated in Equation 5.17.

$$m_{p(modified)} = \alpha_{avg}(0.071{Q_c}^{1/3}z^{5/3} + 0.0018Q_c)$$

$$m_{p(modified)} = \alpha_{avg}m_p \quad (5.17)$$

$m_{p(modified)}$= modified vertical mass flow rate in axisymmetric plume at smoke elevation (kg/s)

To determine the modified exhaust rate the same process explained in Section 2.4.3 is used with the new modified vertical mass flow rate. The temperature of the smoke

layer is modified using the modified mass flow rate value. This is shown in Equation 5.18.

$$T_{s(modified)} = T_o + \frac{KQ_c}{m_{p(modified)} c_p} \quad (5.18)$$

c_p= specific heat of plume gases (1.0 kJ/kgK)

T_o= ambient temperature (℃)

K = fraction of convective heat release contained in smoke layer, dimensionless

$T_{s(modified)}$= average smoke layer temperature (℃)

The density of smoke is then calculated with the modified temperature value, shown in Equation 5.19.

$$\rho_{modified} = \rho_o + \frac{T_o}{T_{s(modified)}} \quad (5.19)$$

ρ_o= density of air at ambient (kg/m^3)

$\rho_{modified}$= density of smoke (kg/m^3)

Lastly, Equation 5.20 determines the volumetric flow rate using the modified mass flow rate and density of smoke.

$$V_{modified} = \frac{m_{p(modified)}}{\rho_{modified}} \quad (5.20)$$

$V_{modified}$ = volumetric flow rate of smoke exhaust (m^3/s)

The intent of this modification method is to calculate a new volumetric exhaust rate ($V_{modified}$) to stabilize the layer at the intended design height despite the increase in smoke production. The modification method and engineering tool proposed is validated for multiple simulations and discussed Section 5.4.

5.4 Engineering Tool Validation

In order to accept the engineering tool presented in Section 5.3, the modified exhaust rate determined by alpha must be validated in FDS. The following section provides numerous examples of configurations using the modified exhaust rate determined for each individual case given the average alpha value.

Table 5.12 presents each validation simulation run in FDS. The table includes the original exhaust rate to stabilize the layer at 8 m calculated by the method addressed in Section 2.4.3, the average alpha value as determined in Section 5.2.1, and modified exhaust rate value as determined by the method explained in Section 5.3.3. The method to obtain the modified exhaust rate from the alpha value is explained Section 5.3. The modified exhaust is applied to the same simulation configurations with the same makeup air velocity so the ceiling vent exhaust rate is the only variation between simulations. The intent of the modified exhaust rate is to stabilize the layer at the design height, which is 8 m.

Table 5.12: Modified Exhaust Rates for Validation Simulations

Simulation Name	Velocity	Original Exhaust Rate (m^3/s)	Average Alpha (α)	Modified Exhaust Rate (m^3/s)	Figure
SOA	1.25	18.66	1.18	21.79	5.39
	1.75	18.66	1.39	25.44	5.40
SOA_rvent	1.75	18.66	1.15	21.96	5.41
SOB	1.75	18.66	1.19	21.27	5.42
STA	1.75	27.92	1.31	35.57	5.43
SFA	1.75	39.36	1.22	46.60	5.44
SOA_rdoor	1.25	18.66	1.25	23.01	5.45
	1.75	18.66	1.61	29.61	5.46

From the 1 MW fire simulation titled SOA, the make of up air velocity of 1.25 m/s resulted in a numerical alpha value of 1.18 alpha. This same simulation with a 1.75 m/s velocity results in a 1.39 alpha value. The modified exhaust rates are applied, and the results for the 1.25 m/s and 1.75 m/s configurations are shown in Figures 5.39 and 5.40 respectively. In both figures, the original 0 m/s smoke layer height which stabilizes at 7.8 m, is compared to the smoke layer height with the additional makeup air velocity, and the corrected smoke layer height with the modified exhaust rate with the same makeup air velocity. The legend indicates the velocity and exhaust rate used for each simulation.

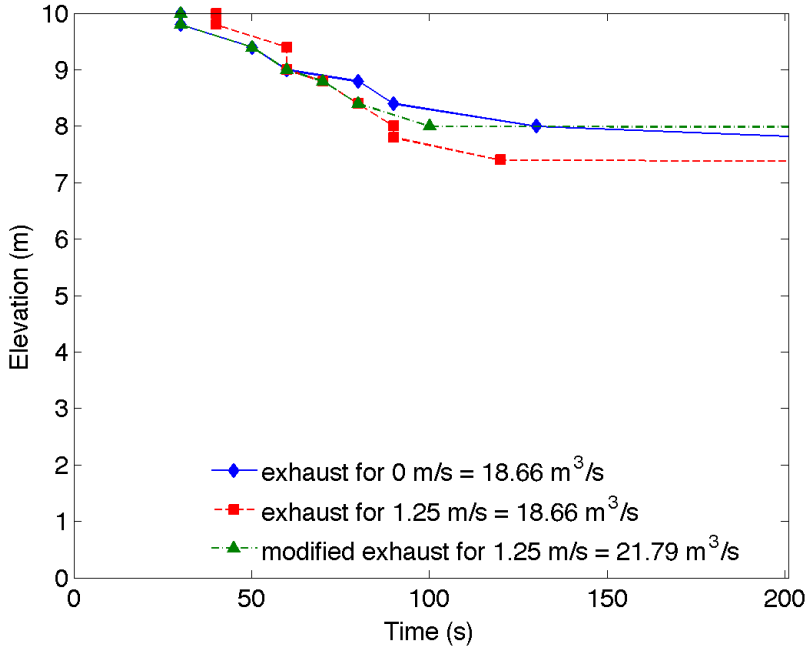

Figure 5.39: Validation Simulation for SOA 1.25 m/s

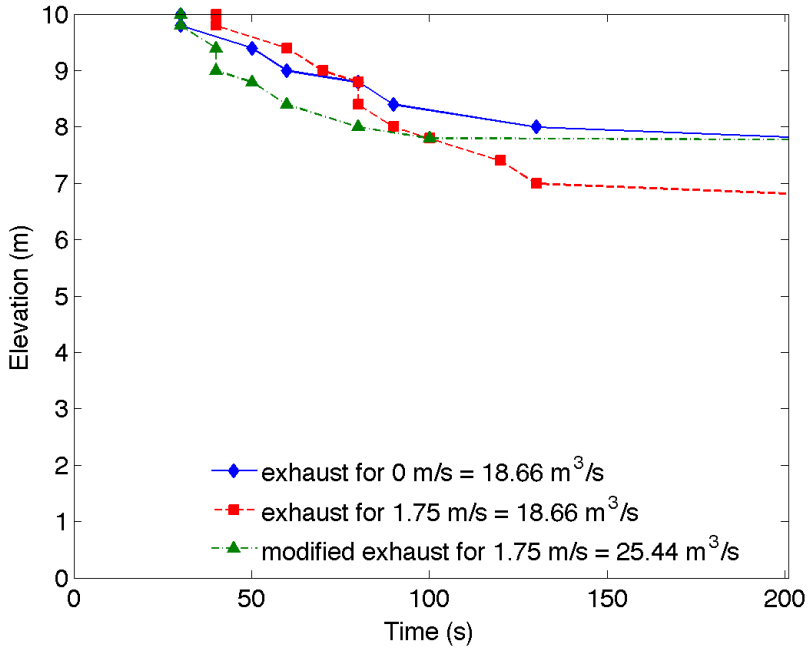

Figure 5.40: Validation Simulation for SOA 1.75 m/s

Both the results in Figures 5.39 and 5.40 indicate that the modified exhaust rate correctly stabilizes the layer at the original smoke layer height with a 0 m/s makeup air velocity. The smoke layer height is approximately 7.8 m.

The same process is validated for the most extreme velocity 1.75 m/s, for the simulations titled SOA_rvent, SOB, STA, and SFA. The configuration details of these simulations are detailed in Section 3.4.3. The smoke layer height of the original 0 m/s velocity case, the 1.75 m/s velocity case, both with the original exhaust rate and with the modified exhaust rate is presented Figures 5.41 - 5.44.

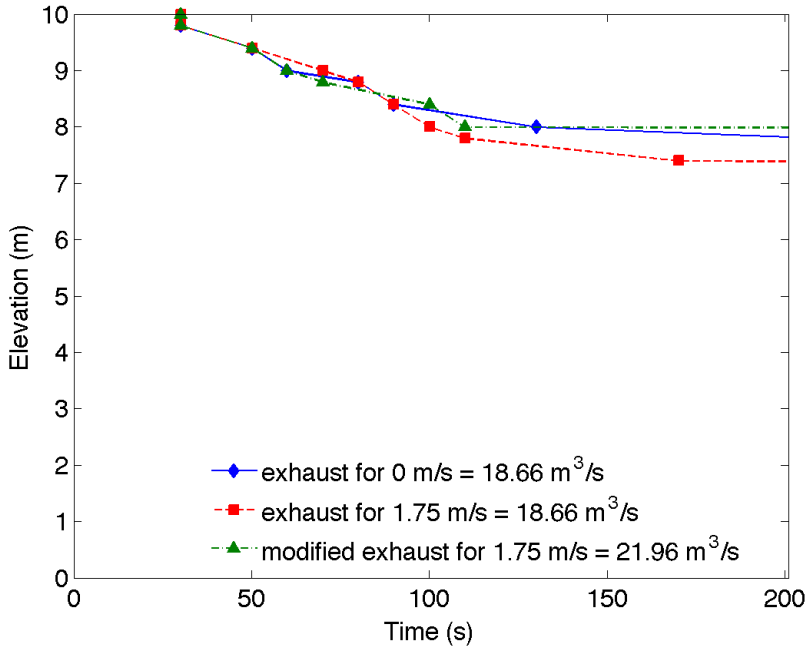

Figure 5.41: Validation Simulation for SOA_rvent 1.75 m/s

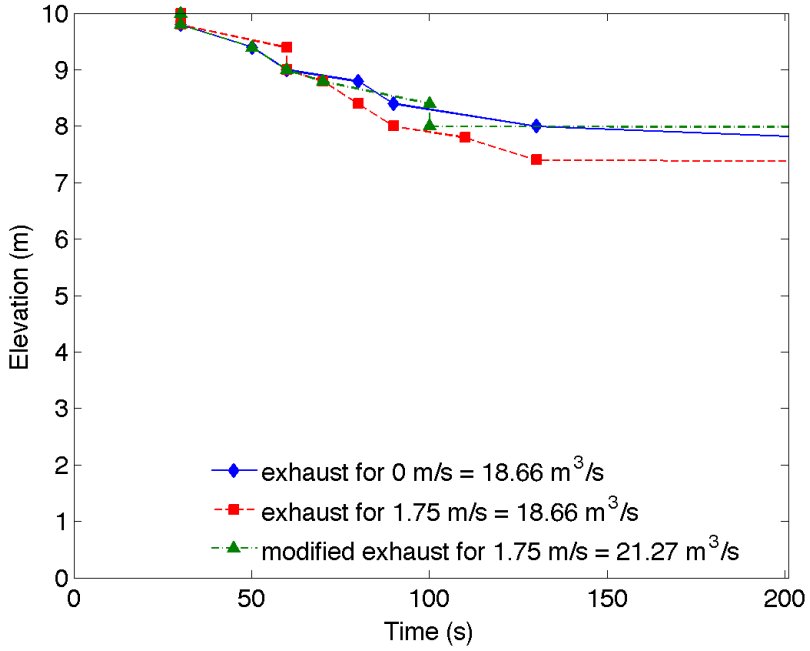

Figure 5.42: Validation Simulation for SOB 1.75 m/s

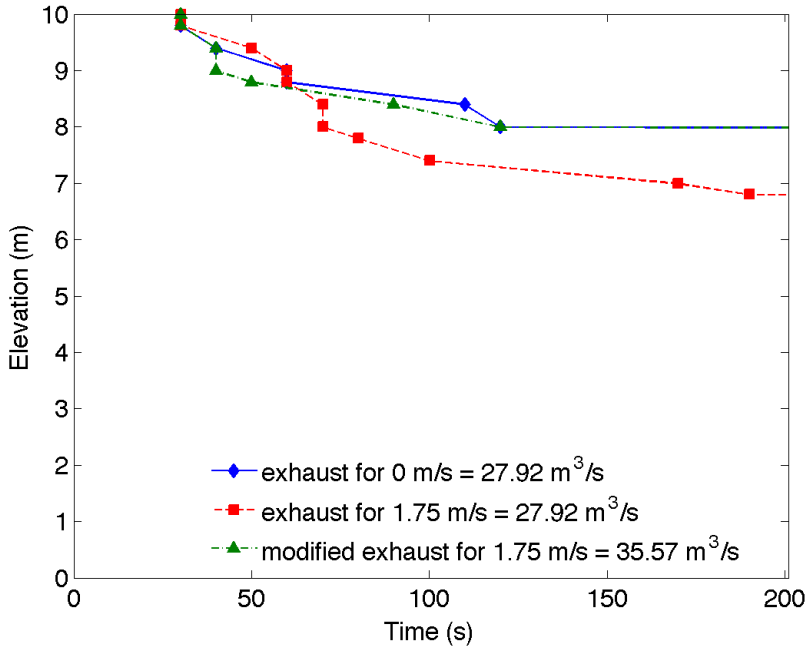

Figure 5.43: Validation Simulation for STA 1.75 m/s

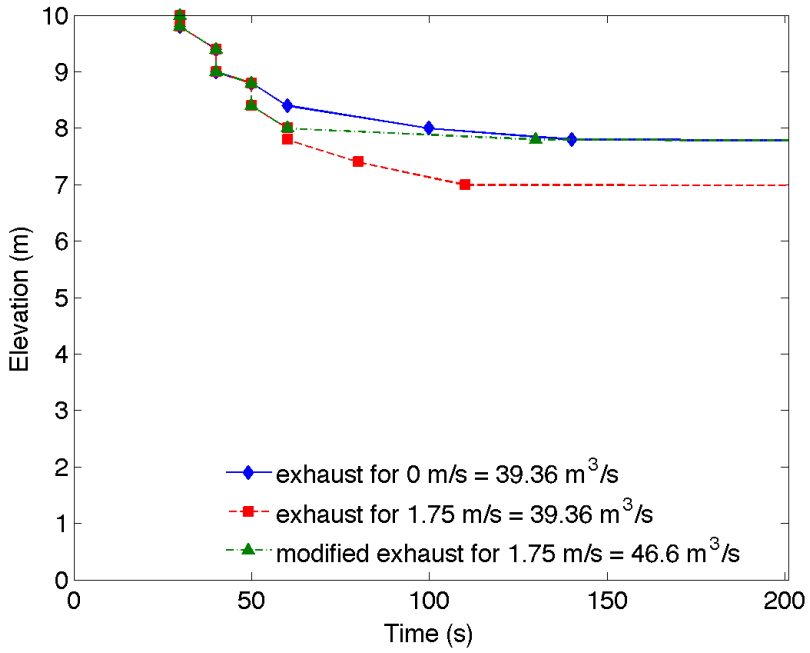

Figure 5.44: Validation Simulation for SFA 1.75 m/s

The results for Figures 5.41 - 5.44, indicate that modified exhaust rate corrects for the additional volume of smoke production by stabilizing the smoke layer at the approximate design height of 8 m.

The SOA_rdoor simulation detailed in Section 3.4.3., is also run to test the alpha values presented in Section 5.2.1. For this simulation configuration the alpha values had standard deviation values exceeding 2% for velocities above 1 m/s, as presented in Table 5.6. In order to determine if taking an average value is appropriate the modified exhaust rates for 1.25 m/s and 1.75 m/s are run to evaluate the smoke layer height. The smoke layer height results are shown in Figure 5.45 and Figure 5.46, for the 1.25 m/s and 1.75 m/s velocity, respectively.

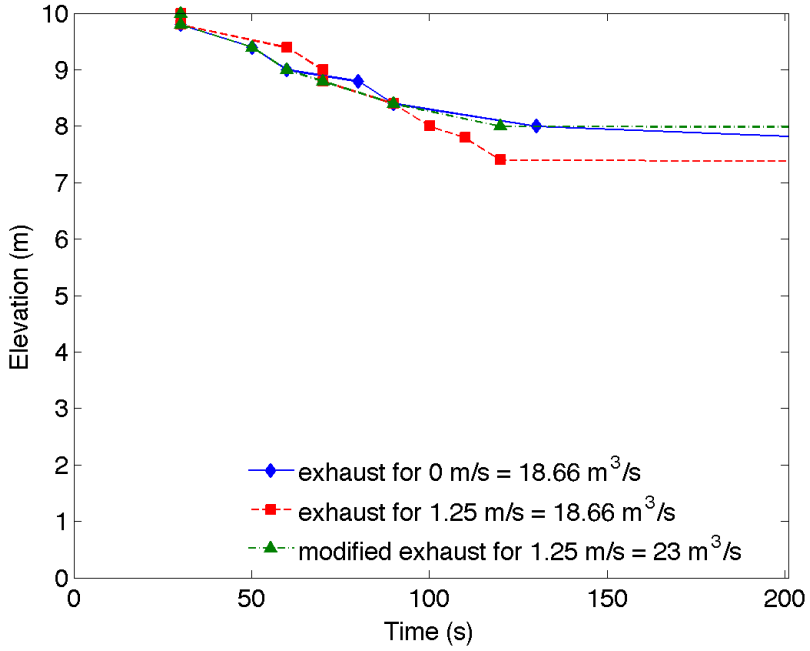

Figure 5.45: Validation Simulation for SOA_rdoor 1.25 m/s

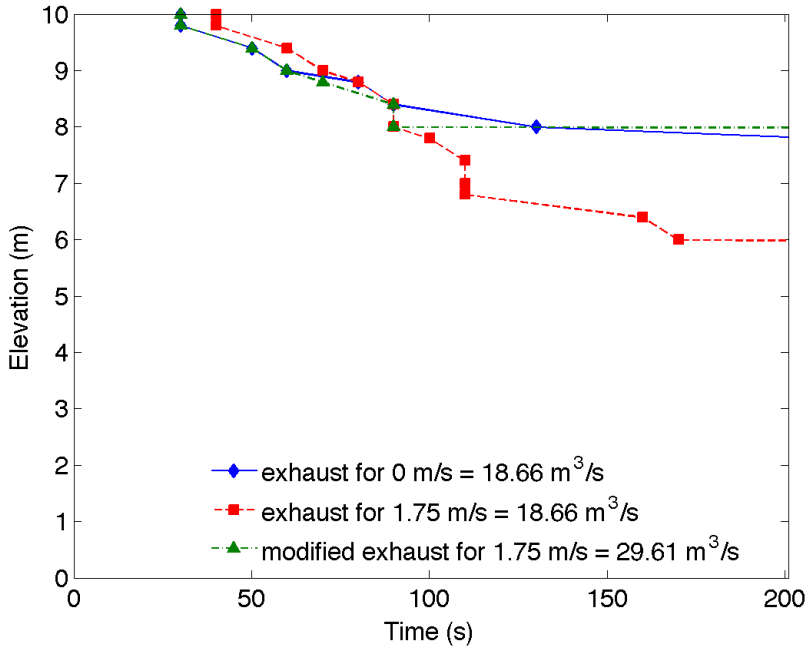

Figure 5.46: Validation Simulation for SOA_rdoor 1.75 m/s

The results in Figure 5.45 and 5.46 indicate that average alpha value used to determine the modified exhaust rate appropriately stabilized the smoke layer at 8 m. It

is concluded that the average alpha value for the SOA_rdoor simulations is taken appropriately despite the increased standard deviation value.

Overall, the results presented in Figures 5.39 - 5.46, indicate that modified exhaust rate accurately corrects for the additional volume of smoke production created by the increase in makeup air. The results validate the use of the alpha value to determine the exhaust rate necessary to stabilize the layer at the original design height with the makeup air velocity exceeding 1 m/s.

5.5 Limitations of the Smoke Production Design Tool

The following engineering design tool is limited by the scope of the FDS study. The study utilizes 1 MW, 2.5 MW, and 5 MW fire. It is suggested that the tool not apply to fire sizes, which exceed a maximum heat release rate of 5 MW. In addition, in the application of parameter $u^*a^*z^*$, makeup air velocity should not exceed 1.75 m/s.

The current study uses a 10 meter tall atria. The average alpha factor is found to remain relatively constant within the plume region for a 10 meter tall space. However, the constant alpha value with elevation, has not been explicitly concluded for space taller than 10 m. The engineering tool is limited to maximum atria of 10 meters in heights.

It is also important to consider the engineering tool is designed for potential “worst case” scenarios, as the makeup air is injected very close to an axisymmetric fire. If the makeup air is introduced further from the edge of the flame, the apparent affect of the airflow velocity will be reduced. As this section concludes, the alpha factor is greater for makeup air located at the base of the flame. Makeup air introduced by a raised vent does not show as significant an affect as the vent located on floor level. Again within the following set limits, the results portray “worst case” conditions.

Chapter 6

Heat Flux and Separation Distance - Results and Design Tool

This chapter presents and discusses the results of the four simulation configurations. The configuration details of each model are included in Section 3.5. The results are presented using the heat flux gauge devices also explained in Section 3.5.

The results are used to determine the impact of the makeup air velocity on the heat flux and therefore separation distance of fuel packages. Further the results are used to develop an engineering tool that assists in accounting for the impact of makeup air velocities exceeding 1 m/s.

6.1 1 MW Fire Results

The results for the 1 MW were compiled to plot the heat flux vs. the distance from the center of the burner. Both the floor and elevated gauges were plotted for each makeup air velocity considered. The floor and elevated heat flux gauge results for a 1 MW fire are plotted in Figure 6.1 and 6.2 respectively.

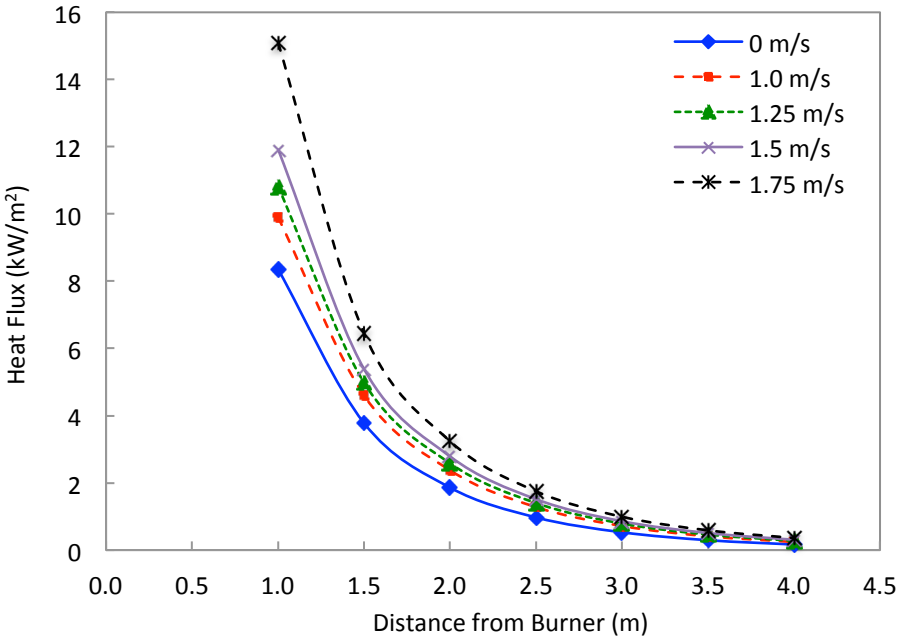

Figure 6.1: 1 MW fire, Heat Flux gauges located on Floor

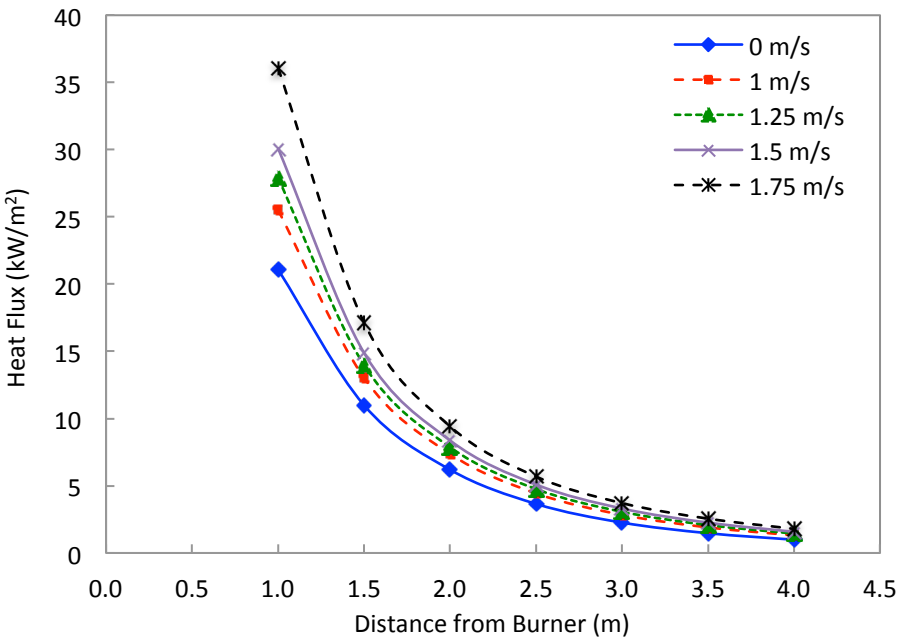

Figure 6.2: 1 MW fire, Heat Flux gauges elevated at half the mean flame height

The results in Figure 6.1 and 6.2 show the velocity of the makeup air directly affects the heat flux value. The makeup air tilts the flame and plume, increasing the heat flux in the direction of the airflow. This effect is greatest at distances closer to the burner.

6.2 5 MW Fire Results

The same plots are created for the 5 MW fire case, both the floor and elevated gauge results are shown in Figure 6.3 and Figure 6.4 respectively.

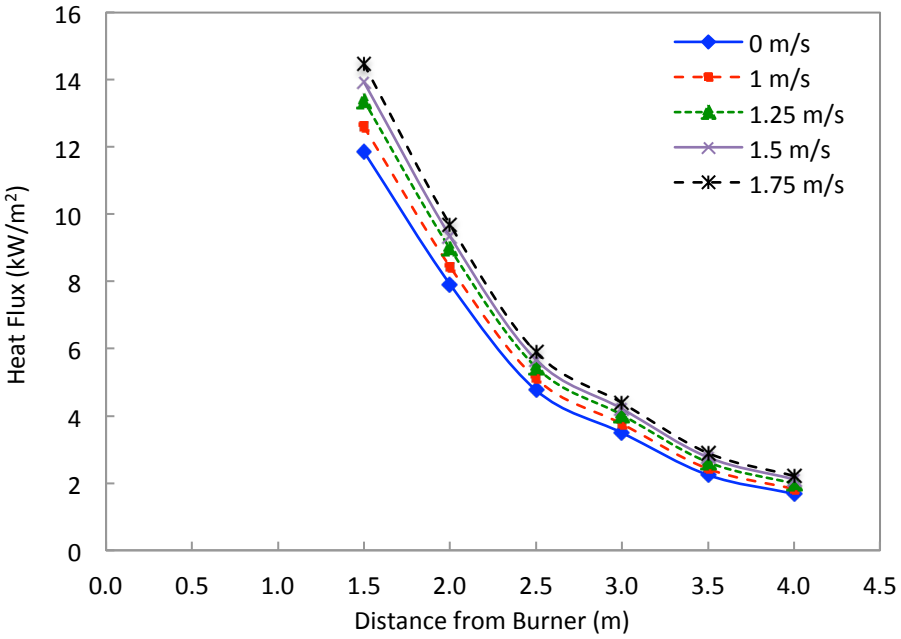

Figure 6.3: 5 MW fire, Heat Flux gauges located on Floor

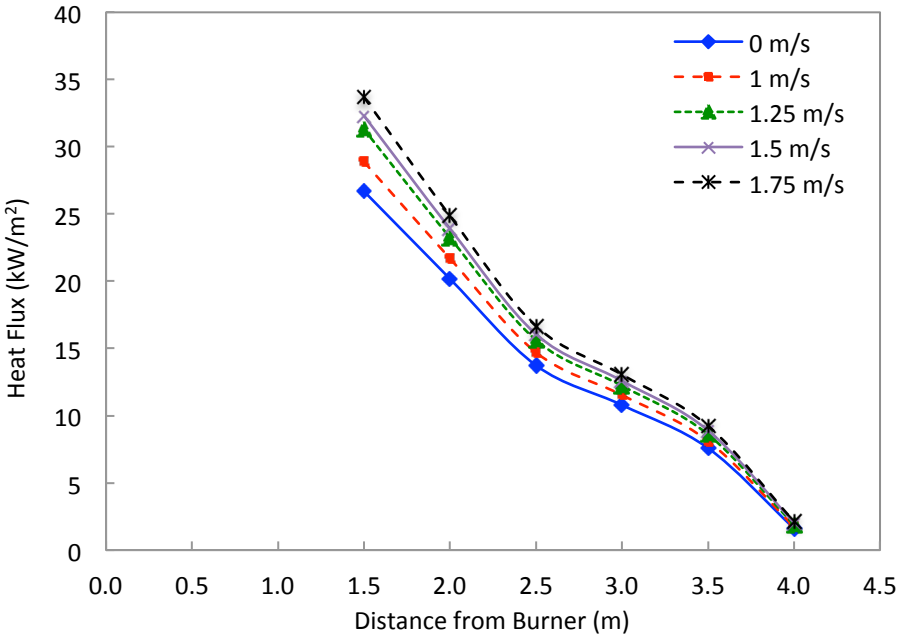

Figure 6.4: 5 MW fire, Heat Flux gauges elevated at half the mean flame height

The results in Figure 6.3 and 6.4 show relatively consistent effects when compared with the 1 MW fire plots. The effects of makeup air velocity increase show consistent trends, and are also intensified closer to the burner.

6.3 Separation Distance Analysis

In order to develop separation distance approximations, a 10 kW/m^2 threshold is defined as the heat flux ($\dot{q}_{r,net}''$), to ignite a neighboring object.

The separation distance for all velocities is determined using the heat flux curves in Figure 6.1-6.4, by interpolating the distance at which 10 kW/m^2 threshold is reached. Tables 6.1 and 6.2 present the distance where the heat flux reaches 10 kW/m^2. This

data is then plotted and shown in Figures 6.5 and 6.6 for the 1 MW and 5 MW configurations respectively.

Table 6.1: 1 MW, Separation Distance

Velocity	Separation Distance (m)	
	Floor Gauge	Elevated Gauge
0.00	-	1.50
1.00	1.00	1.71
1.25	1.06	1.77
1.50	1.10	1.83
1.75	1.27	1.95

Table 6.2: 5 MW fire, Separation Distance

Velocity	Separation Distance (m)	
	Floor Gauge	Elevated Gauge
0.00	1.74	3.12
1.00	1.81	3.22
1.25	1.88	3.31
1.50	1.93	3.35
1.75	1.97	3.40

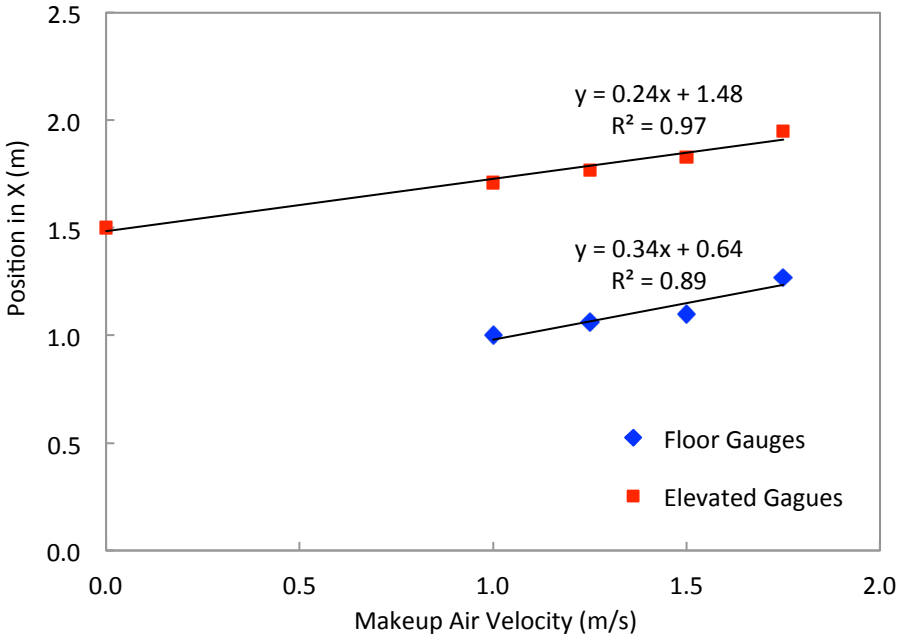

Figure 6.5: 1 MW Fire, Separation Distance vs. Makeup velocity

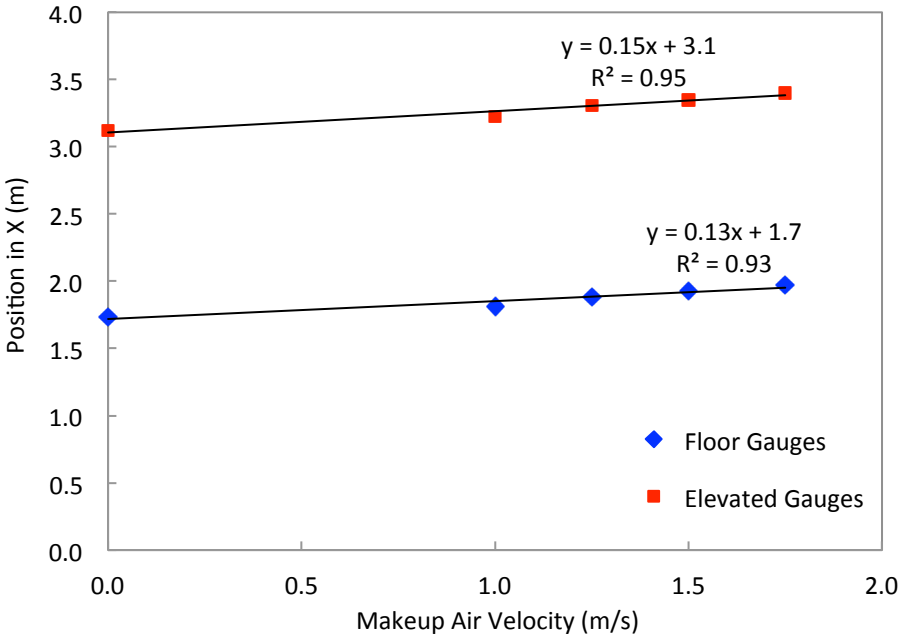

Figure 6.6: 5 MW fire, Separation Distance vs. Makeup velocity

The results show the separation distance increases linearly with makeup air velocity for both the 1 MW and 5 MW case. A best-fit line equation is fitted for the data to define the trend, and the R-squared statistical value is shown. Both the elevated and floor gauges show a strong agreement to the best-fit line.

6.4 Point Source Model Comparison

The point source model defines the separation distance, in regards to the radiative portion of the heat release rate of the fire, the radiant flux required for piloted ignition, and the orientation of the angle between the normal to the target and the line of sight from the target to the point source location. The point source model utilizes these components to define separation distance in terms of the typical entrainment rates of the fire size and does not account for increased makeup air velocities. The results of the point source model calculation is therefore compared to the FDS configuration where makeup air duct is set to a 0 m/s velocity.

6.4.1 Floor Gauges

The point source model considers the orientation of the gauge. As explained in Section 3.5 the floor gauge is oriented to face upwards. The heat flux gauges located on the floor for the 1 MW simulation never reached 10 kW/m^2 as stated in Table 6.1. The point source model calculation for the 5 MW fire with the heat flux gauge position on the floor, is defined in Equation 6.1-6.3. Equations 6.1 and 6.2 account for the orientation of the gauge by defining z_l as the mean flame height, L as the distance from the center of the burner, and R as the hypotenuse established as the separation distance.

$$R = \sqrt{\left(\frac{z_l}{2}\right)^2 + L^2} \tag{6.1}$$

$$\cos(\theta) = \frac{\left(\frac{z_l}{2}\right)}{\sqrt{\left(\frac{z_l}{2}\right)^2 + L^2}} \tag{6.2}$$

Equations 6.1 and 6.2 are applied the point source model for separation distance as shown in Equation 6.3.

$$\dot{q}_r'' = \frac{Q_r \cos(\theta)}{4\pi R^2} = \frac{Q_r}{4\pi} \frac{\left(\frac{z_l}{2}\right)}{\left(\left(\frac{z_l}{2}\right)^2 + L^2\right)^{\frac{3}{2}}} \tag{6.3}$$

$$L = \sqrt{\left(\frac{Q_r\left(\frac{z_l}{2}\right)}{4\pi(q_r'')}\right)^{2/3} - \left(\frac{z_l}{2}\right)^2} = \sqrt{\left(\frac{0.3(5000\text{kW})(2.1\text{m})}{4\pi(10\frac{\text{kW}}{\text{m}^2})}\right)^{2/3} - (2.1\text{ m})^2} = 2.04\text{ m}$$

The point source model defines the separation distance of the floor gauge, L, to be approximately 2.04 m.

6.4.2 Elevated Gauges

The same process is applied to the elevated gauge for both the 1 MW and 5 MW fire simulations. The elevated gauge is located at mean flame height elevation, z_l, and facing towards the flame. Therefore the orientation factor $\cos(\theta)$ is equal to 1. The separation distance, R, is equal to the distance from the center of the burner, L. Applying Equation 6.3, the separation distance for the point source model for the 1 MW and 5 MW fire is 1.54 m and 3.45 m, respectively.

6.5 Heat Flux Calculation Comparison

Table 6.3 presents the separation distance calculated using the point source model compared with separation distance determined by the FDS results.

Table 6.3: Separation Distance Model Comparisons

Fire Size	Floor Gauge		Elevated Gauge	
	Point Source	FDS Results	Point Source	FDS Results
1 MW	-	-	1.54 m	1.5 m
5 MW	2.04 m	1.74 m	3.45 m	3.12 m

The results show a close comparison for the elevated gauge for the 1 MW fire, and over 85% accuracy for the 5 MW gauges. As stated in Section 2.6.3 the point source model is accurate up to 90% if the separation distance is greater than the twice the burner diameter, and up to 80% if the separation distance is greater than the burner

diameter. In this study the separation distance is slightly less than twice the diameter of the burner, so the data will lie within this 80-90% accuracy range.

6.6 Separation Distance Design Tool

The linear relationship shown in Figure 6.5 and 6.6 is used to craft an analytical comparison. Similar to Section 5.1.1, an alpha (α) value, is created to compare the separation distance found at a specific makeup air velocity greater than 0 m/s over the separation distance found with 0 m/s makeup air velocity from the duct mounted vent. This ratio is shown in Equation 6.4.

$$\text{Alpha } (\alpha) = \frac{\text{Separation Distance @ 1,1.25,1.5,1.75 m/s}}{\text{Separation Distance@ 0 m/s}} \quad (6.4)$$

This alpha value reflects the percent increase in separation distance required to successfully maintain radiant heat flux values below 10 kW/m^2. Table 6.1 presents the alpha values for the 1 MW and 5 MW fire sizes. For the 1 MW fire size configuration, the floor gauges never reached 10 kW/m^2 at 0 m/s as shown in Figure 6.5, so the data cannot be applied. Table 6.4 presents the alpha factors for the following makeup air velocities and fire sizes based on the simulation results presented in Section 6.3.

Table 6.4: Alpha factor results for 1 and 5 MW fire simulations

Makeup Air Velocity	1 MW		5 MW	
	Floor	Elevated	Floor	Elevated
1 m/s	-	1.14	1.04	1.03
1.25 m/s	-	1.18	1.09	1.06
1.5 m/s	-	1.22	1.11	1.07
1.75 m/s	-	1.30	1.13	1.09

In order to apply the alpha factor for multiple size fires a similar engineering design tool is created as in Section 6.4. The X-axis is defined as the same momentum parameter defined Section 6.3. The alpha factor vs. the momentum parameter $u^*a^*z^*$, is graphed in Figure 6.7.

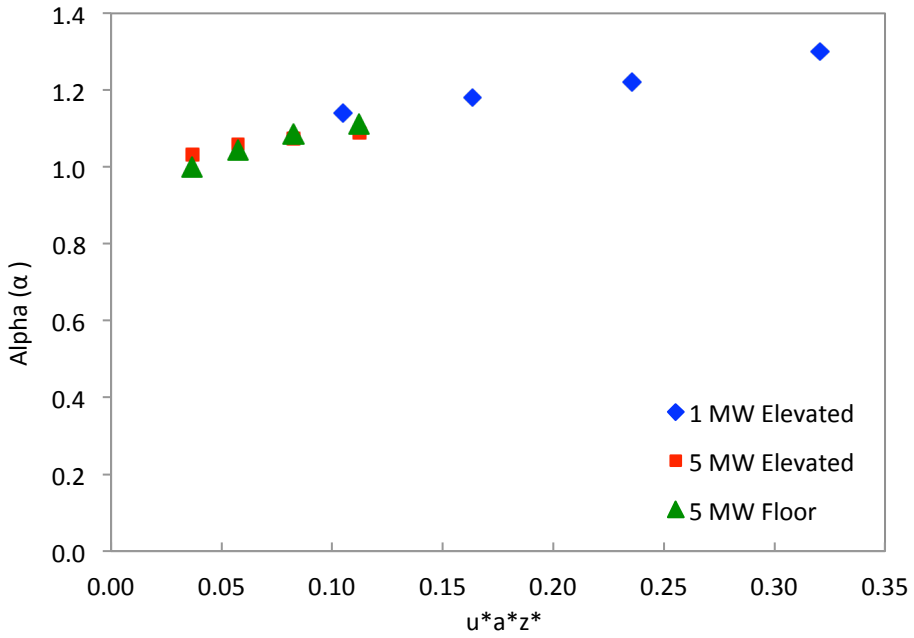

Figure 6.7: Alpha values presented for all Simulations

The graph shows a very consistent linear agreement between data sets for both the 1 MW and 5 MW fire. The same graph is presented with a best-fit line to include all of the data sets, shown in Figure 6.8. The data presented in Figure 6.8, shows strong

agreement when the data is collapsed into one best-fit line, with an R-squared value of 0.95.

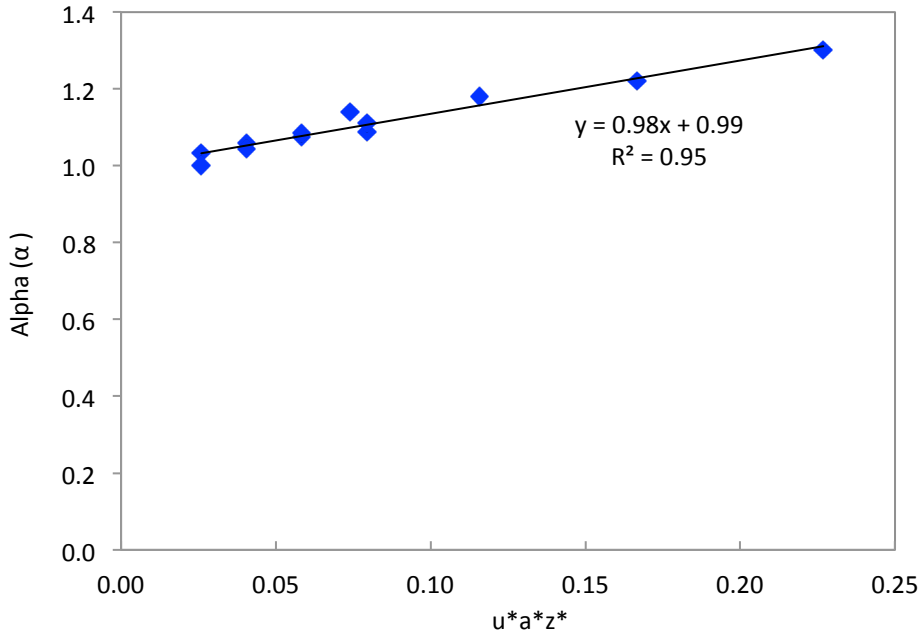

Figure 6.8: Alpha values presented as one data set

The data presented in Figure 6.8 is then be utilized as an engineering design tool. By determining the $u^*a^*z^*$ value for a given configuration as defined by Equation 6.12. an alpha factor is obtained from the best-fit line, as shown in Figure 6.8. An expression defined by the best-fit line equation, is used to determine the alpha factor as a function of the momentum ratio in Equation 6.5.

$$\text{Alpha } (\alpha) = 0.98(u^*a^*z^*) + 0.99 \qquad (6.5)$$

The alpha factor, α, calculated using Equation 6.5 is then applied to the point source model, shown in Equation 6.6. This alpha factor directly adjusts the separation

distance, L, to account for makeup velocity when the possible fuel package is in line with the increased airflow.

$$L = \alpha \sqrt{\left(\frac{Q_r\left(\frac{z_l}{2}\right)}{4\pi(q_r'')}\right)^{2/3} - \left(\frac{z_l}{2}\right)^2} \tag{6.6}$$

6.7 Limitations of the Separation Distance Design Tool

There are limitations to the design tool proposed in Figure 6.8. The design tool proposed is developed solely using the data presented in Section 6.5. The study utilizes a 1 MW and 5 MW fire. The tool should not be applied for fire sizes which exceed a maximum heat release rate of 5 MW. In addition the parameter $u^*a^*z^*$ is based off of makeup air velocities, which do not exceed 1.75 m/s in the simulations conducted in this study. It is suggested the modification tool not apply if the makeup air velocity is designed to exceed 1.75 m/s.

The heat flux design uses the same model configuration with a duct mounted makeup air vent located close to the axisymmetric fire. The smoke production results show that the duct mounted makeup air vent centrally located on the floor at the base of fire is a potential "worst case" scenario. Therefore, the heat flux study only uses this configuration set up to generate conservative solutions.

Chapter 7

Summary and Recommendations for Future Work

7.1 Summary

The primary purpose of this study is to develop engineering methods to assess the impact of increased makeup air velocity in atria. The current restriction defined by NFPA 92 states that makeup air must not exceed 1 m/s during the operation of a mechanical smoke exhaust system. This limitation demands large areas of passive openings and mechanical ventilation at low elevations, which not only limits creative and aesthetic atria designs but also presents significant costs. Many engineering designers use alternative methods to exceed the limit of the code, claiming that 1 m/s is too restrictive.

Past studies have concluded that the makeup air restriction defined by 1 m/s is not overly restrictive. Past CFD models studies have concluded that makeup air velocities exceeding 1 m/s disturb the plume. Increased makeup air leads to increased air entrainment of the fire plume and creates higher volumes of smoke, which descends the smoke layer.

The present study has confirmed these finding using FDS 6.0. The original suggestion from Heskestad, and Mudan and Croce has proven appropriate in past studies in CFD.

The original study initiated by ASHRAE, undertaken by Hadjisophocleous at Carleton University and the University of Maryland study by Kerber and Milke, in 2007 also conclude these results. The present study simulated similar CFD model configurations from Hadjisophocleous and Kerber study, in confirm consistent results using FDS 6.0. The study obtains relatively similar results while applying original design considerations such as extending the boundary domain, and using the smoke layer interface diagnostics.

The present study advances the conclusions of past simulations by addressing potential resolutions to increased makeup air in atria. The study observes makeup air injection very close to the base of the fire at various elevations with a variety of vent sizes. The intent of this design was to introduce “worst case” scenarios, by injecting makeup air very close to an axisymmetric fire. As the makeup air is introduced further from the edge of the flame, the apparent affect of the airflow velocity will be reduced.

The mass flow rate diagnostic created is used to isolate the influence of additional makeup air and quantify the value to a percent increase of entrainment rate and smoke layer depth. Specifically the increase of entrainment and smoke production is determined by comparing the increased makeup air velocity to the same simulation with no additional makeup air. The percent increase is defined as an alpha factor.

A parameter defined as, $u^*a^*z^*$, measures the strength of the forced horizontal airflow with respect to the buoyant vertical flow of the fire plume. The ratio quantifies the energy of air from the duct mounted makeup air towards the flame or plume in the horizontal direction to the energy provided by the fire source in the vertical direction. A parameter value is set for every simulation configuration with varying fire size, makeup air velocity, and vent location, to the results of the percent increase in smoke production obtained in FDS. A comparison tool in form of a graph is created in order to observe a linear trend line between all data points. The trend line observes an R-squared, coefficient of determination, value of 0.75 for all simulation configuration data.

The trend line is used as an engineering correlation. By knowing the fire size, burner area, makeup air vent size, vent elevation, and makeup air velocity, an engineering designer can use the correlation to determine the alpha factor appropriate for the design. The alpha factor consequently translates to an increased exhaust rate appropriate to rectify the increase in smoke production to the original intended design height.

In addition to the smoke entrainment rate increase, the radiant heat flux of the fire was investigated to observe potential effects of increased forced airflow at the flame. NFPA 92 defines the distance between fuel packages in order to prevent the spread of fire. Empirical calculations as well as the FDS study imply that the increased makeup air creates a significant tilt of the flame. Radiant heat flux gauges are used to analyze

and quantify the increased affects. The results permit that the flame tilt produces higher heat flux values in line with the increased airflow velocity.

Similar to the smoke production method, an engineering tool was created in correlation with the NFPA 92 point source model. The radiant heat flux results of increased airflow were compared to the same simulation without an increase of makeup air. The comparison also defined a percent increase value expressed as alpha.

Using the same, $u^*a^*z^*$ parameter, the results are compared to the alpha factor and a linear trend line is developed. The trend line is used to generate an alpha factor, which can be applied to the point source model.

The present study concludes that makeup air of 1 m/s or higher does tilt and increase the entrainment rate of the plume. The plume disturbance creates larger volumes of smoke within the plume and increases radiant heat flux in line with the airflow. An engineering design tool for both the increased smoke production and increased radiant heat flux is presented in order to allow for the increased makeup air velocity. The design for additional makeup air velocity is therefore permitted within atria and the necessary area of makeup air supply is subsequently reduced.

7.2 Recommendations for Future Work

After completion of the current study, recommendations regarding future work are made. Although this study confirms past research and also proposes possible alternative methods to increase makeup air velocity in atria, additional studies regarding makeup air should be conducted.

NFPA 92, along with the current study and past studies focus on the *velocity* (m/s) of makeup air. However, each study that has been concluded has introduced the airflow not only at different elevations, and different directions, but also at different volumetric rates. The volume of airflow (m^3/s) is not directly considered when the adverse affects of the plume are remarked. It is evident from past studies that if a very large opening close to the fire and has a makeup air velocity of 1.5 m/s, compared to a smaller vent in this study, the distress on the fire plume likely will be different. As such, this led to questions being raised as to whether the velocity (rather than volumetric flow rate) was the correct parameter to be used in design. The engineering tool proposed in this study includes the volumetric flow influence with the $u^*a^*z^*$ parameter. However, it is suggested that future work be conducted to more thoroughly quantify the volumetric rate of makeup air as opposed to velocity in order to provide an improved set of guidelines.

This study focuses on the smaller classification of atria, mainly 10 meter height compartments. Consequently, the research may be indicating that the effects of

makeup air being introduced near the base of the fire may only have an impact at lower elevations, and that once the smoke moves away from the area of disturbance, the plume acts as an axisymmetric plume in the classic case. With simulations only conducted at the two ceiling heights, it is not clear whether this effect occurs gradually or whether there is a threshold height at which this occurs. Further, it is unclear if the trend observed at the 30 m ceiling height continues at taller ceiling heights.

The FDS study was completed with a propane gas burner, located within the center of the atrium. It is recommended that future work, investigate different fuel types, fire size, and various fire locations the atria.

Lastly, all of the previous analyses of the impact of makeup air velocity have been conducted numerically, using FDS. It is suggested experimental testing be conducted at a tall height to confirm that the simulations are accurate and to provide a source for calibrating the numerical simulations.

Chapter 8

References

[1] National Institute of Standards and Technology, Fire Dynamics Simulator, Version 6.0, http://www.fire.nist.gov/fds/

[2] Klote, J.H., Milke, J.A., Turnbull, P.G., Ahmed K., and Ferreira M.J., "Handbook of Smoke Control Engineering," ASHRAE, Atlanta, GA, 2012.

[3] NFPA 92, "Standard for Smoke Control Systems", National Fire Protection Association, Quincy, MA, 2012 Edition.

[4] McGrattan, K., McDermott, R., Hostikka, S., and Floyd, J., "Fire Dynamics Simulator (Version 6) users guide," NIST Special Publication 1019-5, National Institute of Standards and Technology, Gaithersburg, MD, 2013.

[5] Cooper, L. Y., Harkleroad, M., Quintiere, J., and Rinkinen, W., "An Experimental Study of Upper Hot Layer Stratification in Full-Scale Multiroom Fire Scenarios," Paper 81-HT-9, the American Society of Mechanical Engineers, 1981.

[6] Madrzykowski, D., and Vettori, R., "A Sprinkler Fire Suppression Algorithm," Journal of Fire Protection Engineering, 4, pp. 151–164, 1992.

[7] "Fire Modeling Software." Fire Modeling Programs. May 2014. <http://www.nist.gov/el/fire_protection/buildings/fire-modeling-programs.cfm>.

[8] McGrattan, K. "Fire Dynamics Simulator Technical Reference Guide Volume 3: Validation", National institute of Standards and Technology, 2013.

[9] Nielsen, J. "Validation Study of Fire Dynamics Simulator", Student Report, Aalborg University, 2013.

[10] Quintiere, J. "Fundamentals of Fire Phenomena." Wiley & Sons, 2006. Print.

[11] Modak, A.T., Thermal Radiation from Pool Fires, Combustion and Flame, 30, pp. 251-265, 1977.

[12] Nelson, H., "FPETool: Fire Protection Engineering Tools for Hazard Estimation," National Institute of Standards and Technology, Gaithersburg, MD, 1990.

[13] Beyler, C., "Fire Hazard Calculations for Large, Open Hydrocarbon Fires," Chapter 3-10 in SFPE Handbook of Fire Protection Engineering. (4th Edition), P.J. DiNenno (ed.). National Fire Protection Association, Quincy, MA, 2008.

[14] Karlsson, B., and Quintiere, J. G. "Enclosure Fire Dynamics", CRC Press, Boca Raton, FL, 2000.

[15] Hadjisophocleous, G. and Zhou, J., "Maximum Velocity of Makeup Air for Smoke Management Systems in Atria and other Large Spaces", ASHRAE RP 1300, Carleton University, Ottawa, 2007.

[16] Kerber, S. and Milke, J. "Using FDS to Simulate Smoke Layer Interface Height in a Simple Atrium," Fire Technology, 43, pp. 45–75, 2007.

[17] P.H. Thomas, "The Size of Flames from Natural Fires," Ninth Symposium (International) on Combustion, Combustion Institute, Pittsburgh, pp. 844–859, 1962.

[18] Mudan, K.S., and Croce, P.A., Fire hazard calculations for large open hydrocarbon fires. SFPE Handbook of Fire Protection Engineering, NFPA, Quincy, MA, pp. 3-271, 2002.

[19] Heskestad, G., Engineering relations for fire plumes, Fire Safety Journal, Vol. 7, pp. 25-32, 1984.

[20] Souza, V.T.D., and Milke, J.A., Modeling smoke layer interface height as a function of makeup air supply velocity for atrium design. Fire Safety Journal 6, 2004.

[21] Milke, J.A., "Smoke Management in Covered Malls and Atria," Chapter 4-13 in SFPE Handbook of Fire Protection Engineering. (3rd Edition), P.J. DiNenno (ed.). National Fire Protection Association, Quincy, MA, 2002.

[22] Hadjisophocleous, G. "Maximum Velocity of Makeup Air for Smoke Management Systems in Atria and Other Large Spaces ASHRAE RP 1300," American Society for Heating Refrigerating and Air-Conditioning Engineers, 2007.

[23] International Building Code 2012, International Code Council, Country Club Hills IL. 2013.

[24] Spratt, D. an A.J.M. Heselden. "Efficient extraction of smoke from a thin layer under a ceiling", Fire Research Note 1001, Fire Research Station. Building Research Establishment, Garston, UK. 1974.